Linear Polyene Electronic Structure and Potential Surfaces

BRUCE S. HUDSON

Department of Chemistry
University of Oregon
Eugene, Oregon

BRYAN E. KOHLER

Department of Chemistry
Wesleyan University
Middletown, Connecticut

KLAUS SCHULTEN

Department of Physics
Technische Universität München
Garching, Federal Republic of Germany

EXCITED STATES, VOL. 6

ISBN 0-12-227206-4

I. Introduction

Polyenes are linear conjugated chains of carbon atoms joined by alternating double and single bonds and are deservedly the objects of a good deal of experimental and theoretical attention. There are many reasons for this, including the historical importance of these systems in the development of molecular quantum theory, the fundamental importance of cis–trans photoisomerization, which is the distinctive photochemistry of these molecules, and the fact that polyene chromophores play starring roles in biologically important photoprocesses, such as vision and energy production in the purple-membrane *Halobacterium halobium*. In both of these biological examples, the electronic structure of the polyene and how it changes upon excitation is of key importance. Until relatively recently, this structure was thought to be rather simple, similar to that of other conjugated systems such as the polyacenes, and well described by approximate molecular orbital ideas. Recent experimental and theoretical discoveries have revealed that this is not the case: Polyene electronic structure is both more complicated and more interesting than was previously thought.

In 1972 Hudson and Kohler reported mixed crystal absorption spectra for α,ω-diphenyl-1,3,5,7-octatetraene that showed the presence of an excited singlet state, nearly forbidden in absorption, below the dipole-allowed state (B_u in C_{2h}) previously thought to be the lowest lying excited singlet. In an accompanying publication, Schulten and Karplus (1972) provided a theoretical rationalization of this finding. The characterization of this state as a "doubly excited" A_g state, which is only poorly described without extensive configuration interaction, followed from their calculations. Hudson and Kohler (1972, 1973) further recognized that this ordering of electronic states, 2^1A_g below 1^1B_u, must be a very general feature of polyene electronic structure because it rationalized aspects of the spectroscopic behavior of these molecules that had previously been thought to be anomalous. Using already published low-resolution spectra and other photophysical data, they were able to argue that this state ordering should hold for all polyenes except, perhaps, the shortest ones, butadiene and hexatriene. Again, this received support from the theoretical work of Schulten and Karplus who found that

at least for the first few members of the series, the energy gap between the excited A_g and B_u states was not a strong function of the length of the polyene chain. A review presented in 1974 (by Hudson and Kohler) covered much of the long history of this field, including both early experiments and theory. In the ensuing years, much has been learned both experimentally and theoretically about polyene electronic structure and photochemistry. Thus, it seems timely to examine both the data and the interpretive constructs that pertain to polyene electronic structure with the aim of producing as coherent a picture as possible of what is known and what needs to be learned. This is the aim of this article.

II. Ground-State Geometry

The most detailed picture of the ground-state structure of unperturbed linear polyenes comes from electron diffraction studies of butadiene and hexatriene (Kuchitsu *et al.*, 1967; Haugen and Traetteberg, 1966, 1967; Traetteberg, 1968a,b). The results of two independent determinations of the structure of butadiene are shown in Fig. 1. The comparison of these results is of interest in several respects. The structure of Traetteberg [panel (b) of Fig. 1] was determined from the electron diffraction data with a minimum of structural assumptions. Planarity was not assumed, and the C—H bond distances and bond angles were only restricted by the constraint that there

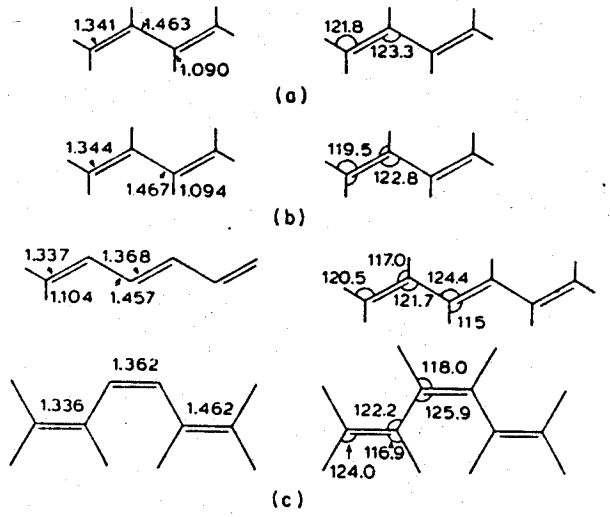

Fig. 1. Electron diffraction structures of butadiene and hexatriene. (a) Kuchitsu *et al.* (1967); (b) Haugen and Traetteberg (1966); (c) Traetteberg (1968a,b).

be a center of inversion symmetry. A planar configuration was found to produce the best fit to the data. The fit of the calculated intensity function to that observed was excellent. The analysis of Kuchitsu *et al.* [panel (a) of Fig. 1] differs from that of Traetteberg in three respects. First, it is a constrained refinement in which all of the C—H bond lengths and C=C—H bond angles were assumed to be equal, and the molecular symmetry was assumed to be C_{2h} and therefore planar. Second, the distances between atoms have been corrected to their equilibrium values using estimated harmonic force constants. Third, the structure shown, termed the "average structure," was refined to fit both the electron diffraction data and four inertial constants for butadiene (CHHCHCHCHH) and two isotopic species (CDDCHCHCDD and CDDCDCDCDD) obtained from infrared and Raman studies. Structure (a) of Fig. 1 is therefore the most accurate determination in terms of statistical reliability, whereas structure (b) is more free of predetermined constraints. The close similarity of the structures obtained using these two different methods of analysis is strong evidence of their validity.

The Raman and infrared spectroscopic data of Cole *et al.* (1967) and Marais *et al.* (1962), which were used in the determination of the average structure of butadiene, have also been analyzed directly. Cole *et al.* derived a C—C central bond-length value of 1.464 Å and a C=C—C bond angle of 123.2 ± 0.2°, while Marais *et al.* obtained C—C = 1.476 Å and a C=C—C angle of 122.9°. Although these purely spectroscopic determinations require a number of structural assumptions, these assumptions appear to be quite reasonable given the agreement with the electron diffraction results.

The structure of both the trans and cis forms of 1,3,5-hexatriene have also been determined by electron diffraction (Traetteberg, 1968a,b). For *trans*-hexatriene several planar and nonplanar models were considered, and a planar structure was found to give the best fit to the data (Fig. 1).

From the point of view of π-electron theory, the most interesting results of these studies of polyene structure are probably the demonstrated planarity and the values of the carbon–carbon bond lengths. Values of the double- and single-bond lengths are summarized in Fig. 2, which covers the results of all of the electron diffraction studies including the estimated range of uncertainty. A number of reasonably reliable conclusions can be drawn from these results:

1. The single-bond lengths are considerably shorter than 1.54 Å.
2. The double-bond lengths are quite close to the value of 1.333 Å for ethylene.
3. There is, however, a significant lengthening of the central double bond of hexatriene relative to the terminal double bonds (Traetteberg,

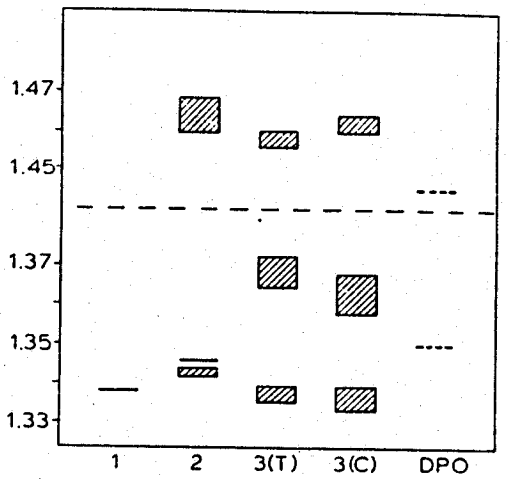

Fig. 2. The variation of polyene bond lengths with number of double bonds. Data from Fig. 1 plus the diphenyloctatetraene (DPO) data of Fig. 3.

1968a,b). This point is of particular interest because of its relevance to the existence of bond alternation in long polyenes.

4. There is some indication that the length of the single bonds in hexatriene is shorter than in butadiene.

The only noncarotenoid polyene which has been investigated by X-ray crystallography appears to be diphenyloctatetraene (Drenth and Wiebenga, 1955). The results of this study are shown in Fig. 3. The orthorhombic crystal form was studied at −100°C, a single isotropic thermal parameter was used for all atoms, and the hydrogen atoms were located. The centrosymmetric molecule has a planar polyene chain with the planes of the phenyl groups rotated relative to this plane by 5.4°. The standard deviation of the carbon–carbon bond lengths summarized in Fig. 3 is 0.004 Å.

It is interesting to compare the results of this study to the electron diffraction and spectroscopic results for butadiene and hexatriene. The double bonds of diphenyloctatetraene are found to be of equal length (1.350 Å) compared to the average double-bond length for *trans*-hexatriene of 1.353 Å.

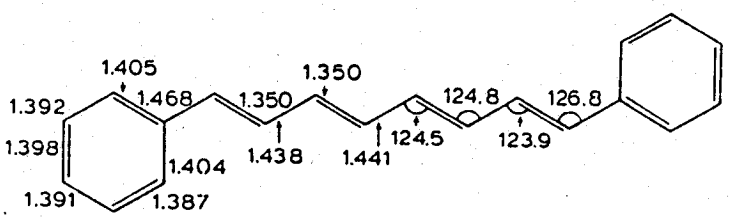

Fig. 3. The molecular structure of 1,8-diphenyloctatetraene (Drenth and Wiebenga, 1955).

The polyene single bonds of diphenyloctatetraene have lengths of 1.438 and 1.441 Å. This is significantly shorter than the values of 1.465 and 1.457 Å observed for butadiene and hexatriene.

Detailed crystallographic studies of carotenoid polyenes have been compared in a paper by Bart and MacGillavry (1968). The results of these studies will not be discussed in detail here because these carotenoid species clearly exhibit structural effects due to their methyl substitution and crystal packing. The single- and double-bond lengths of the four independent carotene-like structures exhibit some variation with position in the chain (single-bond lengths decreasing and double-bond lengths increasing toward the center of the chain), but this trend is probably due to special features of the molecules studied, rather than reflecting an intrinsic property of the polyene chain (Bart and MacGillavry, 1968). This is one of several examples of the fact that carotenoid polyenes may not be good models for the unsubstituted molecules and *vice versa* when detailed quantitative comparisons are needed.

Clearly, additional detailed information on the ground-state structures of longer polyenes is needed. The available data indicates that although there is clear alternation of the bond lengths of the shorter polyenes (ca. 1.35 and 1.45 Å), increasing the chain length decreases the mean single-bond length and increases the double-bond length for those bonds near the chain center. Some highly accurate structural information on a significantly longer polyene could do much to help our understanding of the connection between electronic structure and nuclear position.

III. Electronic States

A. Theoretical Overview

With the planar geometry detailed in Section II, the separation of σ and π electrons in the manner used successfully for the benzenoid hydrocarbons follows quite naturally. This separation assumes that the σ and π electrons move independently and that, to good approximation, the state of the σ electrons is frozen. This frozen core, together with the nuclear frame, provides an effective Hamiltonian for the motion of the π electrons. A variety of Hamiltonians for treating the π electrons have been suggested ranging in complexity from a simple particle-in-a-box formulation to semiempirical Hamiltonians derived using *ab initio* methods. Since the simplest picture reflects the main features of more sophisticated treatments, we review it here in order to establish a frame of reference for discussing further both the theoretical and experimental work.

In the simplest description the carbon atoms in the polyene are sp^2 hybridized. The hybrid orbitals, together with the hydrogen 1s orbitals, are

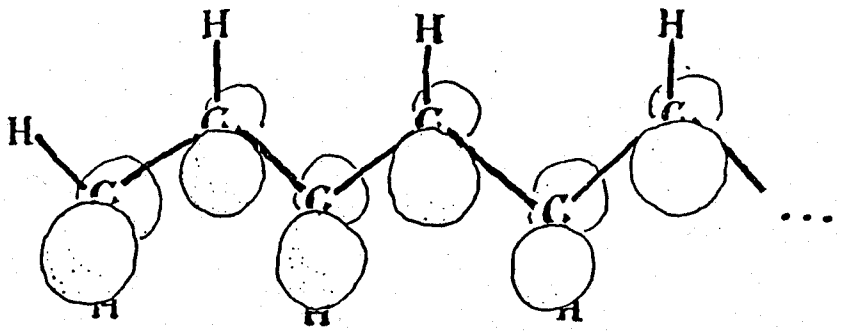

Fig. 4. A pictorial representation of the linear polyene π atomic orbitals.

combined to provide bonding molecular orbitals of sigma symmetry for the hydrogen 1s and three of the carbon 2s, 2p electrons. The remaining electrons (one π electron per carbon atom) are free to move in the frame of the 2p π orbitals as illustrated in Fig. 4.

The wave functions of the individual π electrons are then described by linear combinations of the 2p orbitals chosen to diagonalize the one-electron part of an effective Hamiltonian (possibly including the self-consistent field contribution of the electron–electron repulsion). In an alternative description, the electrons are free to carry out a continuous motion in the plane of the carbon frame governed by an effective potential rather than move in the discrete set of atomic orbitals. The motion of the individual π electrons is then accounted for by wave functions reminiscent of free-electron gas states. In either description, the wave functions conform to the symmetry properties of polyenes and can be classified according to how they transform under C_{2h}. Complete classification follows from noting whether or not the orbitals change sign under inversion at the symmetry center or under 180° rotation around the symmetry axis. The corresponding symmetry labels are u and g for the inversion and b and a for the rotation. Since the atomic 2p orbitals change sign under reflection in the symmetry plane, the character of the π-electron orbitals is restricted to only two symmetry classes, a_u and b_g, excluding the classes a_g and b_u. When ordered with respect to increasing energy, the symmetry character of the π-electron orbitals alternate between a_u and b_g, starting with a_u. As an illustration Table 1 shows the π-electron orbitals for octatetraene.

Wave functions to describe the electronic states of polyenes (the general polyene has formula $C_{2n}H_{2n+2}$ and contains $2n$ π electrons) are constructed by assigning the π electrons to orbitals in a Slater determinant. We denote these orbital configurations by corresponding occupation diagrams as sketched in the accompanying tabulation for the ground state and the first excited B_u state of octatetraene.

TABLE I

PPP-SCF Molecular Orbitals of Octatetraene[a]

Symmetry	Energy (eV)	Coefficients of atomic orbitals: 1	2	3	4	5	6	7	8
a_u	−14.6	0.189	0.296	0.412	0.455	0.455	0.412	0.296	0.189
b_g	−13.5	0.351	0.454	0.370	0.185	−0.185	−0.370	−0.454	−0.351
a_u	−11.8	0.445	0.406	−0.103	−0.356	−0.356	−0.103	0.406	0.445
b_g	−9.8	0.378	0.205	−0.428	−0.368	0.368	0.428	−0.205	−0.378
a_u	−1.4	0.378	−0.205	−0.428	0.363	0.363	−0.428	−0.205	0.378
b_g	0.6	0.445	−0.406	−0.103	0.356	−0.356	0.103	0.406	−0.445
a_u	2.3	0.351	−0.454	0.370	−0.185	−0.185	0.370	−0.454	0.351
b_g	3.4	0.188	−0.296	0.412	−0.455	0.455	−0.412	0.296	−0.189

[a] PPP, Pariser, Parr, and Pople; SCF, self-consistent field; evaluated on the basis of the PPP Hamiltonian [Eq. (2)] with the energy parameters as given in Section IV.

Ground A_g state	Excited B_u state
--O—O—	—O—O—
--O—O—	—O—O—
—O—O—	—O—O—
--O—O—	—x—O—
—x—x—	—O—x—
—x—x—	—x—x—
—x—x—	—x—x—
—x—x—	—x—x—

Since C_{2h} is an Abelian group, the overall symmetry of the $2n$ electron state is unambiguously determined by the product of the characters of the occupied orbitals according to the multiplication rules:

$$a \times a = b \times b = a \qquad g \times g = u \times u = g$$
$$a \times b = b \times a = b \qquad g \times u = u \times g = u$$

These rules show that all π-electron states of polyenes are of either A_g or B_u symmetry, distinguishing the $2n$ electron states by capital letters A, B. Since the σ-electron orbitals in the frozen core are all doubly occupied, the ground and all π-electron excited states of polyenes are also either A_g or B_u. However, if excitations involve σ electrons or Rydberg orbitals, the electronic states may also assume A_u or B_g characteristics.

Since in the π-electron ground state all orbitals are doubly occupied, one expects the ground state to have A_g characteristics. Promoting one electron in the ground state from the highest occupied to the lowest unoccupied orbital will always produce a configuration of symmetry B_u. The lowest energy (in the orbital picture) A_g configurations will come from either the promotion of one electron by two (or, because of the symmetry alternation of the energy-ordered orbitals, any even number) orbitals or by the promotion of two electrons by an odd number of orbitals.

If electron correlation is neglected, i.e., if one considers each of the electrons to move independently in an average potential determined by the rest, the energies of these configurations are approximately the sum of orbital energies. In this case the ordering of electronic states (configurations) would be A_g, B_u, A_g for the first three. For one-photon processes the excitation $A_g \rightarrow B_u$ is allowed and $A_g \rightarrow A_g$ is forbidden. For two-photon absorption the selection rules are complementary, i.e., $A_g \rightarrow A_g$ is allowed and $A_g \rightarrow B_u$ is forbidden. These selection rules will be relaxed for molecules deformed either statically or dynamically from C_{2h} symmetry.

B. *Experimental Overview*

Under medium resolution conditions (room-temperature solutions or samples in disordered rigid glasses), the spectroscopic properties of all linear polyenes are strikingly similar. In the near-ultraviolet or visible

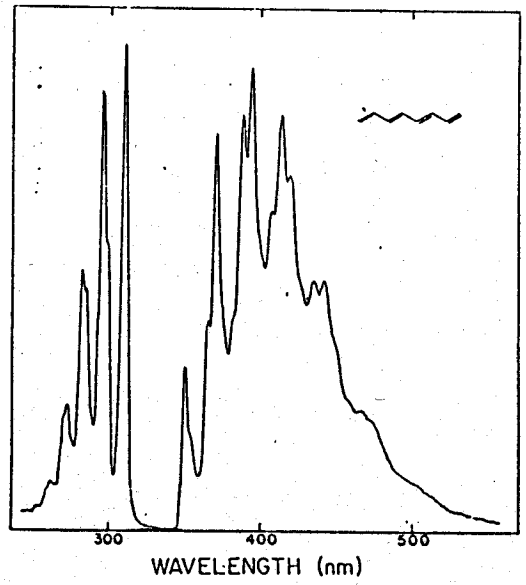

Fig. 5. The absorption (left) and fluorescene (right) spectra of octatetraene in 3-methylpentane at 77 K.

spectra, depending on the length of the conjugated chain, there is a strong structured absorption band. Figure 5 shows the appearance of this band for *all trans* 1,3,5,7-octatetraene. As the conjugated chain length increases, this band shifts to lower energy and increases in intensity.

For a given set of conditions, the observed bandwidths in this absorption decrease with increasing conjugated chain length. Thus the longer systems exhibit more resolved vibrational structure. At this level of resolution the vibronic development is completely described by a progression in two modes, a single-bond-stretching mode at approximately 1200 cm^{-1} and a double-bond-stretching mode at approximately 1600 cm^{-1}. For the short polyenes, butadiene and hexatriene, the degree of resolution in condensed-phase solution is such that these modes are not resolved thus giving rise to apparent intervals of approximately 1440 cm^{-1}.

The Franck-Condon envelope of this absorption band is relatively narrow with the maximum intensity occurring at either the origin (octatetraene or longer) or the first vibronic feature (butadiene and hexatriene). There is universal agreement that this band is properly assigned as the $A_g \rightarrow B_u$ transition. The energy, intensity, and vibronic structure associated with this band are well accounted for by simple molecular orbital treatments as described above.

In butadiene, the spectrum to the high-energy side of the first strong absorption band is dominated by features assignable to Rydberg transitions. In hexatriene and longer systems, transitions to additional valence states

can be seen. Of the unsubstituted polyenes, hexatriene has been studied rather intensively. Gavin *et al.* (1973) measured absorption spectra for both the cis and trans isomers in the 5.8–8.6 eV range (up to 3.7 eV above the $^1A_g \rightarrow {}^1B_u$ band) and have assigned their transitions to $1^1A_g \rightarrow 2^1B_u$ (6.54 eV), $1^1A_g \rightarrow 3^1B_u$ (7.37 eV, tentative), and a $^1A_g \rightarrow$ Rydberg series starting at 7.71 eV and leading to an ionization potential of 8.27 eV. In the room-temperature gas-phase or disordered condensed-phase solutions the resolution is such that only transitions from the ^1A_g ground state to excited ^1B_u states are observed.

Octatetraene and longer polyenes fluoresce. The origin of this fluorescence is significantly shifted from the $1^1A_g \rightarrow 1^1B_u$ absorption origin, and the Franck–Condon envelope is generally somewhat broader with the intensity maximum occurring at the second or third vibrational band. The appearance of a typical fluorescence spectrum and its relation to the strongly allowed $1^1A_g \rightarrow 1^1B_u$ absorption is shown in Fig. 5. Because approximate molecular orbital theories predict 1^1B_u to be the lowest energy excited singlet state, and because these theories quite reasonably account for the properties of the $1^1A_g \rightarrow 1^1B_u$ transition seen in absorption, the emission was originally thought to originate from the 1^1B_u excited state. This left the problem of accounting for the lack of overlap between absorption and emission. This lack of overlap was rationalized on the basis of Franck–Condon forbiddeness. That is, it was hypothesized that the equilibrium nuclear geometry was so different in the 1^1A_g and 1^1B_u states that the origin bands for absorption and emission were unobservable. This hypothesis held fast for decades despite the fact that the Franck–Condon envelope for the polyene $1^1B_u \rightarrow 1^1A_g$ absorption was relatively narrow and completely different from those of other molecules such as ethylene, known to exhibit Franck–Condon forbiddenness. The comparison is, in fact, quite striking. The maximum intensity vibronic feature in the butadiene $^1A_g \rightarrow {}^1B_u$ absorption spectrum is the first feature seen after the origin and is of comparable intensity to the 0–0 band. In ethylene the intensity maximum occurs at approximately the seventeenth vibronic band and is of order 10^6 times more intense than the first feature whose assignments have ranged from $0 \rightarrow 10$ to $0 \rightarrow 0$ (Robin, 1975). Furthermore, as Hudson and Kohler (1972, 1973) pointed out, the assignment of the polyene spectrum as Franck–Condon forbidden was at odds with the observed emission lifetimes and solvent shift behavior of the absorption spectrum. It is now well established for the longer molecules that the emission derives in fact from a different excited state than the one responsible for the strong absorption. This state is directly observable provided that the spectra are sufficiently resolved. Figure 6 shows a superposition of ordinary absorption and emission for octatetraene in a *n*-octane host crystal at liquid helium temperatures.

With the improved resolution afforded by low-temperature mixed-crystal techniques it is very clear that in absorption, a set of very weak features lies

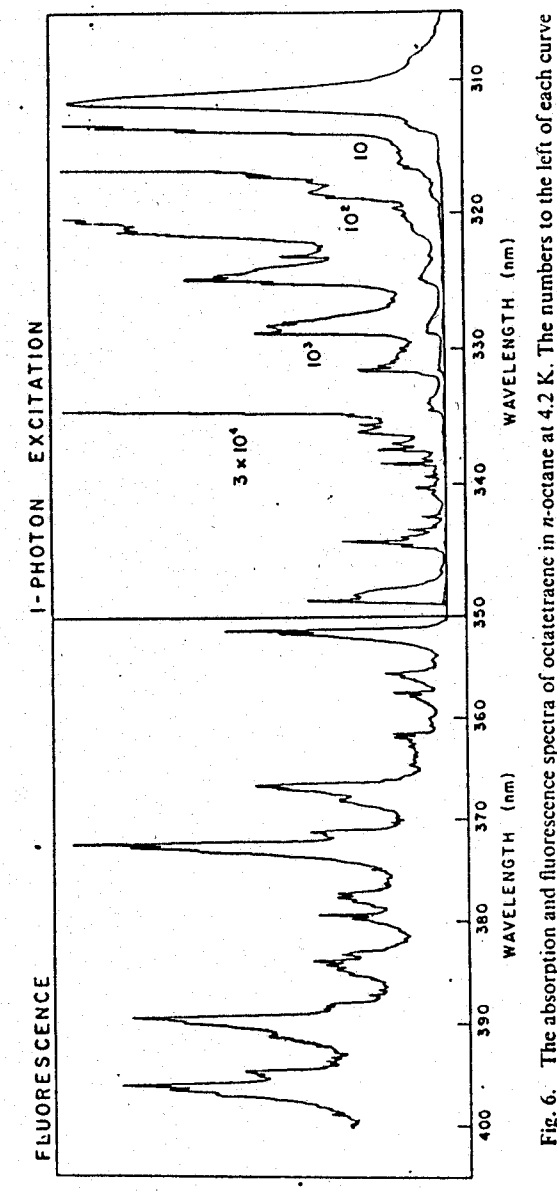

Fig. 6. The absorption and fluorescence spectra of octatetraene in *n*-octane at 4.2 K. The numbers to the left of each curve represent signal scale expansions relative to that of the curve at the far right.

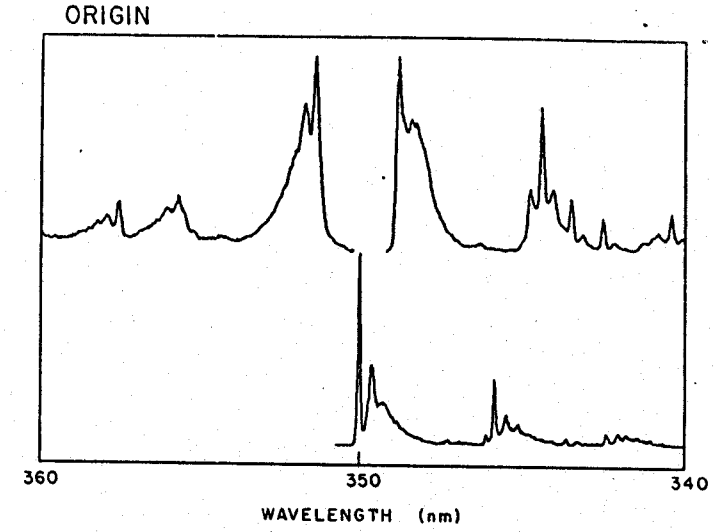

Fig. 7. The fluorescence (upper left), one-photon excitation (upper right), and two-photon excitation spectra (bottom) of octatetraene in *n*-octane at 4.2 K.

to the low-energy side of the origin of the $1^1A_g \rightarrow 1^1B_u$ transition. The lowest energy absorption is quite close to, but not coincident with, the origin of the emission spectrum. Excitation of either the weak or the strong bands gives the same emission spectrum which, when energy transfer is ruled out by a photoselection experiment (Hudson and Kohler, 1973), establishes that the weak, low-energy absorption bands are intrinsic to octatetraene. That the weak, low-energy absorption band derives from a symmetry-forbidden transition is suggested by both the weakness of the absorption and the vibrational development. That this transition is in fact properly assigned as $2^1A_g \rightarrow 1^1A_g$ is unambiguously established through a comparison of the one-photon forbidden, two-photon allowed character of the origin. This comparison (Fig. 7) establishes that the transition is g to g. Of course, if because of either less vibrational resolution or lower site symmetry the strict complementarity of the one- and two-photon spectra had not obtained, the assignment of the transition would have been dependent on either a determination of the absolute two-photon cross section and/or a detailed vibrational analysis.

The realization that there is a dipole-forbidden state below the 1^1B_u state completely rationalized the otherwise anomalous fluorescence properties of the linear polyenes. Conversely, polyene fluorescence, even in low-resolution experiments, can be used to reliably locate the 2^1A_g state in a number of polyenes.

For comparison to theory it is most useful to determine excitation energies for the isolated unsubstituted molecule. In the case of $1^1A_g \rightarrow 1^1B_u$ this can

TABLE 2

FREE-MOLECULE ^1A_g AND ^1B_u EXCITATION ENERGIES FOR UNSUBSTITUTED TRANS POLYENES

Molecule	$1^1A_g \rightarrow 2^1A_g$		$1^1A_g \rightarrow 1^1B_u$	
	O–O (eV)	Vertical[a] (eV)	O–O (eV)	Vertical (eV)
Ethylene	—	—	5.99[b,f]	7.65[f,g,h]
Butadiene	—	—	5.73[i]	5.91[h,i]
Hexatriene	—	—	4.93[j]	4.93[j]
Octatetraene	3.59[c,k]	3.97[d–f,k]	4.40[l]	4.40[l]
Decapentaene	3.10[c,l]	3.48[d–f,l]	4.02[l]	4.02[c,l]
Dodecahexaene	2.73[l]	2.91[d–f,l]	3.65[l]	3.65[c,l]

[a] Vertical excitation taken to be the energy of the most intense vibronic band.
[b] Longest wavelength feature seen by Wilkerson and Mulliken (1955).
[c] Corrected to the gas phase using simple solvent shift theory.
[d] Estimated from the fluorescence spectrum assuming mirror symmetry between absorption and emmission.
[e] Vibronic patterns for the gas and condensed phases assumed similar.
[f] Wilkerson and Mulliken (1955).
[g] Zelikoff and Watanabe (1953).
[h] Jones and Taylor (1955).
[i] Price and Walsh (1940).
[j] Gavin *et al.* (1973).
[k] Gavin *et al.* (1978).
[l] D'Amico *et al.* (1980).

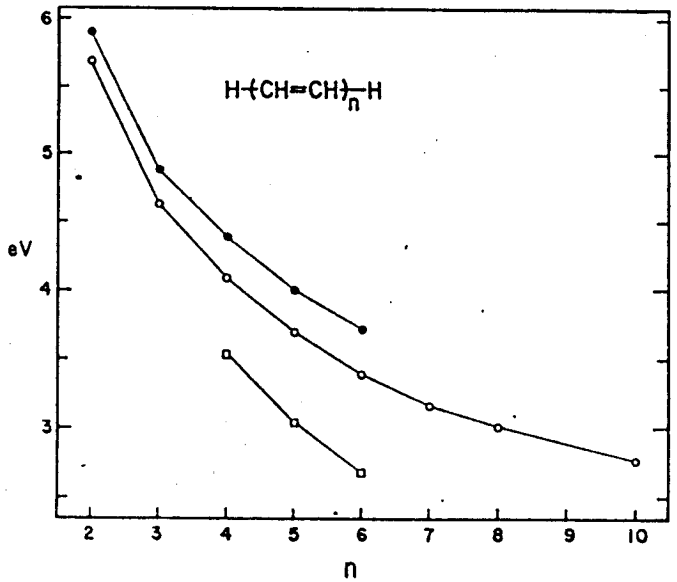

Fig. 8. The excitation energies (eV) of the two lowest energy excited states of unsubstituted linear polyenes as a function of chain length. For the 1^1B_u state, both hexane solution and gas-phase data are shown: ●, 1^1B_u (gas); ○, 1^1B_u (hexane); □, 2^1A_g (hexane). (See citations from Table 2.)

be accomplished directly for butadiene through decapentaene. For longer polyenes the solution excitation energies can be extrapolated to the gas phase using simple solvent shift theory to analyze data obtained in a number of different solvents. A similar approach can be employed for the fluorescence spectra to obtain $2^1A_g \rightarrow 1^1A_g$ excitation energies. The energies derived in this way for compounds containing 1–6 double bonds are tabulated in Table 2 and displayed graphically in Fig. 8.

IV. Electronic Structure: Theory

The experimental evidence for the 2^1A_g state below the 1^1B_u state in polyenes with eight and more π electrons calls for a revision of the molecular orbital (MO) theoretical description of these molecules. The older theoretical picture was based on three key assumptions which need to be reinvestigated in light of the failure of such a picture to properly describe the 2^1A_g states. These assumptions are the following:

1. Electron repulsion has only a weak influence on the electron motion; therefore, the electrons move independently and low-energy excited states involve the excitation of single electrons from the closed-shell ground state.
2. The motion of σ and π electrons is separated; the electrons move only in a minimum set of orbitals corresponding to the atomic 2p π orbitals.
3. The equilibrium geometries in ground and excited states are nearly identical; i.e., one can assume vertical transitions in the ground-state equilibrium geometry to describe the ordering of excited states.

Investigations following the experimental observations of the 2^1A_g state have shown that all three assumptions contribute to the shortcomings of earlier descriptions of polyene spectra. However, it is mainly assumption (1) which falls short in accounting even approximately for the nature of the 2^1A_g state. We will therefore discuss only this aspect of polyene excited states. However, the shortcomings of assumptions (2) and (3) ought to be examined before any quantitative comparisons between predicted and observed spectral transitions are made. Fortunately, for an understanding of the origin of the 2^1A_g state one can rely only on qualitative arguments and calculations, and we will emphasize these in this article.

The motion of conjugated π electrons is governed by two opposing interactions: the Hückel resonance interaction, which tends to delocalize the π electrons over the whole molecular frame and induces frequent encounters of the π electrons on common atomic sites, and the Coulomb repulsion interaction, which tends to prevent close encounters and thereby induces a localization of π electrons at different atomic sites. The latter behavior is often referred to as correlated motion of several electrons since the state of

an individual electron depends strongly on the position of the others. Similarly, the delocalized motion of the electrons is referred to as uncorrelated since the electrons move independently and do not avoid close encounters. The common applications of the MO theory in the past had been founded on a belief in independent electron motion. This has certainly met with great success in assigning the prominent spectral transitions of linear polyene spectroscopy (Salem, 1966; Suzuki, 1967). The opposite view of a strongly correlated motion of π electrons had been taken by the valence bond (VB) theory (Simonetta *et al.*, 1968); this theory, however, met with little success in assigning previously observed transitions and, therefore, was largely dismissed.

However, we will see that the failure of the MO description in accounting for the 2^1A_g state is at the same time a belated justification of the VB theory in that the 2^1A_g state has its parentage in a typical VB excitation (Schulten and Karplus, 1972). In any case, the observation of the 2^1A_g state has borne out the fact that resonance and repulsion both have to be correctly accounted for simultaneously by a proper theory of π, π^* states. For a more detailed discussion we have to introduce the effective Hamiltonian which governs the simultaneous motion of π electrons.

The effective Hamiltonian most often employed for π systems is that originally suggested by Pariser, Parr, and Pople (PPP) (Salem, 1966; Suzuki, 1967). The most concise presentation is in terms of creation (annihilation) operators $C^+_{n\sigma}$ ($C_{n\sigma}$) which create (annihilate) a π-electron spin σ in atomic orbital p_n. The orbitals are assumed to be mutually orthogonal (Campion and Karplus, 1973). The operators $C^+_{n\sigma}$ and $C_{n\sigma}$ are introduced to assure that the system of π electrons described conforms to the Pauli exclusion principle. This is achieved by requiring that the following anticommutation rules are obeyed (Fetter and Walecka, 1971; Tavan and Schulten, 1980):

$$[C^+_m, C^+_{n\rho}]_+ = 0, \qquad [C_{m\sigma}, C_{n\rho}]_+ = 0, \qquad [C^+_{m\sigma}, C_{n\rho}]_+ = \delta_{mn} \tag{1}$$

where $[a,b]_+ = ab + ba$. The following two combinations of creation and annihilation operators account for the motion of π electrons: $C^+_{n\sigma}C_{m\sigma}$ describes the jump of an electron with spin σ from orbital p_m to orbital p_n and $C^+_{n\sigma}C_{n\sigma}$ measures the occupancy of the spin orbital $p_n|\frac{1}{2},\sigma)$. The PPP Hamiltonian is then

$$H = H^{(0)} + H^{(1)} + H^{(2)} \tag{2a}$$

where $H^{(0)}$ denotes the nuclear repulsion (independent of the electrons)

$$H^{(0)} = \sum_{n<m} R_{nm} \tag{2b}$$

$H^{(1)}$ accounts for the electron–nuclear attraction and Hückel resonance

interaction which acts on *one* electron at a time

$$H^{(1)} = \sum_{m,\sigma}\left(-I_m - \sum_{n\neq m} R_{nm}\right)C^+_{m\sigma}C_{m\sigma} + \sum_{m,\sigma}(t_{m,m+1}C^+_{m\sigma}C_{m+1\sigma} + t_{m,m-1}C^+_{m\sigma}C_{m-1\sigma}) \tag{2c}$$

and $H^{(2)}$ represents the Coulomb repulsion between electrons

$$H^{(2)} = \frac{1}{2}\sum_{\substack{n,m\\ \sigma,\rho}}{}' R_{nm}C^+_{n\rho}C_{n\rho}C^+_{m\sigma}C_{m\sigma} \tag{2d}$$

where the summation excludes all terms $(n,\rho) = (m,\sigma)$. The Hamiltonian is based on a set of energy parameters which are related in an approximative way to energy expectation values of the set of atomic orbitals p_n: R_{nm} is the effective Coulomb interaction between electrons and nuclei at sites n and m; I_n is the effective ionization potential of a π electron at site n and $t_{m,m+1}$ is the Hückel resonance integral between centers m and $m+1$.

The difficulty in describing the π-electron behavior lies in the large number of degrees of freedom of the many-electron motion. Even under the restriction to a minimum set of atomic orbitals and disregarding nuclear motion, a system of $2N$ π electrons can assume $\binom{4N}{2N}$ different states (Tavan and Schulten, 1980), i.e., 12,870 for octateraene. A considerable reduction of this large number, albeit connected with great computational effort, can be achieved by including only states corresponding to a specific total spin quantum number, of which there are 1764 corresponding to singlet configurations (Tavan and Schulten, 1980). In the case that both the one- and two-electron part of the Hamiltonian $H^{(1)}$ and $H^{(2)}$ have to be included in the description, there exists no *a priori* selection criterion for reducing the number of π-electron states to a practical level without compromising the ability to reasonably describe π, π^* spectra. A most noteworthy new approach in this respect is the theory of Herrick (1981). Following earlier suggestions in the theory of nuclear structure, Herrick splits the many-electron Hamiltonian into two contributions $H = H_0 + V$, where the "zero-order" Hamiltonian H_0 entails contributions of $H^{(1)}$ as well as $H^{(2)}$ and obeys a dynamical symmetry which can be exploited to considerably reduce the number of π-electron states included in a description of the π, π^* spectra. In fact, Herrick's basis states diagonalize H_0, a result which is most significant in view of the fact that H_0 provides a reasonable qualitative description of the polyene spectra. Thus, Herrick's basis states yield a compact description of the π electronic states.

The results of Herrick's treatment may be very roughly stated in simple terms using a familiar model. The one-electron molecular orbitals for a

near polyene of n atoms have orbital energies which may be written as $m)=\alpha+2\beta\sin[m\pi/(n+1)]$, $m=j, j-1, \ldots, -j, j=(n-1)/2$. For $m\pi/(n+1)$ ear zero (the Fermi surface), the levels are approximately equally spaced. n SU(2) pseudorotation symmetry-group operator is found which, in fact, as equally spaced energy levels that match the Hückel levels at the Fermi irface. The resulting pseudorotation orbitals are similar to Hückel orbitals or short polyenes, but for long polyenes the low-lying excitations are more calized near the ends of the polyene chain. Excited states are highly degenerate for this orbital spectrum. Inclusion of an approximate form for lectron repulsion in the total Hamiltonian preserves an SU(2) symmetry hich permits exact evaluation of the resulting wave functions for which this egeneracy is split. It will be very interesting to see what form the conguration interaction (CI) matrix takes in this basis set and how the eigenectors in a limited CI treatment using this basis set compare with similarly uncated CI using uncorrelated MOs.

The description of π-electron motion is greatly simplified if either $H^{(1)}$ or $I^{(2)}$ is assumed to dominate π-electron motion. The resulting two limiting ases for the PPP Hamiltonian yield the independent-particle (MO) behavior duced by $H^{(1)}$ and the Dirac–Heisenberg (VB) behavior induced by $H^{(2)}$. hese limiting cases are both of interest because systems governed by $H^{(1)}$ s well as by $H^{(2)}$ have been found.

The limit of the independent-particle model will not be dealt with here, s it should be well known to the reader. We may just recall that in this odel the self-consisent one-particle contribution to $H^{(2)}$ is accounted for the ground state and that excited states are constructed by promoting a ngle electron from occupied to unoccupied orbitals.

The analysis of the π system in the limit of strong Coulomb repulsion is ss familiar to spectroscopists, although well known in solid-state science, it will be presented here in some detail (Ohmine and Schulten, 1982). We rst disregard the "mobility" of the electrons due to the Hückel resonance rms. The lowest energy states of the π system are then given by the eitler–London-type determinants which are the eigenstates of $H^{(2)}$. They e of the form

$$\Psi = |p_1\sigma_1 p_2\sigma_2 \cdots p_n\sigma_n| \tag{3}$$

which each atomic orbital is occupied once. All 2^{2N} different spin conurations have the same energy. Higher in energy are the single, double, ..., nic VB structures in which one, two, ..., atomic orbitals are doubly cupied. If the one-electron terms $t_{m,m\pm1}$ which allow electrons to move their neighboring sites are taken into account, the spin degeneracy is fted. To see what happens we consider a pair of nearest neighbor electrons.

Their possible single determinant wave functions are

$$\begin{aligned} \Psi_1 &= |p_1\alpha p_2\alpha|, & \Psi_2 &= |p_1\beta p_2\beta| \\ \bar{\Psi}_3 &= |p_1\alpha p_2\beta|, & \bar{\Psi}_4 &= |p_1\beta p_2\alpha| \\ \Psi_5 &= |p_1\alpha p_1\beta|, & \Psi_6 &= |p_2\alpha p_2\beta| \end{aligned} \tag{4}$$

where we used for the spin functions the notation $|1/2, 1/2\rangle = \alpha$ and $|1/2, -1/2\rangle = \beta$. The wave functions Ψ_1 and Ψ_2 of neighboring electrons with parallel spins represent triplet states. The wave functions $\bar{\Psi}_3$ and $\bar{\Psi}_4$ of neighboring electrons with antiparallel spins can be coupled to a triplet and a singlet state, i.e., $\Psi_3 = (1/\sqrt{2})(\bar{\Psi}_3 - \bar{\Psi}_4)$ and $\Psi_4 = (1/\sqrt{2})(\bar{\Psi}_3 + \bar{\Psi}_4)$, respectively. The ionic states Ψ_5 and Ψ_6 are of singlet character. The spin eigenstates Ψ_i yield the Hamiltonian matrix

$$H_{12} = \begin{bmatrix} R_{12} & 0 & 0 & 0 & 0 & 0 \\ 0 & R_{12} & 0 & 0 & 0 & 0 \\ 0 & 0 & R_{12} & 0 & 0 & 0 \\ 0 & 0 & 0 & R_{12} & 2t_{12} & 2t_{12} \\ 0 & 0 & 0 & 2t_{12} & R_{22} & 0 \\ 0 & 0 & 0 & 2t_{12} & 0 & R_{11} \end{bmatrix} \tag{5}$$

The covalent triplet states Ψ_1, Ψ_2, Ψ_3 are not coupled in this Hamiltonian, the covalent singlet state Ψ_4 is coupled to the ionic states Ψ_5 and Ψ_6, and thus experiences lowering in energy, i.e., a splitting from the triplet-state levels. The energy splitting $2J$ of the singlet and triplet covalent states can be evaluated readily from second-order perturbation theory (assuming $R_{22} = R_{11}$),

$$2J = -2[t_{12}^2/(R_{11} - R_{12})] \tag{6}$$

For a system of π electrons the effect of the resonance integrals $t_{m,m\pm1}$ may be cast formally into the Heisenberg spin Hamiltonian

$$H^{\text{Hei}} = \sum_m J(\mathbf{S}_m \cdot \mathbf{S}_{m+1} - \tfrac{1}{4}) \tag{7}$$

where $\mathbf{S}_m$ denotes the spin vector operator for an electron residing at the mth atomic site. To simplify the discussion we assume here and in the following a polyene with all bond lengths equal, i.e., $R_{m,m} = R_{11}$ and $t_{m,m\pm1} = t_{12}$ for all m.

It is readily verified that this Hamiltonian predicts the same energy lowering for a two-electron system as described above. The net effect of the resonance integrals t_{12} is then to lower the energy of spin configurations in proportion to the number of neighboring singlet pairs they contain. As a result the covalent wave functions [Eq. (3)] will split into a band of "spin

near polyene of n atoms have orbital energies which may be written as $m)=\alpha+2\beta\sin[m\pi/(n+1)]$, $m=j, j-1, \ldots, -j, j=(n-1)/2$. For $m\pi/(n+1)$ ear zero (the Fermi surface), the levels are approximately equally spaced. n SU(2) pseudorotation symmetry-group operator is found which, in fact, as equally spaced energy levels that match the Hückel levels at the Fermi irface. The resulting pseudorotation orbitals are similar to Hückel orbitals or short polyenes, but for long polyenes the low-lying excitations are more ocalized near the ends of the polyene chain. Excited states are highly degenerate for this orbital spectrum. Inclusion of an approximate form for lectron repulsion in the total Hamiltonian preserves an SU(2) symmetry hich permits exact evaluation of the resulting wave functions for which this egeneracy is split. It will be very interesting to see what form the configuration interaction (CI) matrix takes in this basis set and how the eigenectors in a limited CI treatment using this basis set compare with similarly uncated CI using uncorrelated MOs.

The description of π-electron motion is greatly simplified if either $H^{(1)}$ or $I^{(2)}$ is assumed to dominate π-electron motion. The resulting two limiting ases for the PPP Hamiltonian yield the independent-particle (MO) behavior duced by $H^{(1)}$ and the Dirac–Heisenberg (VB) behavior induced by $H^{(2)}$. hese limiting cases are both of interest because systems governed by $H^{(1)}$ s well as by $H^{(2)}$ have been found.

The limit of the independent-particle model will not be dealt with here, s it should be well known to the reader. We may just recall that in this odel the self-consisent one-particle contribution to $H^{(2)}$ is accounted for the ground state and that excited states are constructed by promoting a ngle electron from occupied to unoccupied orbitals.

The analysis of the π system in the limit of strong Coulomb repulsion is ss familiar to spectroscopists, although well known in solid-state science, o it will be presented here in some detail (Ohmine and Schulten, 1982). We rst disregard the "mobility" of the electrons due to the Hückel resonance rms. The lowest energy states of the π system are then given by the eitler–London-type determinants which are the eigenstates of $H^{(2)}$. They e of the form

$$\Psi = |p_1\sigma_1 p_2\sigma_2 \cdots p_n\sigma_n| \tag{3}$$

which each atomic orbital is occupied once. All 2^{2N} different spin configurations have the same energy. Higher in energy are the single, double, ..., nic VB structures in which one, two, ..., atomic orbitals are doubly ccupied. If the one-electron terms $t_{m,m\pm1}$ which allow electrons to move to their neighboring sites are taken into account, the spin degeneracy is fted. To see what happens we consider a pair of nearest neighbor electrons.

Their possible single determinant wave functions are

$$\begin{aligned} \Psi_1 &= |p_1\alpha p_2\alpha|, & \Psi_2 &= |p_1\beta p_2\beta| \\ \bar{\Psi}_3 &= |p_1\alpha p_2\beta|, & \bar{\Psi}_4 &= |p_1\beta p_2\alpha| \\ \Psi_5 &= |p_1\alpha p_1\beta|, & \Psi_6 &= |p_2\alpha p_2\beta| \end{aligned} \tag{4}$$

where we used for the spin functions the notation $|1/2, 1/2\rangle = \alpha$ and $|1/2, -1/2\rangle = \beta$. The wave functions Ψ_1 and Ψ_2 of neighboring electrons with parallel spins represent triplet states. The wave functions $\bar{\Psi}_3$ and $\bar{\Psi}_4$ of neighboring electrons with antiparallel spins can be coupled to a triplet and a singlet state, i.e., $\Psi_3 = (1/\sqrt{2})(\bar{\Psi}_3 - \bar{\Psi}_4)$ and $\Psi_4 = (1/\sqrt{2})(\bar{\Psi}_3 + \bar{\Psi}_4)$, respectively. The ionic states Ψ_5 and Ψ_6 are of singlet character. The spin eigenstates Ψ_i yield the Hamiltonian matrix

$$H_{12} = \begin{bmatrix} R_{12} & 0 & 0 & 0 & 0 & 0 \\ 0 & R_{12} & 0 & 0 & 0 & 0 \\ 0 & 0 & R_{12} & 0 & 0 & 0 \\ 0 & 0 & 0 & R_{12} & 2t_{12} & 2t_{12} \\ 0 & 0 & 0 & 2t_{12} & R_{22} & 0 \\ 0 & 0 & 0 & 2t_{12} & 0 & R_{11} \end{bmatrix} \tag{5}$$

The covalent triplet states Ψ_1, Ψ_2, Ψ_3 are not coupled in this Hamiltonian, the covalent singlet state Ψ_4 is coupled to the ionic states Ψ_5 and Ψ_6, and thus experiences lowering in energy, i.e., a splitting from the triplet-state levels. The energy splitting $2J$ of the singlet and triplet covalent states can be evaluated readily from second-order perturbation theory (assuming $R_{22} = R_{11}$),

$$2J = -2[t_{12}^2/(R_{11} - R_{12})] \tag{6}$$

For a system of π electrons the effect of the resonance integrals $t_{m,m\pm1}$ may be cast formally into the Heisenberg spin Hamiltonian

$$H^{\text{Hei}} = \sum_m J(\mathbf{S}_m \cdot \mathbf{S}_{m+1} - \tfrac{1}{4}) \tag{7}$$

where $\mathbf{S}_m$ denotes the spin vector operator for an electron residing at the mth atomic site. To simplify the discussion we assume here and in the following a polyene with all bond lengths equal, i.e., $R_{m,m} = R_{11}$ and $t_{m,m\pm1} = t_{12}$ for all m.

It is readily verified that this Hamiltonian predicts the same energy lowering for a two-electron system as described above. The net effect of the resonance integrals t_{12} is then to lower the energy of spin configurations in proportion to the number of neighboring singlet pairs they contain. As a result the covalent wave functions [Eq. (3)] will split into a band of "spin

near polyene of n atoms have orbital energies which may be written as $m)=\alpha+2\beta\sin[m\pi/(n+1)]$, $m=j, j-1, \ldots, -j, j=(n-1)/2$. For $m\pi/(n+1)$ ear zero (the Fermi surface), the levels are approximately equally spaced. n SU(2) pseudorotation symmetry-group operator is found which, in fact, as equally spaced energy levels that match the Hückel levels at the Fermi irface. The resulting pseudorotation orbitals are similar to Hückel orbitals or short polyenes, but for long polyenes the low-lying excitations are more calized near the ends of the polyene chain. Excited states are highly degenerate for this orbital spectrum. Inclusion of an approximate form for lectron repulsion in the total Hamiltonian preserves an SU(2) symmetry hich permits exact evaluation of the resulting wave functions for which this egeneracy is split. It will be very interesting to see what form the configuration interaction (CI) matrix takes in this basis set and how the eigenectors in a limited CI treatment using this basis set compare with similarly uncated CI using uncorrelated MOs.

The description of π-electron motion is greatly simplified if either $H^{(1)}$ or $I^{(2)}$ is assumed to dominate π-electron motion. The resulting two limiting ases for the PPP Hamiltonian yield the independent-particle (MO) behavior duced by $H^{(1)}$ and the Dirac–Heisenberg (VB) behavior induced by $H^{(2)}$. hese limiting cases are both of interest because systems governed by $H^{(1)}$ s well as by $H^{(2)}$ have been found.

The limit of the independent-particle model will not be dealt with here, s it should be well known to the reader. We may just recall that in this odel the self-consisent one-particle contribution to $H^{(2)}$ is accounted for the ground state and that excited states are constructed by promoting a ngle electron from occupied to unoccupied orbitals.

The analysis of the π system in the limit of strong Coulomb repulsion is ss familiar to spectroscopists, although well known in solid-state science, it will be presented here in some detail (Ohmine and Schulten, 1982). We rst disregard the "mobility" of the electrons due to the Hückel resonance rms. The lowest energy states of the π system are then given by the eitler–London-type determinants which are the eigenstates of $H^{(2)}$. They e of the form

$$\Psi = |p_1\sigma_1 p_2\sigma_2 \cdots p_n\sigma_n| \tag{3}$$

which each atomic orbital is occupied once. All 2^{2N} different spin configurations have the same energy. Higher in energy are the single, double, ..., nic VB structures in which one, two, ..., atomic orbitals are doubly cupied. If the one-electron terms $t_{m,m\pm1}$ which allow electrons to move their neighboring sites are taken into account, the spin degeneracy is fted. To see what happens we consider a pair of nearest neighbor electrons.

Their possible single determinant wave functions are

$$\begin{aligned} \Psi_1 &= |p_1\alpha p_2\alpha|, & \Psi_2 &= |p_1\beta p_2\beta| \\ \bar{\Psi}_3 &= |p_1\alpha p_2\beta|, & \bar{\Psi}_4 &= |p_1\beta p_2\alpha| \\ \Psi_5 &= |p_1\alpha p_1\beta|, & \Psi_6 &= |p_2\alpha p_2\beta| \end{aligned} \tag{4}$$

where we used for the spin functions the notation $|1/2, 1/2\rangle = \alpha$ and $|1/2, -1/2\rangle = \beta$. The wave functions Ψ_1 and Ψ_2 of neighboring electrons with parallel spins represent triplet states. The wave functions $\bar{\Psi}_3$ and $\bar{\Psi}_4$ of neighboring electrons with antiparallel spins can be coupled to a triplet and a singlet state, i.e., $\Psi_3 = (1/\sqrt{2})(\bar{\Psi}_3 - \bar{\Psi}_4)$ and $\Psi_4 = (1/\sqrt{2})(\bar{\Psi}_3 + \bar{\Psi}_4)$, respectively. The ionic states Ψ_5 and Ψ_6 are of singlet character. The spin eigenstates Ψ_i yield the Hamiltonian matrix

$$H_{12} = \begin{bmatrix} R_{12} & 0 & 0 & 0 & 0 & 0 \\ 0 & R_{12} & 0 & 0 & 0 & 0 \\ 0 & 0 & R_{12} & 0 & 0 & 0 \\ 0 & 0 & 0 & R_{12} & 2t_{12} & 2t_{12} \\ 0 & 0 & 0 & 2t_{12} & R_{22} & 0 \\ 0 & 0 & 0 & 2t_{12} & 0 & R_{11} \end{bmatrix} \tag{5}$$

The covalent triplet states Ψ_1, Ψ_2, Ψ_3 are not coupled in this Hamiltonian, the covalent singlet state Ψ_4 is coupled to the ionic states Ψ_5 and Ψ_6, and thus experiences lowering in energy, i.e., a splitting from the triplet-state levels. The energy splitting $2J$ of the singlet and triplet covalent states can be evaluated readily from second-order perturbation theory (assuming $R_{22} = R_{11}$),

$$2J = -2[t_{12}^2/(R_{11} - R_{12})] \tag{6}$$

For a system of π electrons the effect of the resonance integrals $t_{m,m\pm1}$ may be cast formally into the Heisenberg spin Hamiltonian

$$H^{\text{Hei}} = \sum_m J(\mathbf{S}_m \cdot \mathbf{S}_{m+1} - \tfrac{1}{4}) \tag{7}$$

where $\mathbf{S}_m$ denotes the spin vector operator for an electron residing at the mth atomic site. To simplify the discussion we assume here and in the following a polyene with all bond lengths equal, i.e., $R_{m,m} = R_{11}$ and $t_{m,m\pm1} = t_{12}$ for all m.

It is readily verified that this Hamiltonian predicts the same energy lowering for a two-electron system as described above. The net effect of the resonance integrals t_{12} is then to lower the energy of spin configurations in proportion to the number of neighboring singlet pairs they contain. As a result the covalent wave functions [Eq. (3)] will split into a band of "spin

wave" states with spin configuration corresponding to a maximum number of neighboring singlet pairs, i.e., to the bond structure lowest in energy:

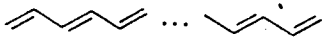

The set of covalent structures [Eq. (3)] does not, of course, allow a complete description of the π-electron motion. Single ionic, double ionic, etc., structures need to be included in a complete expansion of the electronic wave functions. For strong electron repulsion, i.e., $R_{11} - R_{12} \gg t_{12}$, the bands of covalent, single ionic, etc., structures are clearly separated in energy by the amount needed to move an electron to a neighboring occupied site. Hence, in the VB limit one can expect that ionic structures are not important for low-energy excited states. One can show that transitions between all states in the covalent band are one-photon forbidden and only transitions between covalent and ionic states can be allowed.

The effect of a transition from the VB limit to the MO limit can now be qualitatively described as follows: In the VB limit of strong Coulomb repulsion, i.e., $R_{11} - R_{12} \gg t_{12}$, the electronic states separate into a band of covalent low-energy, optically forbidden states and bands of single, double, ..., ionic high-energy states which are (partially) dipole allowed from the covalent ground state. If the Coulomb forces become weaker, i.e., $R_{11} - R_{12}$ decrease to values of the order t_{12}, the spin–spin interaction [Eq. (6)] and hence the width of the covalent and ionic bands increase, whereas the band gap decreases until covalent and ionic states become interspersed.

To illustrate these qualitative conclusions we approximate the PPP Hamiltonian by the Hubbard Hamiltonian ($t = t_{12}$, $R = R_{11} - R_{12}$)

$$H^{\text{Hub}} = t \sum_{m,\sigma} (C^+_{m\sigma} C_{m+1\sigma} + C^+_{m+1\sigma} C_{m\sigma}) + R \sum_m C^+_{m\sigma} C_{m\sigma} C^+_{m\rho} C_{m\rho} \qquad (8)$$

This approximation neglects the Coulomb repulsion between second, third, etc., neighbors, i.e., assumes $R_{13} = R_{14}$, etc., $= 0$. The Hubbard Hamiltonian may be divided by $|t|$ so that all energies are measured in units of $|t|$, i.e., we deal with the Hamiltonian

$$H^{\text{Hub}} = -\sum_{m,\sigma} (C^+_{m\sigma} C_{m+1\sigma} + C^+_{m+1\sigma} C_{m\sigma}) + \frac{R}{|t|} \sum_m C^+_{m\sigma} C_{m\sigma} C^+_{m\rho} C_{m\rho} \qquad (9)$$

This identifies the quantity $U = R/|t|$ as the relevant parameter for a characterization of the π-electron motion and suggests that we study the spectrum of H^{Hub} as a function of U.

In Fig. 9, the spectrum of butadiene is presented for U values ranging from $U = 0$ (MO limit) to $U = 8$ (near the VB limit). The spectrum has been evaluated in three basis sets: (1) a MO–SCF basis set including the SCF ground state; (2) a VB basis set including all those VB structures effectively accounted for by the Heisenberg Hamiltonian, namely, all covalent structures and all structures generated from them by moving a single electron to its adjacent site; and (3) the complete basis set.

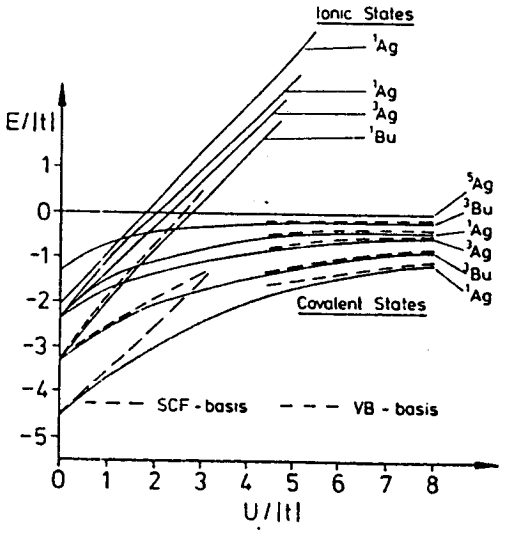

Fig. 9. The energies of the states of butadiene as a function of the ratio of the electron repulsion parameter to the resonance parameter. The solid line is for the complete basis set; the dashed curves from the right are for the VB basis; and the dashed curves from the left are for the MO–SCF basis.

The spectrum for the Hubbard Hamiltonian in Fig. 9 separates for large U (i.e., the VB limit) into two bands of covalent and of ionic excitations. Since increasing $U = R/|t|$ implies an increase of the energy to move an electron to an occupied atomic site, the band of ionic states rises linearly with U. The covalent band is well described by a VB description according to the Heisenberg model. The lowest state in this band 1^1A_g corresponds clearly to the spin configuration 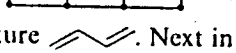 with two singlet pairs corresponding to the bond structure . Next in energy are states with only one singlet pair and one triplet pair 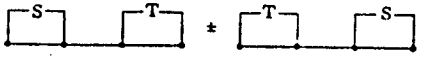 giving rise to the two triplet states 1^3B_u and 1^3A_g. These states are referred to as spin wave states because the triplet pair which originates from a spin flip in the ground state oscillates over the polyene chain. Highest in energy are the states  without any singlet pair. These states give rise to the states 2^1A_g, 2^3B_u, and 1^5A_g because two triplets can couple

to singlet, triplet, and quintet total spin states. Since, to an important degree, the resulting singlet state corresponds to the spin-coupling situation

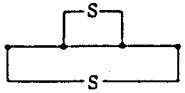

in which the second and third electron spins are in a singlet alignment, this state is lower in energy than 2^3B_u and 1^5A_g and corresponds to the bond structure 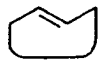 . Since in an ionic configuration two of the four electrons are necessarily in a singlet spin alignment, the band of ionic states entails only singlet and triplet states.

Of interest, as it relates to earlier treatments of polyene spectra, are the predictions of the MO–SCF model for the 1^1A_g, 1^3B_u, and the *ionic* 1^1B_u states. The MO–SCF states are found in close agreement with the exact results for small U values. However, since the MO–SCF assumption of independent electron motion induces frequent electron encounters, i.e., a great proportion of ionic contributions to the wave functions, the MO–SCF predictions rise linearly with U. The 1^3B_u MO–SCF state rises with only half the slope because according to the Pauli exclusion principle, the two triplet electrons cannot meet on a common atomic site. Figure 9 demonstrates that the MO–SCF description matches well the ionic ^1B_u state but that the covalent 1^3B_u and 1^1A_g states are only poorly described for medium and large U values. This finding can actually be generalized in that the MO–SCF description of excited states constructed by single-electron promotions from the SCF ground state tends to closely approximate the states of ionic character, but in many instances it only very poorly describes the states of covalent character.

The connection between these considerations and real polyene spectra follows from the results in Fig. 9 around $U = 1.5$ because this value corresponds to the interaction parameters suggested for conjugated π systems. At $U = 1.5$ the covalent and ionic bands are found to be interspersed and one expects, therefore, that polyene spectra in the low-energy regime should show both kinds of excitations. This is exactly what has been established by the recent observations of the polyene singlet states: The ^1B_u state is of the ionic variety and the 2^1A_g state is of the covalent variety. The description in Fig. 9 yields another important characterization of the 2^1A_g state as being the composite of two triplet excitations. The parentage of the 2^1A_g state is also reflected by the fact that its excitation energy is determined to be about twice the excitation energy of the lowest triplet state 1^3B_u. It follows from these considerations that in longer polyenes, many possible combinations of two covalent triplet states exist that yield covalent singlet states, i.e., $^3B_u \times {}^3A_g \rightarrow {}^1B_u$, etc. To explore the practical significance of the above discussion we make a comparison of calculations for octatetraene

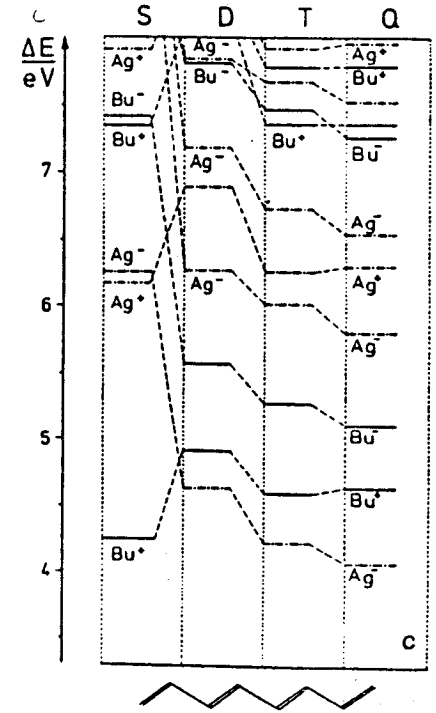

Fig. 10. The PPP–SCF–CI excitation energies of octatetraene for four different levels of CI (from Tavan and Schulten, 1979).

with the spectroscopic observations. For this purpose we present in Fig. 10 the results of a calculation of the spectrum of the PPP Hamiltonian [Eq. (2)] with realistic interaction parameters (Schulten *et al.*, 1976; Tavan and Schulten, 1979). The parameters are based on the standard geometry of polyenes with 120° angles between adjacent carbon–carbon bonds and bond distances of 1.35 Å for double bonds and 1.46 Å for single bonds. The resonance integrals are chosen according to the empirical formula

$$t_{m,m+1} = [2.60 - 3.21(r_{m,m+1} - 1.397)]\ \text{eV} \tag{10}$$

where the bond length $r_{m,m+1}$ is in angstrom units. The Coulomb matrix elements are taken from the Ohno expression

$$R_{mn} = \frac{19.397}{[(14.397/R_{11})^2 + r_{mn}^2]^{1/2}}\ \text{eV} \tag{11}$$

where r_{mn} is the distance between the atomic sites m and n in angstrom units. The one-center repulsion integral is chosen such that $R_{11} = 11.13$ eV and the ionization energy I in Eq. (2c) is chosen to be $I = 11.16$ eV. Except for a slight change of expression [Eq. (10)], these parameters have been suggested previously by other workers in connection with MO–SCF calculations.

The resulting singlet spectrum of octatetraene is presented in Fig. 10. The corresponding calculations have been carried out in four basis sets: these include all single excitations from the SCF ground state (S), double excitations (D), all triple excitations (T), and also all quadruple excitations (Q). The increase of the basis set is to account progressively for π-electron correlation due to electron repulsion which is only accounted for in a crude way in the smallest (S) basis. The spectra predicted for the different basis sets show very clearly the importance of π-electron correlation on the π-electron excitations. By far the largest effect occurs in going from the (S) to the (D) description; this leads to a strong decrease of the excitations which qualify as covalent spin–wave excitations in the VB description and to an increase of those excitations which qualify as ionic excitations in that description, e.g., the optically allowed 1^1B_u state. The net result of the introduction of double excitations is to intersperse covalent and ionic excitations. Since double excitations have such a profound effect on the description of the covalent excited states and dominate the wave functions, the covalent states are sometimes loosely referred to as doubly excited states. In fact, the 2^1A_g and 2^1B_u covalent states in this (D) description assume 58% double excited character, whereas the ionic 1^1B_u state assumes only 4% of this character. This aspect of the 2^1A_g and 2^1B_u states is in keeping with the characterization of these states in the VB limit as composites of two triplet excitations. It is quite apparent that such composite excitations can only be constructed by including at least double excitations with respect to the ground state. The electron configurations which contribute to the 1^1A_g ground state and the 2^1A_g and 1^1B_u excited states are presented in Table 3. However, since the MO description is rather ill suited for a description of the 2^1A_g state, none of the properties of this state are immediately obvious from such a description. A better picture of the character of this state is achieved by an excitonic (localized orbital) description (Schulten and Karplus, 1972; Schulten *et al.*, 1976; Tavan and Schulten, 1979).

Figure 10 demonstrates that higher excitations, i.e., triple and quadruple, also affect the spectrum of octatetraene, however, only to a small degree. These excitations do not give rise to a reordering of excitations, but they do affect the relative energy of the excited states, in particular the gap between the 2^1A_g and the 1^1B_u states. In fact, it has been found that only a full (Q) basis set can account for the tendency of the 2^1A_g–1^1B_u energy gap to increase with increasing polyene length (Fig. 8). Higher excitations also contribute to a general red shift of the polyene spectrum relative to the (D) predictions. In fact, spectra resulting from a (D) basis set in the limit of infinite π systems experience a kind of ultraviolet catastrophe in that infinite excitation energies are predicted. The reasons for this behavior lie in an unbalanced account of the effect of electron correlation in ground and excited states. To properly

TABLE 3

CI COEFFICIENTS IN OCTATETRAENE

Configuration	1^1A_g	2^1A_g	1^1B_u	Configuration	1^1A_g	2^1A_g	1^1B_u
------ ------ ------ ------ -x--x- -x--x- -x--x- -x--x-	0.95	0.11	0.00	------ ------ ------ ----x- -x--x- -x---- -x--x- -x--x-	0.02	−0.43	0.00
------ ------ ------ ----x- -x---- -x--x- -x--x- -x--x-	0.00	0.00	0.97	------ ------ ------ -x--x- ------ -x--x- -x--x- -x--x-	−0.14	0.59	0.00
------ ------ ----x- ------ -x---- -x--x- -x--x- -x--x-	−0.02	0.43	0.00	------ ------ ----x- ----x- -x---- -x---- -x--x- -x--x-	0.10	−0.29	0.00

repair this imbalance one would have to include infinitely high excitations. For moderately large polyenes, quadruple excitations appear to be sufficient for a proper description. This aspect of higher excitations is discussed in detail in Schulten *et al.* (1976) and Tavan and Schulten (1979). Schulten *et al.* (1976, 1980) and Tavan and Schulten (1979) provide a correction formula for the excitation energy of (D) calculations which corrects the excitation energies without needing recourse to the more extended descriptions.

With this discussion of the theory of polyene spectroscopy at the semiempirical level as background, it is interesting to examine some recent *ab initio* studies of butadiene and hexatriene (Nascimento and Goddard, 1979a,b). Earlier *ab initio* studies of butadiene are cited in these works and were discussed in our previous review (Hudson and Kohler, 1974). The results of these recent calculations for the Rydberg and triplet states of butadiene and hexatriene is discussed in later sections. Emphasis is placed here on the low-lying 2^1A_g and 1^1B_u states. The excitation energies obtained

r these states (in electron volts) are as follows:

State	Butadiene	Hexatriene
2^1A_g	6.8–7.2	5.6–5.9
1^1B_u	6.7	6.2

he range given for the 2^1A_g states represents the results for various degrees CI including some σ excitations. The magnitude of this $\sigma\pi^*$ correlation fect for hexatriene is estimated from the butadiene results. The value ted for the 1^1B_u state of hexatriene, although not actually given by Nascimento and Goddard, can be deduced from the experimental values and fferences between experimental and calculated values which are given. The oted differences between theory and experiment for the 1^1B_u state are 7 and 1.2 eV for butadiene and hexatriene, respectively. It is interesting note that the calculated decrease in the excitation energy for the 1^1B_u state n going from butadiene to hexatriene is at most 0.5 eV, while the experiental value is roughly 1 eV. The reason(s) for this discrepancy remain usive. It has been proposed that it is related to the ionic nature of this cited state.

These *ab initio* calculations confirm the description of the 2^1A_g excited ate of linear polyenes as an excitonic state formed from two ethylenic trip- t excitation (Hostency *et al.*, 1975). In the generalized valence bond (GVB) icture the 2^1A_g state is more nearly a pure doubly excited state than is the ase when delocalized π orbitals are used. The GVB description has more calized orbitals. The use of delocalized orbitals requires inclusion of singly xcited excitations relative to the ground state.

Nascimento and Goddard conclude that their calculations demonstrate at the 1^1B_u excited state is below the 2^1A_g state for both butadiene and exatriene. Their conclusion is ultimately based on a comparison of the *alculated* 2^1A_g excitation energy (5.6–5.9 eV for hexatriene) with the *xperimental* value for the 1^1B_u state (5 eV for hexatriene). The obvious potential fallacy in this argument is that the computational corrections which re needed to lower the ^1B_u excitation energy by 1.2 eV may also lower he 2^1A_g state by a comparable amount. Some estimate of the expected effect an be obtained from examination of the similar situation for benzene. Calculations similar to those performed for hexatriene place the ionic $^1E_{1u}$ tate too high by 1.4 eV. The covalent 1^1E_{2g} state, which has considerable louble-excitation character and a VB description similar to that of the 2^1A_g tate of polyenes, is calculated too high by 0.5 eV (Ziegler and Hudson, 1981, ection X.B.2). Thus, the correction needed for the covalent state is more than ne-third of the ionic state correction. To the extent that these two cases are imilar, it seems that both states of hexatriene will be lowered by improvements in the calculations, but that as postulated by Nascimento and Goddard, there will be a larger decrease for the 1^1B_u state. At present, however, it seems unlikely that current calculations are of sufficient accuracy to determine the state order for these short polyenes.

V. Linear Polyene s-cis, s-trans Isomerization

The conformational equilibrium of polyene chains about their "single" bonds is a unique feature of this π-electron system. Most of our information about this conformational equilibrium comes from studies on butadiene. Structural studies, including the electron diffraction and rotational Raman investigations discussed above and microwave studies of Lide (1962), have shown that the trans conformer of butadiene is the dominant species. Three experimental methods have been used to determine the energy difference between the s-trans and the s-cis conformations of butadiene: thermodynamic determinations of entropy and specific heat combined with vibrational data (Aston *et al.*, 1946; Compton *et al.*, 1976), NMR studies of deuterated butadiene as a function of temperature (Lipnick and Garbisch, 1973), and Raman spectroscopy (Carreira, 1975).

The thermodynamic analyses are based on the use of spectroscopic data to calculate the entropy, heat capacity, and enthalpy of each isomer. In this calculation the vibrational frequencies of the two conformations are assumed to be the same except for those of the low-frequency a_u torsional mode which represents the interconversion coordinate. In the paper by Compton *et al.* (1976), the torsional frequencies obtained by Carreira (1975) are used (163.7 cm^{-1} for s-trans and 137.4 cm^{-1} for s-cis, as discussed below), and all of the vibrations are considered to be harmonic in the thermodynamic calculations. In the older work by Aston *et al.* (1946) the torsional potential function was treated according to the method of Pitzer and Gwinn (1942). The potential parameters $V_{0,t}$, $V_{0,c}$, ΔE_0°, and n_{cis} ($1/n_{trans} = 1 - (1/n_{cis})$ of the formulas

$$V(\theta) = \tfrac{1}{2}V_0(1 - \cos n\theta) + \Delta E_0^\circ \tag{12}$$

were simultaneously adjusted to reproduce the entropy and specific heat data. The resulting potential is shown in Fig. 11. The energy difference between the s-cis and s-trans forms ΔE_0° was found to be 2.43 kcal/mol. Correction for the zero-point difference calculated from the resulting potential reduces this to 2.30 kcal/mol. The barrier energy was determined to be 5 kcal/mol.

The zero-point correction used by Aston *et al.* is probably considerably too large. The value they used of 0.125 kcal/mol may be compared to the value of 0.037 kcal/mol calculated from spectroscopic data of Carreira (1975).

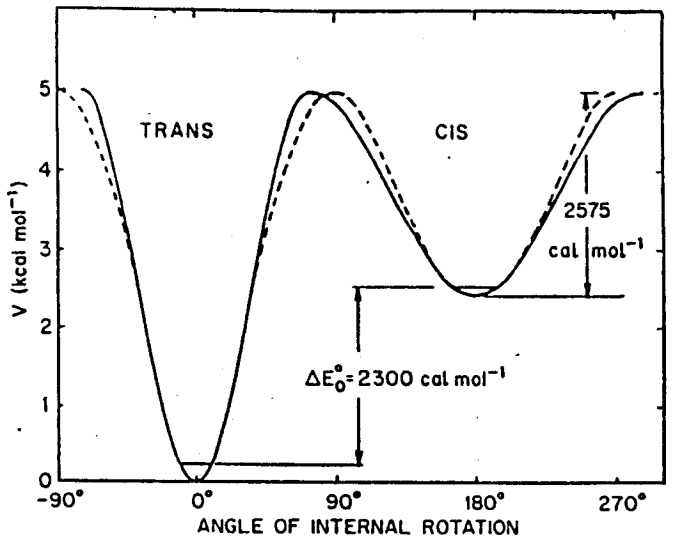

Fig. 11. The potential energy surface of butadiene as determined from an analysis of thermodynamic data (Aston *et al.*, 1946).

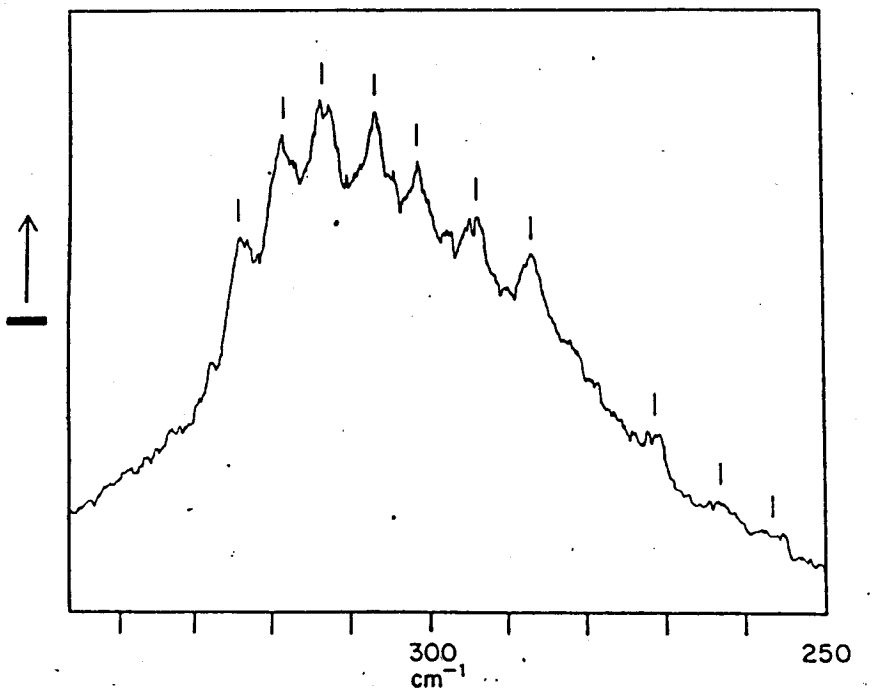

Fig. 12. The Raman spectrum of butadiene in the torsional mode overtone region (Carreira,

The approach used by Compton *et al.* in their analysis of the same thermodynamic data was quite different. They began with the relatively accurate entropy data. The difference between the observed entropy and that calculated for the s-trans isomer is dominated by the entropy of mixing. This permits a determination of the mole fraction of the s-cis isomer with reasonable independence from the assumptions of the statistical thermodynamics. Using the resulting value for the mole fraction of the s-cis isomer, it is possible to calculate the observed heat capacity by varying only the s-cis, s-trans zero-temperature enthalpy difference. The value obtained in this way was 2.49 kcal/mol. Since this is a zero-degree enthalpy difference, it includes the zero-point correction.

The study by Carreira (1975) is based on the Raman spectrum shown in Fig. 12. This band is identified as the set of overtone transitions of the a_u symmetry torsional vibration. The association of the labeled peaks of Fig. 12 with particular torsional transitions can be seen by reference to Fig. 13. The seven transitions at the left are associated with the s-trans conformer, while the three at the right are assigned to the s-cis conformer. The frequencies of the first four s-trans transitions are in excellent agreement with the values deduced from infrared studies. There can be no doubt as to their assignment.

A torsional potential function of the form

$$V(\theta) = \sum_{i=1}^{4} \tfrac{1}{2} V_i (1 - \cos i\theta) \tag{13}$$

was adjusted to reproduce the observed transitions. This is a four-parameter fit to ten data points. The calculated variation in the reduced mass as a

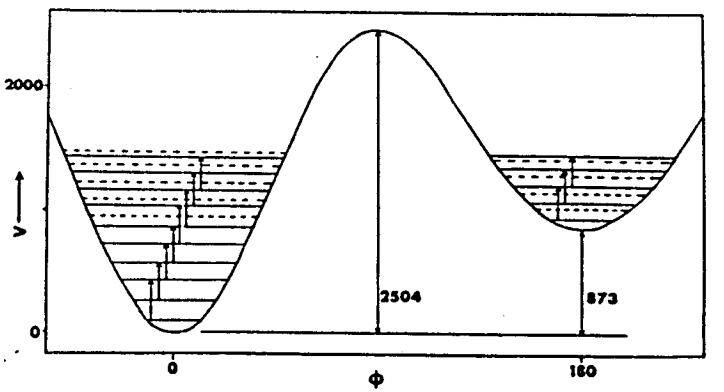

Fig. 13. The potential surface of butadiene as determined from an analysis of the Raman spectrum of Fig. 12. Energies are given in cm^{-1}. The seven lowest transitions marked for the trans minimum and the three for the cis correspond to the marked peaks in Fig. 12 (from Carreira, 1975).

unction of θ was included in the analysis. The resulting function has minima it 0° and 180° with the 180° conformation having higher energy. The energy difference obtained in this way was 2.50 kcal/mol, in excellent agreement with the values of 2.43 and 2.49 kcal/mol from the thermodynamic analysis. The barrier height of 7.15 kcal/mol is considerably higher than the 5 kcal/mol value of Aston *et al.* (1946). This difference is probably a reflection of the different functional forms chosen.

The NMR approach to this problem (Lipnick and Garbisch, 1973) is based on the determination of the temperature dependence of the chemical shift difference δ_{AB} for 2,3-dideuterio-1,3-butadiene:

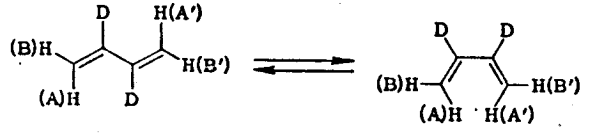

and the coupling constant $J_{CC'}$, for 1,1,4,4-tetradeuterio-1,3-butadiene:

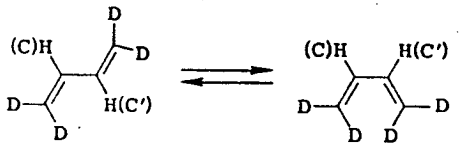

The interconversion rate between the two conformers is very rapid compared to the NMR time scale so that each of these quantities is a weighted average of the values for each conformer. The temperature dependence of these quantities can therefore be related to the ΔH and ΔS values associated with the conformational equilibrium and the four limiting values $(\delta_{AB})_{cis}$, $(\delta_{AB})_{trans}$, $(J_{CC'})_{cis}$, and $(J_{CC'})_{trans}$. The NMR data was collected for liquid butadiene over the temperature range from −103° to +112°C. The two data sets $\delta_{AB}(T)$ and $J_{CC'}(T)$ were not sufficient to determine all six of the above parameters. Therefore, ΔS was fixed on the basis of one of two alternative models as discussed below. The resulting values of ΔH were 2.05 and 2.15 kcal/mol depending on which model was used to evaluate ΔS. These values are somewhat lower but are comparable to those discussed above.

The two models used by Lipnick and Garbisch, Jr. to evaluate the value of ΔS correspond to (a) $\Delta S = 0$ and (b) $\Delta S = R \ln 2 = 1.376$ eu. These are estimates of the entropy differences expected for the case where there is a single planar s-cis isomer (case a) and the case where there are two equal-energy skewed *gauche* isomers. The possibility that the s-cis conformer potential surface has two skew-conformer minima is a reasonable possibility because of the nonbonded interactions between the internal hydrogens in

the planar s-cis geometry. A slight skewing is certainly to be expected unless the π-electron interactions are sufficiently strong that planarity is imposed, probably with an associated outward splay deformation of the molecule. Calculations indicate that the planar geometry has the lowest energy (e.g., Radom and Pople, 1970). Experimental evidence on this point is fairly meager. Lipnick and Garbisch, Jr. concluded in favor of the skewed geometry. Their argument was based on the fact that the derived vicinal 2,3 proton–proton coupling constant for the minor form $(J_{CC'})_{cis}$ depends on the value chosen for ΔS (1.03 Hz for planar s-trans, 5.10 Hz for skewed gauche) and only the higher value corresponds to values obtained for related compounds with planar or 20° skewed geometries ($J = 5.1$–6.5 with skewed values corresponding to the lower end of the range). On the other hand, Compton *et al.* (1976) conclude in favor of a planar s-cis conformation. The basis for this conclusion is in part the experimental value of ΔS, which is closer to the value expected for the single excited s-cis conformation, and a related observation that the hypothesis of two excited conformations in the determination of the entropy of mixing results in a value of ΔH which is not in agreement with that determined by Carreira. This conformational question concerning the planarity of the nontransoid isomer of butadiene is basically undecided at the present time although the weight of evidence is in favor of the planar s-cis geometry. Indirect support for this can be deduced from the values of the potential terms obtained in Carreira's analysis of the vibrational spectrum. If the potential function [Eq. (13)] is truncated to include the first three terms (V_1, V_2, and V_3) then if $4V_2 > V_1 + 9V_3$, the s-cis conformer will have a minimum energy at $\theta = 180°$ (planar). If $4V_2 < V_1 - 9V_3$, there will be a local maximum at 180°. The values obtained by Carreira are $V_1 = 1.72$, $V_2 = 5.91$, and $V_2 = 0.78$ kcal/mol, so $4V_2 = 23.61$ is much greater than $V_1 + 9V_3 = 8.74$. Hence the potential (Fig. 13) has a minimum at 180°.

An interesting and more general aspect of polyene conformational equilibria is that substitution of butadiene position 2 by a methyl group has a significant effect on the s-cis isomer content. Compton *et al.* (1976) have determined that the s-cis isomer of isoprene has an energy relative to the s-trans state of only 1.1 kcal/mol, less than half the value for butadiene. The reason for this difference is that rotation about the central C—C bond in isoprene results in the interchange of one unfavorable steric interaction by another. The result of this change in energy is that at room temperature there is roughly 2.8% of the s-cis isomer expected for butadiene but 11% of the s-cis form for isoprene.

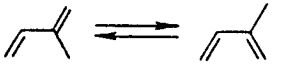

The Raman data in Fig. 12 is the only direct observation of the s-cis isomer of butadiene. There have been several reports of unsuccessful attempts to detect this isomer, including a study by microwave spectroscopy (Lide, 1962) and electric-beam focusing (Novick *et al.*, 1973). This electric-beam-focusing experiment has recently been repeated using an oven temperature of 300°C (Tom Dyke, private communication). At that temperature at least 20% of the population should be in the s-cis form. Again, however, no polar forms were detected. Lide estimated that with the expected dipole moment of roughly 0.4 D it should have been possible to detect the s-cis isomer if it had been present at a mole fraction of 2% or more. The concentration estimated by Compton *et al.* at 298 K is 2.8%. Lide points out that if the s-cis isomer had been nonplanar (*gauche*), it might then have escaped detection because its resonances might have been outside the region searched. The failure of the electric-beam-focusing experiment to detect any dipolar species is not dependent on the detailed geometry of the non-trans form. The failure of these two experiments to detect any polar species could, of course, be due to a particularly small value of the dipole moment. Lide's estimate of 0.4 D was based on the known values for cyclopentadiene and propene. It is interesting to note that if s-cis butadiene had 120° bond angles, then the contribution of the C—H bond vectors to the dipole moment would vanish. Thus, to a first approximation, the only contribution to the dipole moment comes from the C—C double-bond moments, which are expected to be very small.

VI. Polyene Vibrational Spectroscopy and Force Fields

An all-trans polyene with N double bonds has vibrational species given by

$$\Gamma = (4N + 1)a_g + 2Na_u + (2N - 1)b_g + 4Nb_u \qquad (14)$$

The a_g and b_u modes are in-plane, whereas the a_u and b_g modes are out-of-plane. The a_u and b_u modes are active in infrared spectra, whereas the a_g and b_g modes are Raman active. The b_g modes are depolarized ($\rho = 3/4$), and the totally symmetric a_g modes are polarized ($0 < \rho < 3/4$). The general overall linear structure of the polyene chromophore and in particular the low energy of the strongly allowed transition to the ^1B_u state, causes the depolarization ratio to be near 1/3 ($0.2 < \rho < 0.4$) for the a_g modes (Diamond, 1978).

For *cis*-hexatriene the C_{2v} selection rules permit the $13a_1$ vibrations to be both Raman and infrared active. This is also the case for the $12b_1$ modes and the $5b_2$ modes. The $6a_2$ modes are only Raman active. The a_1 and a_2 modes are in plane, whereas the b_1 and b_2 modes are out of plane.

TABLE 4

THE VIBRATIONAL NORMAL MODES OF BUTADIENE[a]

Normal Mode Symmetry, Number, and Type			IR (cm^{-1}) (Gas)	Raman (cm^{-1}) (Solid)	Normal Mode Symmetry, Number, and Type			IR (cm^{-1}) (Gas)	Raman (cm^{-1}) (Solid)
a_g	ν_1	CH_2 a-stretch	ia	3087 M	b_g	ν_{14}	CH bend	ia	976 W
	ν_2	CH stretch	ia	3003 M		ν_{15}	CH_2 wag	ia	912 S
	ν_3	CH_2 s-stretch	ia	2992 S		ν_{16}	CH_2 twist	ia	770 VW
	ν_4	C=C stretch	ia	1630 VS	b_u	ν_{17}	CH_2 a-stretch	3100.6 S	ia
	ν_5	CH_2 s-cis	ia	1438 S		ν_{18}	CH stretch	3054.9 S	ia
	ν_6	CH bend	ia	1280 S		ν_{19}	CH_2 s-stretch	2984.3 S	ia
	ν_7	C—C stretch	ia	1196 S		ν_{20}	C=C stretch	1596.0 S	ia
	ν_8	CH_2 rock	ia	894 W		ν_{21}	CH_2 s-cis	1380.7 W	ia
	ν_9	CCC deform	ia	512 S		ν_{22}	CH bend	1294.3 W	ia
a_u	ν_{10}	CH bend	1013.4 VS	ia		ν_{23}	CH_2 rock	989.7 M	ia
	ν_{11}	CH_2 wag	907.8 VS	ia		ν_{24}	CCC deform	300.6 VW	ia
	ν_{12}	CH_2 twist	522.2 M	ia					
	ν_{13}	C—C torsion	162.3 VW	ia					

[a] From Shimanouchi (1972). W = weak, M = medium, S = strong, V = very.

Reasonably complete vibrational spectroscopic information is available for butadiene (Richards and Nielsen, 1950; Harris, 1964; Abe, 1970; Shimanouchi, 1972), including data for four deuterated species (Abe, 1970) (Table 4). The low-frequency vibrations of butadiene and two of its symmetrical deuterated derivatives have been studied at high resolution by Cole *et al.* (1973). These authors point out an interesting relationship between the in-plane bend (ν_{24}) with b_u symmetry and the torsional mode (ν_{13}), which has a_u symmetry. These modes occur at 300 and 163 cm^{-1} for C_4H_6; for the hypothetical linear species these two modes would be degenerate. This may be related to the strong Coriolis interaction observed for these two modes (Cole *et al.*, 1973).

The vibrational spectroscopy of 1,3,5-hexatriene in both its trans and cis isomers has been studied by Lippincott *et al.* (1959) and Lippincott and Kenney (1962). Their data are shown in Table 5. Similar data are available for 1,3,5,7-octatetraene (Lippincott *et al.*, 1959) (Table 7).

For *trans*-hexatriene the modes are $13a_g + 6a_u + 5b_g + 12b_u$. Table 5 lists all of these modes of each symmetry except for one a_u low-frequency vibration. For octatetraene there are $17a_g + 8a_u + 7b_g + 16b_u$ modes. Table 7 shows that 11 of the $17a_g$ modes have been tentatively identified as having 5 of the $8a_u$ modes, 6 of the $7b_g$ modes, and 14 of the $16b_u$ modes. Many of the missing modes undoubtedly are absent because of accidental degeneracies. Some are at very low frequencies, however, particularly for octatetraene and have not yet been detected. The normal-mode calculations discussed below and also consideration of the behavior expected for certain modes as a function of chain length indicates that many of the low-frequency modes are, in fact, misassigned for hexatriene and octatetraene and that they are actually at lower values than those suggested.

Vibrational data, including Raman depolarization ratios, are also available for several simple substituted polyenes. Examples include the dimethyl tetraene decatetraene (Andrews, 1978) and the diphenylpolyenes with one to four double bonds (Diamond, 1978). The extensive studies of the more complex retinyl polyenes will not be discussed here. For recent accounts of this work see Callender and Honig, 1977.

There have been several recent theoretical treatments of the vibrations of polyenes (Popov and Kogan, 1964; Tric, 1969; Gavin and Rice, 1971; Warshel and Karplus, 1972a; Inagaki *et al.*, 1975; Lasaga *et al.*, 1980). The treatment of Inagaki *et al.* (1975) is a classical modified Urey–Bradley-type force field treatment. The force field parameters were adjusted to fit Raman data for β-carotene or poly(acetylene). The calculations were actually carried out for an infinite chain consisting of the repeating unit $(CH{=}CH)_n$. Only the in-plane motions were calculated. This results in the eight dispersion curves shown in Fig. 14. The poly(acetylene) data is compared to the $\delta = 0$

TABLE 5

THE VIBRATIONAL FREQUENCIES OF THE CIS AND TRANS ISOMERS OF 1,3,5-HEXATRIENE*

Γ	#	$\bar{\nu}$ (cm^{-1})	*trans*-Hexatriene
a_g	1	3085 m	CH_2 antisymmetric stretch
	2	3054 mw	Vinyl CH stretch
	3	3054 mw	trans CH stretch
	4	2989 s	CH_2 symmetric stretch
	5	1623 vs	C=C in-phase stretch
	6	1573 s	C=C out-of-phase stretch
	7	1394 m	CH_2 scissors
	8	1280 m	Vinyl CH in-plane bend
	9	1245 w	C—C stretch
	10	1187 vs	trans CH in-plane bend
	11	1128 m	CH_2 in-plane bend
	12	444 mw	Terminal angle in-plane bend
	13	347 mP	Center angle in-plane bend
a_u	14	1011 s	CH_2 twist
	15	941 m	trans CH out-of-plane bend
	16	899 s	CH_2 wag
	17	658 s	Vinyl CH torsion
	18	475 m	Skeletal
	19		Skeletal
b_g	20	990 mw	CH_2 out-of-plane twist
	21	928 m	trans CH out-of-plane bend
	22	897 m	CH_2 wag
	23	758 w, b	Vinyl CH torsion
	24	395 w	Skeletal
b_u	25	3091 s	CH_2 antisymmetric stretch
	26	3040 s	Vinyl CH stretch
	27	3012 s	trans CH stretch
	28	2953 s	CH_2 symmetric stretch
	29	1623 vs	C=C stretch
	30	1429 s	CH_2 scissors
	31	1294 s	Vinyl CH bend
	32	1255 m	CH_2 rock
	33	1166 m	trans CH bend
	34	1130 s	C—C stretch
	35	590 m	Terminal angle bend
	36	540 s	Center angle bend

* w = weak, m = medium, s = strong, v = very, b = broad, P = polarized.

(continued)

TABLE 5 (*continued*)

Γ	#	$\bar{\nu}$ (cm^{-1}) Raman[b]	$\bar{\nu}$ (cm^{-1}) IR[b]	*cis*-Hexatriene
a_1	1	3097	3110	CH_2 antisymmetric stretch
	2	3030	3050	Vinyl CH stretch
	3	3015		cis CH stretch
	4	3015		CH_2 symmetric stretch
	5	1622		In-phase C=C stretch
	6	1570	1560	Out-of-phase C=C stretch
	7	1392	1395	CH_2 scissors
	8	1314	1315	Vinyl CH in-plane deform
	9	1182	1185	cis CH in-plane deform
	10	1136		CH_2 rock
	11	1083		C—C stretch
	12	393		Skeletal (terminal angle)
	13	167		Skeletal (center angle)
a_2	14	978		CH_2 twist
	15	902		CH_2 wag
	16	883		cis CH out-of-plane deform
	17	709		Vinyl CH torsion
	18	331		Skeletal (terminal angle)
	19	264		Skeletal (center angle)
b_1	20	3097	3110	CH_2 antisymmetric stretch
	21		3080	cis CH stretch
	22	3030	3050	Vinyl CH stretch
	23		3050	CH_2 symmetric stretch
	24		1612	C=C stretch
	25	1448	1449	CH_2 scissors
	26		1280	Vinyl CH in-plane deform
	27	1141	1148	cis CH in-plane deform
	28	1141	1148	CH_2 rock
	29	947	950	C—C stretch
	30	479		Skeletal (terminal angle)
	31	243		Skeletal (center angle)
b_2	32	978	990	CH_2 twist
	33	902	910	CH_2 wag
	34		818	cis CH in-plane deform
	35		589	Vinyl CH torsion
	36	357	358	Skeletal (terminal angle)

[b] From Lippincott and Kenney (1962).

points of this curve. For the finite β-carotene chain, a value of $\delta = \pi/10$ is used, corresponding to an excitation with a wavelength such that $\lambda/2 = n + 1$ for $n = 9$ (the polyene part of β-carotene). Extension of this use of an infinite-chain-dispersion curve to the case of finite polyene chains leads to the general

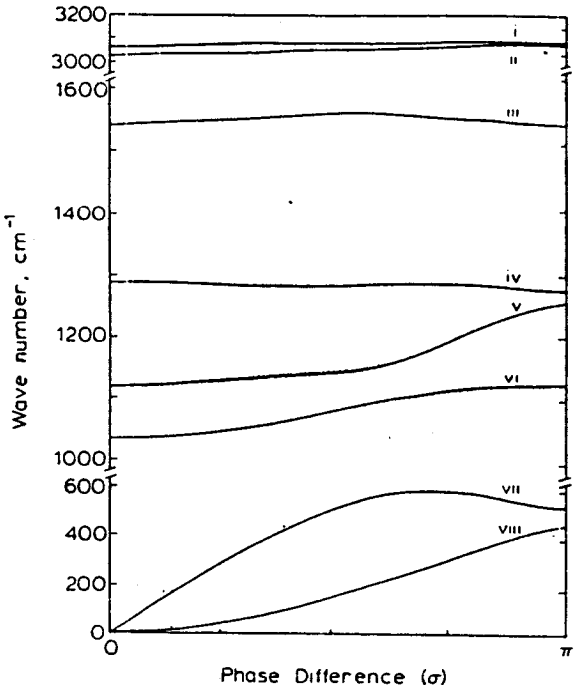

Fig. 14. Dispersion curves for the vibrations of a polyene chain (from Inagaki *et al.*, 1975).

form for a chain of n units

$$\nu_{k,m} = \nu_k(\delta_m), \qquad \delta_m = m\pi/(n+1), \quad m = 1, 2, 3, \ldots, n \tag{15}$$

where k labels the dispersion curve ($k = 1, 2, \ldots, 8$) and m labels the number of half-wavelengths corresponding to the entire chain. The modes with $m = 1$ are expected to have the largest Raman intensity. Note that if the dispersion curve is flat (e.g., for curve III and IV), then a group of modes will have the same value for a given molecule (independent of m) and this will not depend on chain length (independent of n). This aspect of this calculation, which is not in agreement with experiment, is dealt with by the authors by letting the two chain carbon–carbon force constants be different for the two systems in question, i.e., the curves shift with a change in length. The resulting force fields are shown in Table 6. Set I refers to the poly(acetylene) case and set II to the β-carotene case. It is not stated how the parameters of these force fields were adjusted to fit the experiments, and only four comparisons are made with experiment for each force field (branches III–VI). Therefore, it is not clear to what extent this force field is unique. However, there are some features of this force field which make it of interest. First, if we compare the carbon–carbon stretching constants for the infinite

TABLE 6

POLYENE FORCE CONSTANTS[a]

Force constant	Set I	Set II	Force constant	Set I'	Set II'
Urey–Bradley type[b]:			Non-Urey–Bradley type[c]:		
K(C—C)	3.90	3.60	f(C—C)(C=C)	0.50	0.30
K(C=C)	5.50	6.20	f(C—C)(C—C)	−0.10	−0.10
K(C—H)	4.54	4.54	f(C=C)(C=C)	−0.46	−0.46
H(C—C=C)	0.30	0.30	f(H—C=C)(C=C—H)	0.07	0.07
H(H—C=C)	0.15	0.15	f(H—C—C)(C—C—C—H)	0.06	0.06
H(H—C—C)	0.16	0.16			
F(C—C=C)	0.35	0.35			
F(C—C—H)	0.42	0.42			
F(C=C—H)	0.52	0.52			

[a] As determined by Inagaki *et al.* (1975).

[b] In units of md $Å^{-1}$. $F = -0.1$. For general information about the Urey–Bradley force field, see Shimanouchi (1949).

[c] These constants are added to the off-diagonal element in the F matrix. Units are md · $Å^{-1}$ for the stretching–stretching and md · Å rad^{-2} for the bending–bending cross terms.

(set I) and finite (set II) cases, we find that the single-bond force constant increases and the double-bond force constant decreases as the chain length increases.

The other feature of interest is the magnitude and sign of the carbon–carbon bond interaction terms. These are as large as 10% of the diagonal terms. The fact that the interaction between adjacent single and double bonds is positive while those for next-nearest neighbor single bonds f(C—C)(C—C) and double bonds f(C=C)(C=C) are negative is also of interest. This can be rationalized by a version of the valence hybrid argument first proposed for benzene by Scherer and Overend (1961; see Ziegler and Hudson, 1981). This argument, as applied to linear polyenes, considers these species to be combinations of the covalent resonance structures shown here, with the

first structure being the major contributor to the ground state. If we focus on the left terminal double bond, we see that stretching this bond will increase the contribution of the first of the two right-hand structures. This will make it more difficult to stretch the neighboring "single" bond because it has an increased double-bond character. This corresponds to a fairly large positive neighboring-bond-interaction force constant. The same argument applies to stretching either of the single bonds. However, if the terminal double bond is stretched, the central double bond will become weaker due to the increased contribution of these "long-bond" covalent structures. As a result, stretching the terminal double bond will make it easier to stretch the central double bond, giving rise to a negative interaction coefficient. A similar argument applies to the single bonds.

The force field developed by Popov and Kogan (1964) for butadiene and hexatriene includes a C=C diagonal term which is 15% smaller than the value for ethylene and other dienes and a C—C diagonal term which is 50% higher than that for the single bonds of propylene and isobutylene. The relative magnitude of these numbers is consistent with the observed bond lengths. These authors also propose a large negative double-bond interaction constant (13% of the double-bond diagonal term) and a smaller (positive) interaction between double and single bonds.

Tric (1969) performed a calculation for an infinite chain (cyclic boundary conditions) neglecting the interactions between bonds and fixing the hydrogen atoms so that they move with the carbons. These are very severe assumptions.

The approach of Gavin and Rice (1971) and Warshel and Karplus (1972a) is quite different from that of the previously discussed workers since they

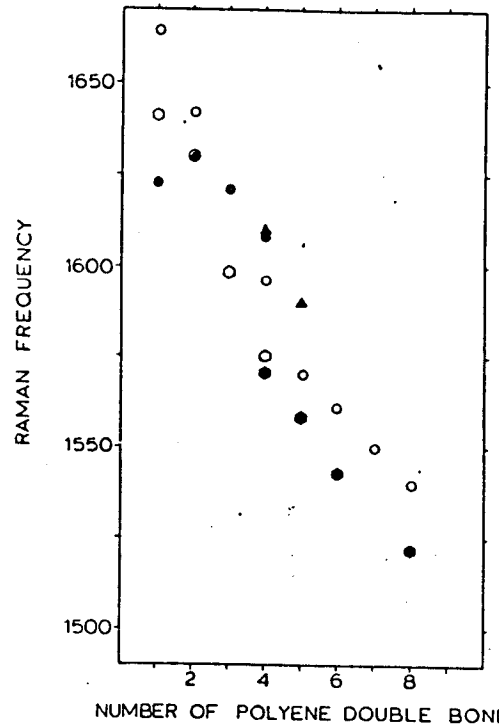

Fig. 15. The frequency of the strongest Raman active mode of several types of linear polyenes: ○, dicarboxylic acid dimethyl ester polyenes; ●, unsubstituted polyenes; ▲, dimethylpolyenes; ⬡, ⬢, diphenylpolyenes in solution (open hexagons) and solid form (solid hexagons).

attempt to incorporate a theory of the π-electron structure of polyenes into the determination of the carbon–carbon force constants. Gavin and Rice use expressions due to Coulson and Longuet-Higgins (1948) to relate diagonal and off-diagonal force constants to bond orders, "self-polarizabilities," and, for the off-diagonal elements, "mutual polarizabilities" of the carbon–carbon bonds. These were obtained from simple Hückel and extended Hückel theory. These calculations result in smaller bond orders, and therefore smaller force constants, for the double bonds in the center of the polyene chain. The opposite effect is observed for the single bonds. The interaction force constants used by Gavin and Rice, derived from these π-electron MO arguments, are positive for nearest neighbor interactions. The "non-nearest-neighbor" interactions are small and *positive*.

The strongest line in the Raman spectra of linear polyenes decreases in frequency as the length of the polyene chain increases (Rimai *et al.*, 1973) (Fig. 15). The origin of this trend is one of the important themes of polyene

vibrational spectroscopy. As noted above, Inagaki *et al.* (1975) account for this behavior by simply adjusting the diagonal force constant values as the chain length changes.

Popov and Kogan (1964) also modify their force constants slightly in going from butadiene to hexatriene, but they argue that agreement with experiment is satisfactory even without this adjustment and that the changes in the observed frequency are due to purely kinematical factors rather than changes in conjugation. However, Gavin and Rice claim that the force-constant set of Popov and Kogan leads to an *increase* in the Raman active double-bond stretch frequency as the chain length increases. In their calculations (Gavin and Rice, 1971) the force constants for the double bonds decrease slightly as the chain length increases, whereas the single-bond force constants increase slightly. The more interesting trend, however, is that for longer polyenes the double bonds toward the middle of the chain are weaker than the terminal bonds.

The treatments by Warshel and Karplus (1972a) and Lasaga *et al.* (1980) are comprehensive and systematic treatments of the potential surface of conjugated systems based on an empirical σ-framework potential function and a semiempirical (PPP–CI) treatment of the π-electron contributions. The treatment of Lasaga *et al.* includes doubly excited configurations in the CI calculation. These authors note that the admixture of doubly excited configurations with the Hartree–Fock ground state will mix in the covalent long-bond C—C=C—C structures which are dominant in the low-lying excited A_g state. These are the resonance structures needed to introduce negative next-nearest neighbor bond interactions as discussed above. Comparison of the results of calculations using single CI with those of double CI shows that the inclusion of double excitations considerably lowers the frequency of the highest energy Raman-active double-bond-stretching vibration and also that it introduces the proper decrease of this vibrational frequency with chain length. Thus, there may be a connection between the extent of configuration interaction and an observable ground-state property.

Table 7 includes the results of two normal-mode calculations for 1,3,5,7-octatetraene for comparison with the available data. The two calculations are in reasonable agreement with each other and with the experimental results. Even better agreement with experiment is found in the work of Lasaga *et al.* (1980). An exception is the lowest frequency b_u mode where the assigned experimental value is clearly too high. The eigenvectors for this and other low-frequency modes are discussed later (Section VII,I). Also, the experimental basis for the assignment of a b_g mode at 223 cm^{-1} is not clear since it is stated (Lippincott *et al.*, 1959) that the Raman spectrum has only a very weak, broad bank at 223 cm^{-1} which may be the overlapping 164-cm^{-1} b_g and 242-cm^{-1} a_g modes. The totally symmetric (a_g) modes in

TABLE 7

VIBRATIONAL DATA AND CALCULATED FREQUENCIES FOR 1,3,5,7-OCTATETRAENE

expt[a]	GR[b]	CFFπ[c]	expt[a]	GR[b]	CFFπ[c]	expt[a]	GR[b]	CFFπ[c]
a_g (In-plane)			a_u (Out-of-plane)			b_u (In-plane)		
3090	3107	3095	1007	1000	1080	3070	3017	3099
—	3029	3082	954	964	1021	3009	3021	3089
—	3016	3079	897	915	951	—	3014	3063
—	3010	3078	839	822	948	2988	3007	3063
3005	2986	2988	816	597	625	2955	2986	2988
1612	1635	1658	—	237	241	—	1607	1655
1608	1595	1625	—	164	166	1631	1575	1583
1432	1378	1441	—	65	63	1405	1374	1426
1304	1328	1361				1279	1310	1345
—	1322	1326	b_g (Out-of-plane)			1229	1295	1305
1285	1271	1301				1179	1244	1265
—	1223	1199	1080	992	1064	1138	1117	1187
1187	1120	1168	958	939	979	1096	915	933
1138	966	955	905	913	871	649	594	600
546	535	593	883	871	840	627	401	450
353	362	337	722	610	631	565	94	106
242	231	264	223	319	322			
			164	156	153			

[a] Experimental values from Lippincott *et al.* (1959) except for the a_g and b_g modes in italics which are from a Raman spectrum obtained by G. Holtom (G. Holtom, W. M. McClain, and B. Kohler, unpublished).

[b] GR, Gavin and Rice (1971).

[c] The results of a CFFπ calculation as described by Warshel and Karplus (1972a) and Hudson and Andrews (1979).

the 1700–1000 cm^{-1} region are of particular interest because some of them are strongly active in the low-lying electronic transitions. The strongly Raman active modes at 1612 and 1608 cm^{-1} correspond to those calculated to be at 1635–1658 and 1595–1625 cm^{-1}. Lasaga *et al.* (1980) calculate these modes to be at 1617 and 1604 cm^{-1}. The eigenvectors from the CFFπ calculation show that the higher frequency mode of this pair (ν_6) is a mixture of carbon–carbon bond stretching and HCC angle bending. The formal double bonds dominate the carbon–carbon bond-stretching component, and the phase of the single-bond component is opposite to that for the double bonds so that one contracts when the other expands. The double-bond stretches are themselves in phase. The form of this normal coordinate closely parallels what we would expect to be the change of bond lengths associated with electronic excitation. The "1608-cm^{-1}" mode (ν_7) has a much smaller single-bond component and has a change of phase between the terminal

and inner double bonds. The modes calculated to be at 1441, 1361, 1326, and 1301 cm^{-1} are mostly angle-deformation modes. The modes at 1199 and 1169 cm^{-1} are primarily single-bond stretching modes, especially the one calculated to be at 1169 cm^{-1}. This mode has its largest amplitude at the central single bond, out of phase with the outer two single bonds, while the higher mode has in-phase single-bond displacements.

VII. Experimental Studies of Excited States

The following sections describe in more detail the current state of our experimental understanding of the excited states of linear conjugated polyenes. Sections VII,A–D deal with experimental techniques which have recently yielded information concerning polyene excitations. Sections VII,E–I are best described as "polyene spectroscopic phenomenology" and include accounts of many observations which are not yet fully understood. Section VII,J describes recent studies of higher states of polyenes and their triplet states.

A. High-Resolution One-Photon Absorption Spectroscopy

The first evidence for the existence of a forbidden polyene transition at an energy lower than the strongly allowed transition to the 1^1B_u state came from absorption and fluorescence studies of diphenyloctatetraene in *n*-alkane matrices and bibenzyl crystals at 4.2 K (Hudson and Kohler, 1972, 1973; see Fig. 16). For particular combinations of polyene and host matrix, these conditions produce well-resolved fluorescence spectra and absorption spectra with a series of sharp bands at an energy below that of the poorly resolved strong transition. The detection of absorption by fluorescence excitation is particularly helpful in these studies. The mechanism of the production of these sharp lines is discussed in Section VII,F.

These early experiments were performed using guest–host systems where the substituted polyene could not have a center of symmetry. As a result, the origin transition for the 1^1A_g–2^1A_g excitation is observable as an overlap between an absorption and an emission band. Presumably, progressions based on false origins are intermixed with series based on the crystal-field-induced origin in these spectra, but their analysis has not been vigorously pursued.

More recent studies of substituted and unsubstituted polyenes using this technique have progressed along two lines. On the one hand, there has been a pursuit of host crystal environments which provide a true centrosymmetric field for the guest molecule. Another theme has been the use of such spectra, even with noncentrosymmetric environments, for the determination of relative state ordering. Recent applications of this method include the work of

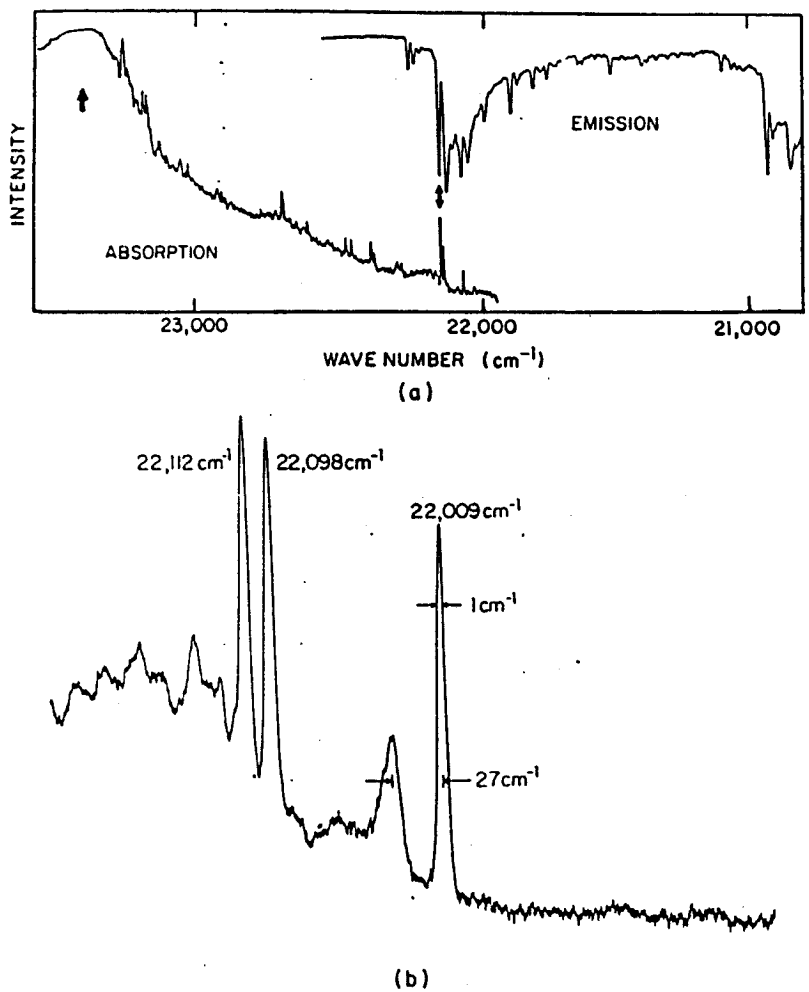

Fig. 16. High-resolution absorption and emission spectra of 1,8-diphenyloctatetraene in bibenzyl at 4.2 K. (a) Comparison of absorption and emission spectra. The origin of the strongly allowed absorption to the 1^1B_u state is indicated by an arrow at the left. (b) Expanded view of the absorption spectrum near the origin region (from Hudson and Kohler, 1973).

Hetherington (1976) on diphenylbutadiene and diphenylhexatriene (Fig. 17; see also Nikitina *et al.*, 1975, 1976, 1977), Andrews (1978) on 2,4,6,8-dodecapentaene (Fig. 18), and Auerbach *et al.* (1981) on 2,12-dimethyltridecahexaene (Fig. 19). The basis of this technique is that the series of sharp lines observed in the absorption spectrum where they are superimposed on a strong, broad continuum are also observed in rough reflection in the

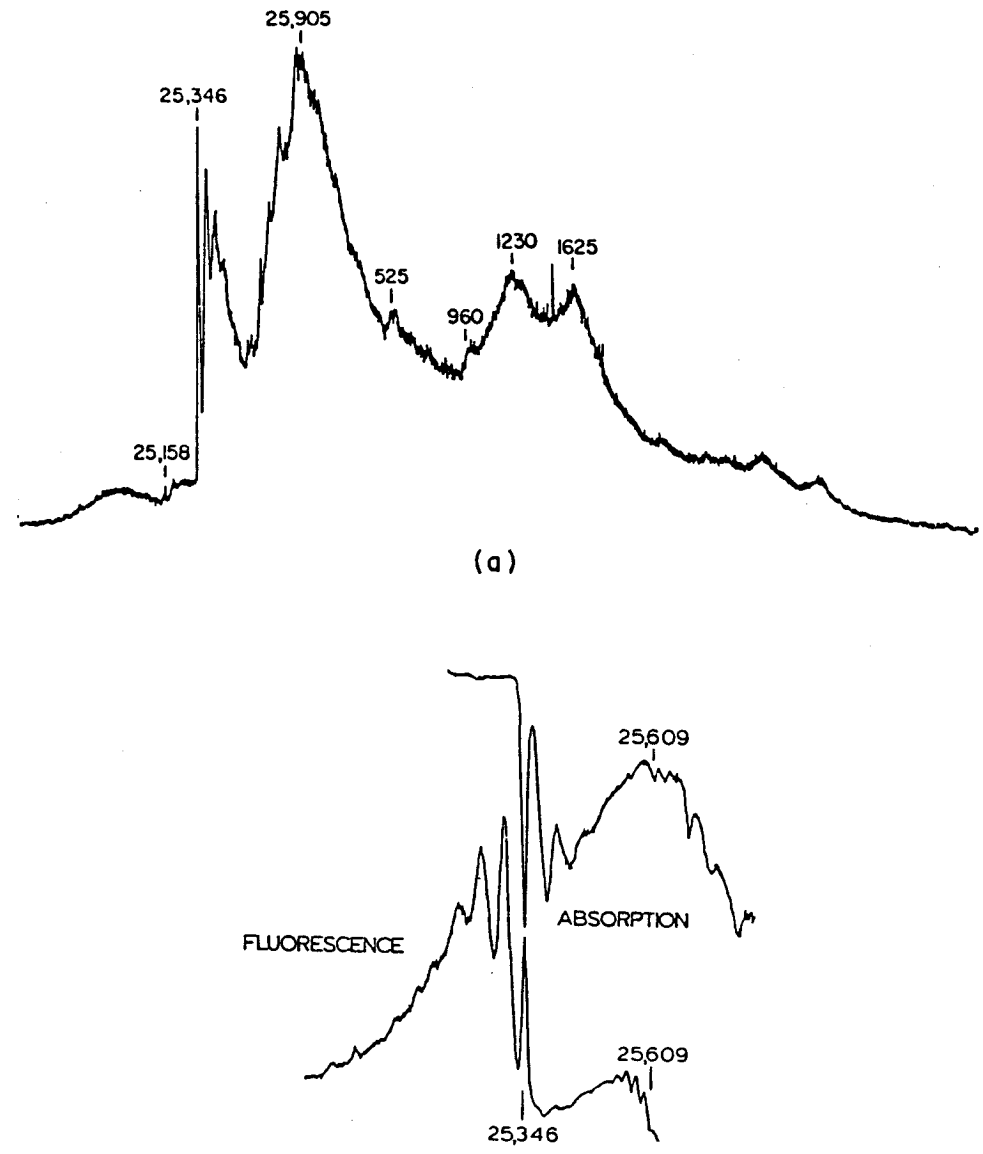

Fig. 17. High-resolution spectra of diphenylhexatriene in nonane at 4.2 K. (a) The absorption spectrum shows the origin of the transition to the 2^1A_g state at 25,346 cm^{-1} and to the 1^1B_u state at 25,905 cm^{-1}. The absorption spectrum actually rises at higher energy but is attenuated due to the lamp intensity decrease. (b) Expanded view of the origin region and a comparison of absorption and fluorescence (from Hetherington, 1976).

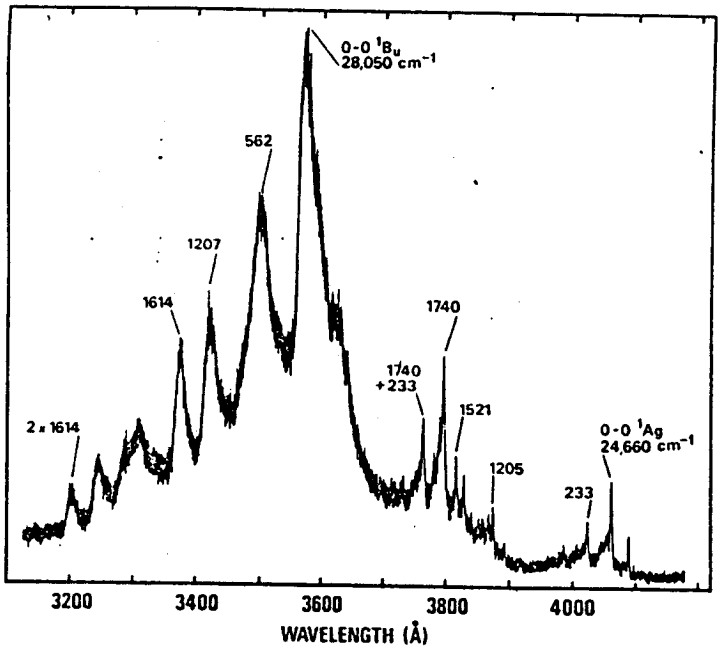

Fig. 18. The fluorescence excitation spectrum of dodecapentaene in undecane at 4.2 K. The sharp features between 4100 and 3700 Å are due to the 2^1A_g state, whereas those in the 3600–3200-Å region are due to the 1^1B_u state. The spectrum is attenuated at shorter wavelengths due to decreasing lamp intensity (Andrews, 1978).

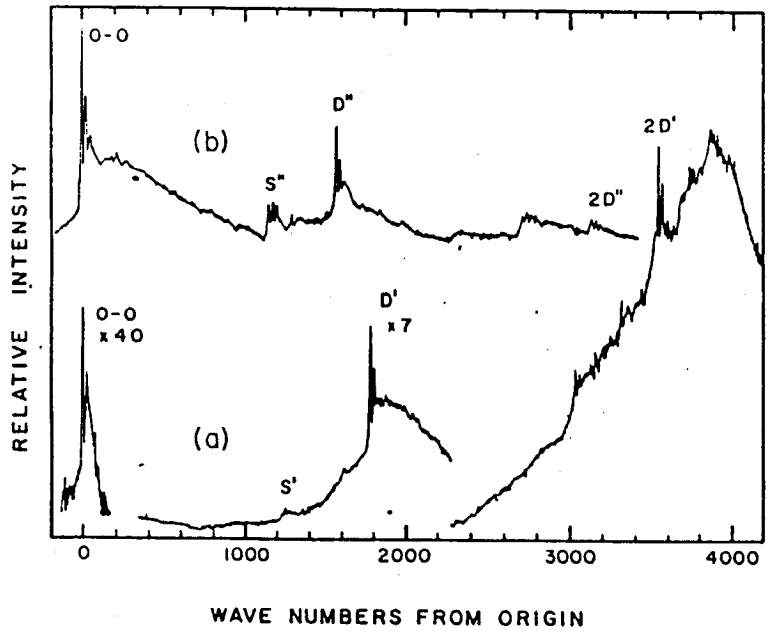

Fig. 19. The 4.2-K fluorescence excitation (a) and fluorescence (b) spectra of 2,12-dimethyltridecahexaene in a quickly grown *n*-undecane polycrystal. Both spectra have been

fluorescence spectrum without the broad continuum. Thus, the weak, sharp lines are associated with the emitting state, whereas the strong, broad bands must be associated with the higher ^1B_u state. This separation into two excited states is supported by radiative lifetime determinations and solvent-effect behavior. This combination of data has now been acquired for the diphenylpolyenes with 2, 3, and 4 polyene double bonds, and for several alkyl and unsubstituted tetraene, pentaene, and hexaene species.

For certain combinations of polyene guest and transparent host, it is found that more than one absorption or fluorescence excitation line overlaps a fluorescence line (Fig. 20). Selective excitation of one absorption transition near the origin results in a simplified emission spectrum with fewer spectral overlaps, perhaps only one. This identifies the multiple overlapping lines as being due to different guest–host packing arrangements or sites, as discussed in Section VII,F. The presence of multiple sites makes vibrational analysis difficult.

The search for a guest–host combination where the spectra reveal a true forbidden transition with a missing origin has been pursued with increasing success by Christensen and Kohler (1975, 1976) for 2,10-dimethylundecapentaene in nonane, by Andrews and Hudson (1978a) for decatetraene in undecane, and by Granville *et al.* (1979, 1980) for octatetraene in octane. In this last case the origin line is completely missing (Figs. 6 and 7). The promoting modes which result in false origins are b_u vibrations, including the lowest frequency in-plane bending mode which flexes the entire chain (Hudson and Andrews, 1979). These are discussed in more detail in Section VII,I.

It has been repeatedly demonstrated that a polyene which has a "forbidden" vibronic pattern in one *n*-alkane host, typically has an "allowed" pattern in other *n*-alkane hosts differing perhaps by only one or two carbon atoms. Some examples are shown in Fig. 36 (see Section VII,F.). This demonstrates the extreme sensitivity of this forbidden transition to small perturbations.

It has been suggested that some of the spectral features of polyenes are due to dimeric forms (Moore and Song, 1973a; Rosenberg, 1975). This objection might be applied to the low-energy sharp bands observed in mixed crystals. The possibility has been excluded by acquiring spectra at various concentrations with a variety of solvents and crystal or matrix preparation methods. Also, fluorescence excitation spectra are equivalent to absorption spectra, which would not be the case for a mixture of monomers and dimers unless they had the same quantum yield and similar emission spectra. Furthermore, no emission is observed to the blue of the origin line. If this were dimer emission, most of the monomer emission would be in this region. If the monomers were nonfluorescent, then the strong monomer transition would not be in the excitation spectrum. Finally, the one- and two-photon

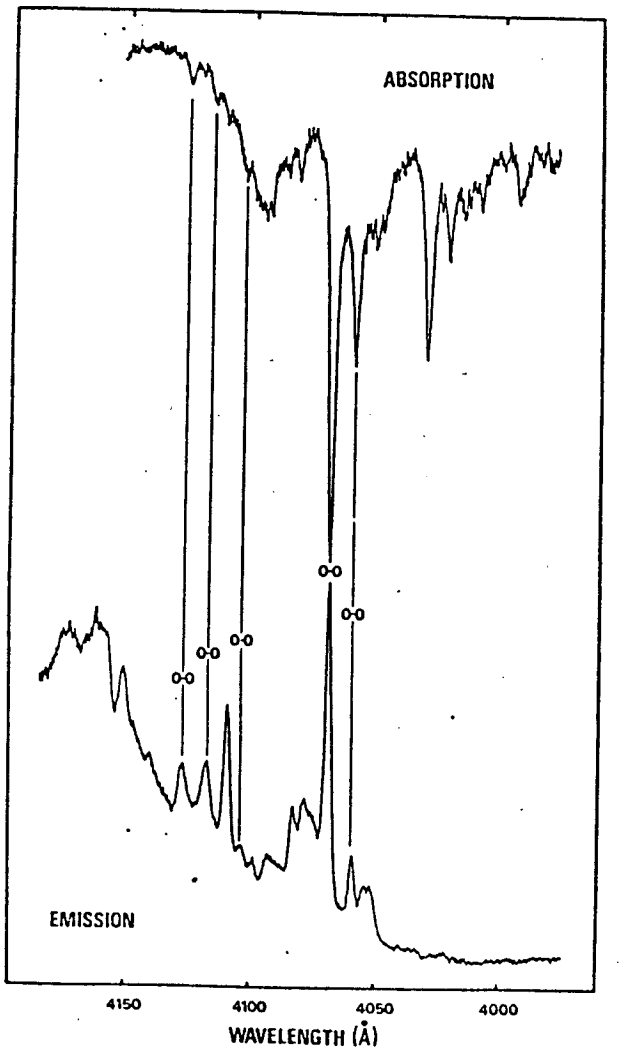

Fig. 20. The absorption and emission spectra of dodecapentaene in tridecane at 4.2 K showing multiple-site effects (Andrews, 1978).

comparison of Granville *et al.* (Fig. 7) for octatetraene in *n*-octane demonstrates that the weak low-energy lines are due to a system with inversion symmetry. The crystal lattice of *n*-octane is such that it is not possible to make a substitutional dimer with inversion symmetry.

Dimers have been observed for stilbene in a bibenzyl host (Hetherington and Hudson, 1979). The dimer spectrum is shifted to lower energy than the monomer by 773 cm^{-1}. Both the monomer and the dimer are fluorescent

and the dimer band goes away at high dilution, as expected. This dimer, at least, has none of the unusual properties which would have to be postulated in order to explain the observed high-resolution spectra on the basis of dimers.

B. Two-Photon Spectroscopy

As has been noted in Section III,A, the symmetry of the unsubstituted all-trans polyenes is such that the π-electron configurations are split into two groups: those of character B_u, which are connected to the A_g ground state by allowed one-photon processes but for which the corresponding two-photon processes are symmetry forbidden, and those of character A_g, for which the selection rules are just reversed. Thus, it is quite clear that the comparison of one- and two-photon spectra, particularly vibrationally resolved spectra, would be most useful in determining the properties of low-lying polyene singlet states. In 1973 Swofford and McClain reported the two-photon fluorescence excitation spectrum for *trans,trans*-1,4-diphenyl-1,3-butadiene in cyclohexane solution at room temperature. They were also able to estimate a two-photon cross section at 28,259 cm^{-1}, which was the lowest energy feature in this spectrum, of 1×10^{-50} cm^4 sec $photon^{-1}$ $molecule^{-1}$. This relatively large cross section is clearly indicative of a two-photon-allowed absorption process. Measurements of the polarization ratio were also in agreement with their assignment of this transition to an ^1A_g state located 200–600 cm^{-1} below the lowest energy ^1B_u state. This assignment is in complete agreement with the somewhat more resolved two-photon excitation spectrum for these molecules in EPA at 77 K reported by Bennett and Birge (1980). Holtom and McClain (1976) extended the measurements of two-photon excitation of fluorescence spectra to the longer diphenylpolyenes: diphenylhexatriene and diphenyloctatetraene. Again, significant cross sections for two-photon absorption to states below the lowest ^1B_u state were observed, although under the conditions of their experiments (room-temperature cyclohexane solutions) it was not possible to make unambiguous assignments. The diffuseness of these two-photon excitation spectra and the large difference in cross section between the onset of absorption and the band maximum was interpreted by these authors to signal a large geometry change in the excited ^1A_g state. By going to a rigid-glass matrix at 77 K, Fang *et al.* (1977, 1978) were able to obtain a considerable improvement in vibronic resolution and reported two-photon excitation of fluorescence spectra for diphenylhexatriene and diphenyloctatetraene.

Fang *et al.* (1977, 1978) found rough coincidence between the lowest energy feature in the two-photon excitation spectrum with the highest energy feature seen in the fluorescence spectra for both diphenylhexatriene and diphenyloctatetraene. Their spectra differ significantly from those obtained

in room-temperature solution by Swofford and McClain (1973) in that the intensity difference between the onset of two-photon absorption and the higher energy portions of the spectrum are not large. In fact, the vibronic development appears relatively simple and is consistent with minor displacements in the double- and single-bond stretching coordinates. A detailed study of the influence of the local environment on the vibronic development of these two-photon spectra would clearly add greatly to our understanding of both the free-molecule and molecule–host potential surfaces.

The bandwidths in both the room-temperature solution and rigid-glass spectra have not allowed a detailed comparison of the one- and two-photon absorption spectra. Granville *et al.* (1979) reported the first two-photon fluorescence excitation spectrum for an unsubstituted linear polyene (*trans*, *trans*-1,3,5,7-octatetraene) and were able to attain sufficient resolution to permit a detailed comparison of the vibrational development in each of the spectra. In their spectra, measured for octatetraene substituted in *n*-octane at 4.2 K, the origin was clearly seen to be one-photon forbidden and two-photon allowed (Granville *et al.*, 1979, 1980) (Fig. 7). This not only confirmed the ^1A_g assignment for the lowest singlet excited state but demonstrated that this state, in this centrosymmetric environment, was not distorted along any odd symmetry coordinate. In particular, their spectra rule out twisted

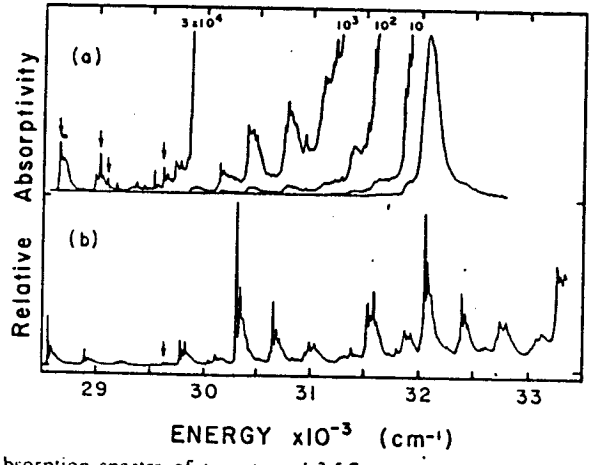

Fig. 21. Absorption spectra of *trans*,*trans*-1,3,5,7-octatetraene in *n*-octane at 4.2 K. (a) One-photon excitation. Arrows indicate the four false origins of the 2^1A_g state and the large peak at 32,100 cm^{-1} is the origin of the 1^1B_u state. (b) Two-photon excitation. The sharp peak at 28,561 cm^{-1} is the origin of the 2^1A_g state and the arrow indicates the weak feature assigned as two quanta of a promoting mode. For both spectra, the relative molar absorptivity is plotted against vacuum wave numbers (from Granville *et al.*, 1980).

(a_u distortion) excited-state geometries in this matrix. Furthermore, the strong transition to the ^1B_u state of the one-photon spectrum is missing in the two-photon spectrum, confirming the strict centrosymmetric nature of the guest in this host (Fig. 21).

To date, attempts to locate the excited ^1A_g state in the shorter, unsubstituted polyenes hexatriene and butadiene have not been successful. Since these molecules do not fluoresce, the fluorescence excitation technique is not available. Attempts to apply both photoionization (Parker *et al.*, 1976, 1978; Johnson, 1976) and thermal blooming (Twarowski and Kliger, 1977; Vaida *et al.*, 1978; Ziegler and Hudson, unpublished) to detect two-photon absorption to the lowest A_g valence state for these molecules have failed, although much has been learned about higher lying states. A major limitation of these techniques is that they require fluid solution or gas-phase samples and this results in poorly resolved spectra.

C. *Electron-Impact Spectroscopy*

Inelastic, variable-angle electron-impact spectroscopy can be a very valuable alternative to optical spectroscopic methods. Transitions to excited states which are forbidden by electric dipole or spin selection rules may be observed by this technique. For a review of results for polyatomic molecules see Kuppermann *et al.* (1979). An excellent brief review of the theory of inelastic electron scattering is given in Lassettre and Skerbele (1974).

Electron-impact spectra are obtained at considerably lower resolution than is typical for optical spectra. The highest resolution used in the spectra discussed below is 25 meV or 200 cm^{-1}. The overlapping intensity resulting from this relatively poor resolution and, more importantly for polyenes, from extreme spectral congestion, can be partially sorted out by obtaining spectra as a function of incident electron energy and scattering angle. For low-energy electrons (of the order of a few tens of electron volts), the angular dependence may be used to distinguish spin and electric dipole-allowed transitions from spin-forbidden (singlet–triplet) transitions (Kuppermann *et al.*, 1979). Spin-allowed but symmetry-forbidden transitions can produce a complex angular distribution such that the intensity as a function of scattering angle shows maxima and minima (Flicker *et al.*, 1978; Mosher *et al.*, 1975; Frueholz *et al.*, 1976; Klump and Lassettre, 1977; Lassetre and Skerbele, 1974).

Two basic physical phenomena lie behind the angular and incident energy dependence of electron-impact scattering transition intensities. Electron-exchange scattering contributes to singlet–triplet transitions. The short-range nature of this interaction results in a nearly isotropic angular distribution. The cross section for spin-forbidden transitions usually peaks a few electron

volts above threshold, and by 50 eV above threshold it will have fallen by more than two orders of magnitude.

Spin-allowed transitions can be induced by the Coulomb interaction between the molecular and incident electrons. Since this is a long-range interaction it can be caused by large-parameter collisions which produce little deflection for high-energy electrons. The dependence of a spin-allowed transition on the incident electron energy per se may be characterized as showing a maximum a few tens of electron volts above threshold with a very gradual falloff at higher energies up to several hundred electron volts.

The variation of the cross section for a spin-allowed transition with scattering angle θ depends to some extent on the nature of the transition and the incident electron energy E_0. For moderate-energy electrons ($E_0 \simeq 40$ eV), electric dipole-allowed transitions show a steep decrease in cross section with increasing angle. An example of this is shown in Fig. 29. The angular variation expected for spin-allowed transitions which are symmetry forbidden is somewhat more complex. We will first give an analysis which is valid for high-energy incident electrons ($E_0 > 400$ eV). This case can be done quantitatively but it is not strictly applicable to most of the polyene spectra reported so far where $E_0 = 20$–90 eV. Thus our conclusions will have to be qualified at the end of this section.

The experimental quantity most directly related to theory is not the scattering angle θ or the incident energy E_0, but rather the momentum transfer S. Since $E = \hbar^2 S^2/2m$, we have

$$\hbar^2 S^2 = 2m[2E_0 - \Delta E - 2(E_0 - \Delta E)^{1/2} E_0^{1/2} \cos\theta] \tag{16}$$

where ΔE is the energy loss and m is the electron mass. The effective wavelength of the perturbation associated with the electron scattering process is

$$\lambda_{\text{eff}} = 2\pi/S \tag{17}$$

Thus, as $S \to 0$ the electron-scattering spectrum approximates the optical limit. As S departs from zero, the higher order transition moments can contribute to the scattering intensity, i.e., λ_{eff} becomes sufficiently small that the dipole approximation is inappropriate. The general behavior expected for a plot of scattering intensity as a function of wavelength is an oscillation, although in a reasonable experimental region there may be only one maximum or only a small inflection on a steep decrease. A calculation and an experiment illustrating this behavior for benzene are presented in Fig. 27 of Ziegler and Hudson, 1982.

Equation (16) indicates that the magnitude of S depends on both ΔE and θ. For a given value of ΔE and E_0, the magnitude of S is minimized by reducing θ to zero. Even at $\theta = 0$, however, $S > 0$. For example, with $\Delta E =$ 5 eV and $\theta = 0$ the value of S for $E_0 = 10$, 50, 100, and 500 eV is 0.48, 0.19,

0.13, and 0.057 Å^{-1}. For an incident energy of 20 eV and $\Delta E = 5$ eV, the value of S at $\theta = 0$, 15, 50, and 80° is 0.31, 0.64, 1.83, and 2.76 Å^{-1}. For example, an angular scan of a 5 eV transition with $E_0 = 20$ eV which started at $\theta = 15°$ might miss a trend toward a small cross section at low momentum transfer indicative of a forbidden transition (see Ziegler and Hudson, 1982, Fig. 27).

In order to examine the angular behavior expected for scattering from linear polyenes in a more quantitative fashion, we briefly repeat the analysis given in Lassettre and Skerbele (1974). These equations are much more compact in atomic units ($m = e = 1$, $h = 2\pi$, length in multiples of a_0, energy in e^2/a_0). In order to avoid confusion and to conform with the usage of Lassettre and Skerbele, we use k to represent an electron wave vector in atomic units, and similarly replace S by K, and ΔE by W in this system. First-order perturbation theory (the Born approximation) for the transition amplitude yields

$$F_n = 2\mu/K^2, \qquad \mu = \left\langle \Psi_n \middle| \sum_j q_j \exp(i\mathbf{k}\cdot\mathbf{r}_j) \middle| \Psi_0 \right\rangle \tag{18}$$

This is related to the experimental cross section by

$$\sigma = (k_f/k_0)|F_n|^2 = (k_f/k_0)(4\mu^2/K^4) \tag{19}$$

It is convenient to define a generalized oscillator strength (following Bethe) as

$$f = (W/2)(k_0/k_f)K^2\sigma = 2W\mu^2/K^2 \tag{20}$$

Expansion of the exponential in Eq. (18) leads to an expression for f in powers of the magnitude of the momentum transfer

$$f = 2W[\mu_1^2 + (\mu_2^2 - 2\mu_1\mu_3)K^2 + (\mu_3^2 - 2\mu_2\mu_4 + 2\mu_1\mu_5)K^4 + \cdots] \tag{21}$$

where

$$\mu_n = (n!)^{-1}\left\langle \Psi_n \middle| \sum_j q_j z_j^n \middle| \Psi_0 \right\rangle \tag{22}$$

The first term μ_1 is the familiar electric dipole transition moment, μ_2 is the transition quadrupole moment, μ_3 the transition octupole moment, etc.

An analysis for the allowed (^1B_u) and forbidden (^1A_g) transitions of polyenes can be given by examining the values expected for these multipole moments. For the ground state–^1B_u transition we know that μ_1 is large, μ_2 and μ_4 are zero by symmetry, μ_3 and μ_5 are expected to be very large. The oscillator strength as a function of K should start at a high value and drop off very rapidly with K since the coefficient of K^2 will be large and negative. For the ground state–^1A_g transition, we expect μ_1 to vanish except for vibronic coupling. This is a significant source of intensity in this case, resulting in

$f \simeq 0.05$ or even larger. However, μ_2 is expected to be particularly large and since μ_3 should be small, the coefficient of the K^2 term should be positive. The sign of the K^4 coefficient in Eq. (21) is hard to guess for linear polyenes. On strict symmetry grounds ($\mu_1 = \mu_3 = \mu_5 = 0, \mu_2, \mu_4 \neq 0$), we would expect a negative value for this coefficient.

This analysis is intended to show that there is a wide variety of possible variations of f and σ with K (and therefore θ). If the coefficient of the K^4 term is small, we expect the K^2 behavior to dominate the generalized oscillator strength. This will result in a cross section which does not depend on K (or θ). However, it is also possible to have a situation where the 1^1A_g–2^1A_g transition cross section reaches a maximum at small K. This is, in fact, the situation expected in the absence of vibronic coupling where we would have $f = 2W(\mu_2^2K^2 - 2\mu_2\mu_4K^4 + \cdots)$. The value of K at which f becomes a maximum may be less than attainable even at $\theta = 0$ for E_0 values in the tens of electron volts and transition energies near 5 eV.

The above analysis leads to a simple picture of electron-impact scattering with a close connection between this technique and optical multipole transitions. However, the scattering of low-energy electrons is much more complex. A dipole-forbidden transition may be made allowed not by multipole terms but rather because the electron severely polarizes the molecule with a consequent lowering of the symmetry of the system. The Born approximation is no longer valid. Because this is a complex phenomenon, a more empirical approach has been adopted (Kuppermann *et al.*, 1979). According to results obtained primarily for atoms and small polyatomics, a distinction can be made between spin-allowed and spin-forbidden transitions on the basis of their angular dependence. Spin-forbidden transitions show an isotropic angular variation, whereas spin-allowed transitions show a steep decrease in intensity with increasing angle. The roughly half-a-dozen molecular transitions which are spin allowed but dipole forbidden seem to generally follow this rule, but there are exceptions (Kuppermann *et al.*, 1979).

The polyenes butadiene (Doering, 1979; Flicker *et al.*, 1978; Mosher *et al.*, 1973a,b) and hexatriene (Frueholz and Kuppermann, 1978; Flicker *et al.*, 1977; Post *et al.*, 1975; Knoop and Oosterhoff, 1973) have been studied by electron-impact spectroscopy. The higher energy transitions (7 eV for butadiene and 6 eV for hexatriene) will be discussed later (Section VII,J). A low-resolution electron-impact spectrum of butadiene is shown in Fig. 22 (Mosher *et al.*, 1973b). The optically allowed transition to the ^1B_u state is seen at 5.92 eV. The weak peaks seen at 3.22 and 4.91 eV are assigned as transitions from the ground state to the two triplet states with ^3B_u and ^3A_g symmetry. The intensity of these transitions relative to that of the 5.92 eV transition to the ^1B_u state increases with increasing scattering angle. The ratio of the intensity of the 4.91 eV transition to that of the

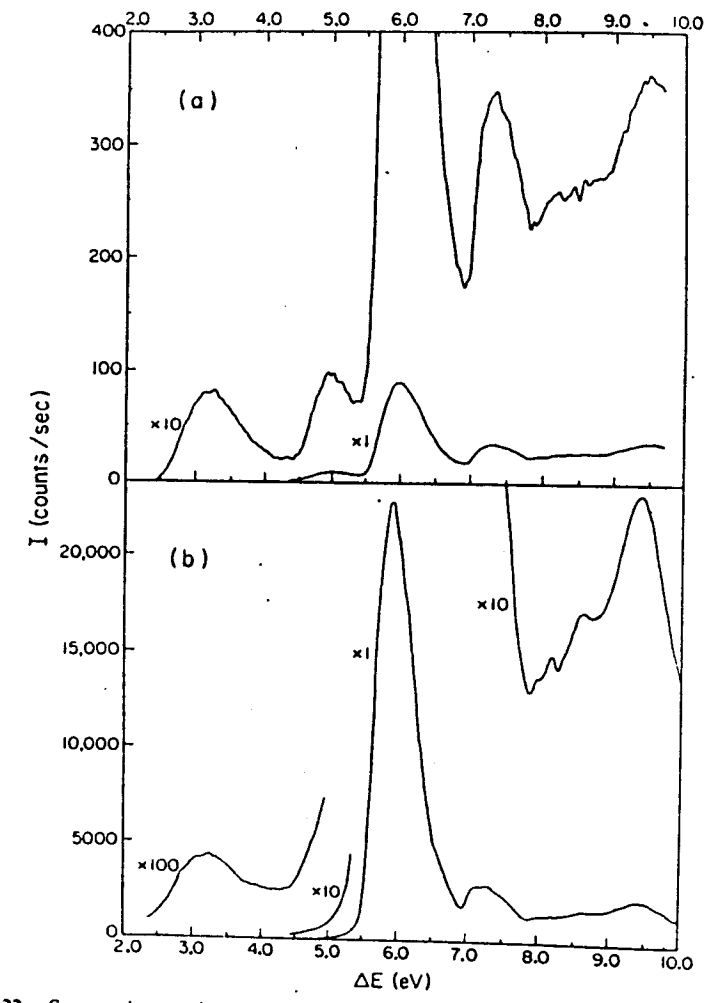

Fig. 22. Survey electron-impact spectra of butadiene. The spectral resolution is 150 meV (1200 cm^{-1}) (from Mosher *et al.*, 1973b): (a) $E_0 = 20$ eV; $\theta = 85°$; (b) $E_0 = 20$ eV; $\theta = 10°$.

allowed 5.92 eV transition changes by a factor of 100 as the angle varies from 17° to 85°. This is the behavior expected for a spin-forbidden transition due to the isotropic nature of exchange scattering. These triplet-state excitation energies are compared to theory and those for other polyenes in Section VIII,J. The spectral resolution of Fig. 22 is 150 meV. A spectrum of butadiene at 70 meV resolution is shown in Fig. 23. At this resolution the vibrational structure of the 6 eV allowed transition is partially resolved. A

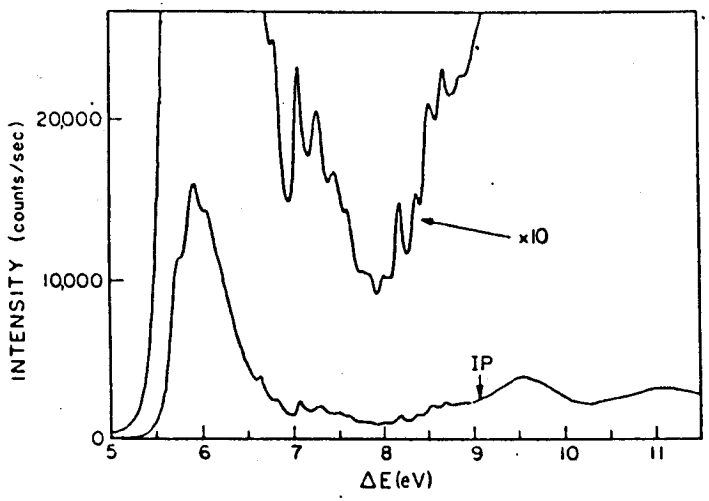

Fig. 23. An electron-impact spectrum of 1,3-butadiene with a resolution of 70 meV, 90 eV incident electron energy, and 0° scattering angle (from Flicker *et al.*, 1978).

series of higher energy transitions is seen above 6.6 eV. Increasing the resolution to 45 meV results in the spectrum labeled B in Fig. 24. The optical absorption spectrum is shown for comparison as trace A. The value of S for this experiment is roughtly 0.12 $Å^{-1}$, which means that it should be quite close to the optical limit. This explains the close agreement between the two spectra. Increasing the resolution to 25 meV (100 cm^{-1} or 4 Å for an optical spectrum at 2100 Å) produces the spectrum of Fig. 25. This spectrum shows a very close correspondence with the optical spectrum.

At this relatively high resolution it is possible to exploit the differential variation of the cross section for different electronic states to detect overlapping transitions. This is illustrated in Fig. 25 by comparison of the spectra obtained at $E_0 = 43$ eV where $S = 0.10$ $Å^{-1}$ (labeled A) with that obtained at $E_0 = 13$ eV where $S = 0.19$ $Å^{-1}$ (labeled B). At the higher momentum transfer there is a relative decrease in intensity in the high-energy region of the spectrum near 5.7 eV. Spectra obtained at a variety of incident energies and angles are consistent with the presence of a transition near 5.7 eV whose intensity peaks at a value of S of a few tenths of $Å^{-1}$ (Doering, 1979). There may also be some other maxima at higher momentum transfer. This behavior is certainly consistent with the qualitative arguments given above if the upper state involved in this transition is the 2^1A_g state.

An alternative point of view concerning this dependence of the spectrum of butadiene on incident energy has been presented (McDiarmid and Doering, 1980). A series of spectra of methyl-substituted butadienes has

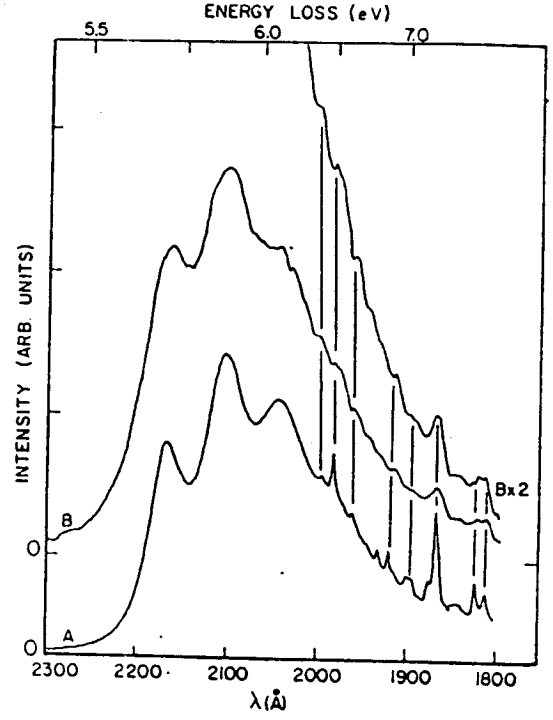

Fig. 24. The optical absorption spectrum (A) and electron-impact spectrum (B) of butadiene. Curve B was obtained with 45 meV resolution, 33.1 eV incident electrons, and 0° scattering angle (Doering, 1979).

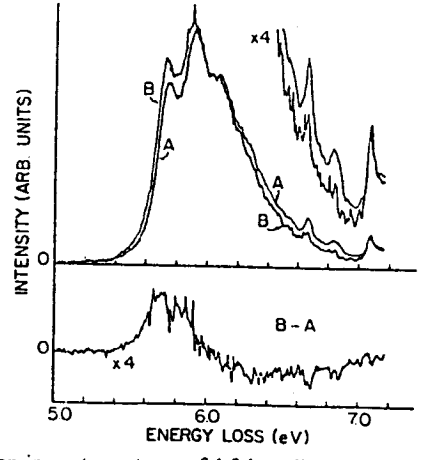

Fig. 25. The electron-impact spectrum of 1,3-butadiene at 4° scattering angle with 43 eV (a) and 13 eV (b) incident electron energies. The two spectra have been normalized to coincide from 6.0 to 6.1 eV. The panel at the bottom is the difference between these two spectra (J. P. Doering, private communication). For an alternative interpretation of similar data see McDiarmid and Doering (1980).

been obtained (Fig. 26). Methyl substitution results in a shift of the transition to lower energy by 0.15–0.2 eV. All of these diene species, with the exception of cyclohexadiene, exhibit the spectral change with excitation energy observed for butadiene. McDiarmid and Doering (1980) argue that this excludes the originally proposed (Doering, 1979) low-lying forbidden-transition hypothesis. The basis for this argument is that methyl substitution is not expected to have the same effect on the B_u and A_g excited states and that one would therefore not expect to see the same spectral pattern for all of these dienes. The authors propose that the observed changes in the electron-impact spectra are due to some intrinsic property of the excited B_u level which gives it an electron-impact cross section which varies with the degree of vibrational excitation. The mechanism for this effect proposed by the authors is not very convincing.

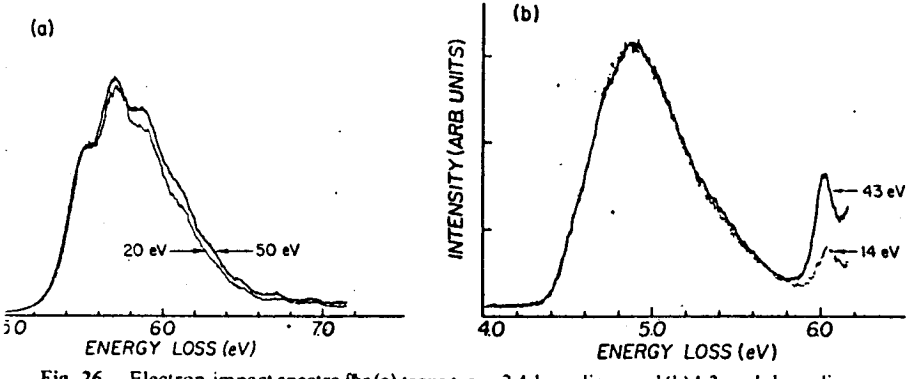

Fig. 26. Electron-impact spectra for (a) *trans,trans*-2,4-hexadiene and (b) 1,3-cyclohexadiene each at 4° scattering angle and two different incident electron energies (McDiarmid and Doering, 1980).

In fact, it seems possible that these observations are consistent with the hypothesis of a low-lying excited A_g state. It is not really known what the effect of methyl substitution will be for this small polyene, but the available data (see Section VIII,G) indicate that both states shift together. Also, the effect on the B_u state is small (0.2 eV) compared to the width of the entire transition (ca. 0.6 eV). Thus, if the effect on the A_g state was, say, 0.1 or 0.3 eV in the same direction, then the differential effect would be only 0.1 eV. It is not clear that this would be noticeable because of the large overall bandwidth.

The observation that cyclohexadiene does not exhibit an incident-energy-dependent spectrum suggests another explanation for this effect for the other dienes. The s-cis conformers, which should be present at 2–3% or

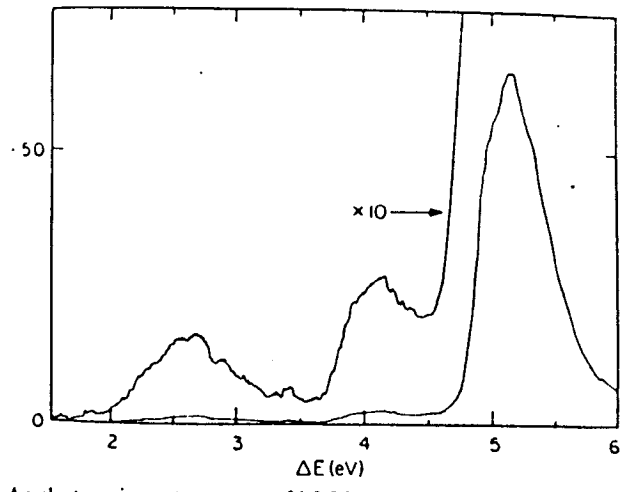

Fig. 27. An electron-impact spectrum of 1,3,5-hexatriene with 40 eV incident electrons and a scattering angle of 70°. The resolution is 100 meV (Flicker *et al.*, 1977).

more for all species studied except cyclohexadiene, may have a spectrum which is shifted slightly from that of the major s-trans isomer. That this is likely is indicated by numerous comparisons including that of cyclohexadiene with *trans,trans*-2,4-hexadiene (Fig. 26). It is also very likely that the two conformers have different dependences of their cross section on E_0 and, therefore, changing E_0 will result in a change in the spectral shape. Since the s-cis conformer probably has its transition at lower energy and a less steep dependence of its cross section on momentum transfer, one would expect a red shift at lower E_0, as observed. Since the observed effect would, according to this hypothesis, depend on the conformer population, the two spectral positions and shapes and the dependence of their cross sections on E_0, it does not seem possible to present a more quantitative comparison with experiment.

The electron-impact spectroscopy of hexatriene has not been investigated with the same degree of detail as that for butadiene. The low-energy region with 100 meV resolution is shown in Fig. 27. Transitions are observed with maxima at 2.6, 4.1, and 5.2 eV. The 5.2 eV transition is clearly the $^1A_g \rightarrow {}^1B_u$ transition. This is shown at 52 meV resolution in Fig. 28. Here the characteristic vibronic structure of the allowed transition is observed.

The variation of the cross section for these three transitions with scattering angle is shown in Fig. 29 (Flicker *et al.*, 1977). The rapid decrease in σ for the allowed transition is expected. The 2.6 eV transition is certainly to a triplet state. The 4.1 eV transition has been assigned as due to the second

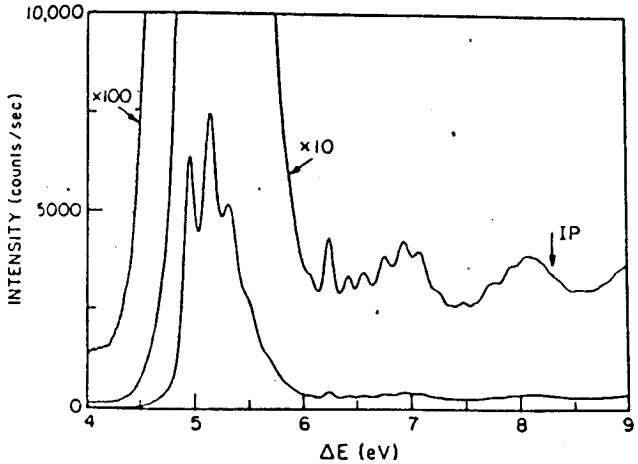

Fig. 28. Electron energy-loss spectrum of 1,3,5-hexatriene with 40 eV incident electrons, 0° scattering angle, 52 meV resolution (Flicker *et al.*, 1977).

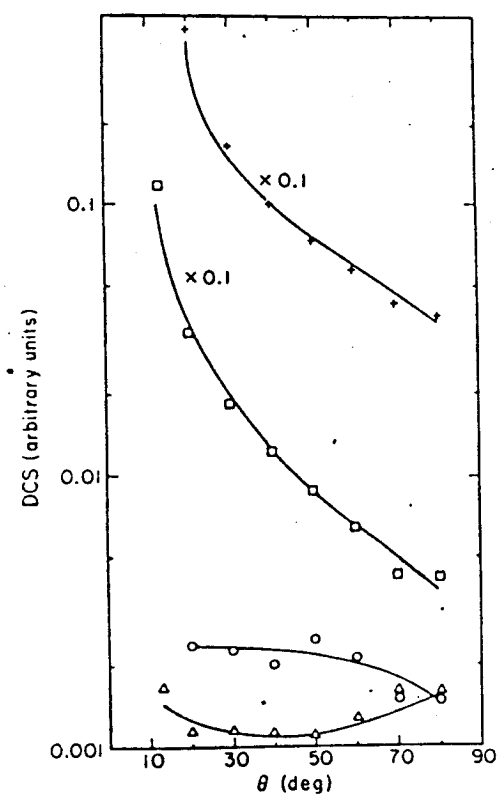

Fig. 29. Relative differential cross sections for the 1^3B_u (△), 1^3A_g (○), and 1^1B_u (□) excited states of 1,3,5-hexatriene for 20 eV incident electrons (elastic, +) (Flicker *et al.*, 1977).

triplet. However, according to the discussion given above, it is possible that this is a transition to a singlet state. It should be noted that the lowest value of S used in these experiments was 0.62 $Å^{-1}$ (E = 20 eV, θ = 20°). This value of S may be so high that a maximum in σ at lower S has been missed. However, the weight of the empirical correlations discussed above would indicate that the assignment of this transition to a triplet state is correct. A particularly relevant test of the empirical correlation would be an angular study of a transition of a polyatomic molecule which has a known dipole-forbidden transition which, like the polyene $^1A_g \rightarrow {}^1A_g$ transition, is quadrupole (two-photon) allowed. In any case the presence of a triplet state at 4.1 eV does not preclude the presence of a singlet state in the 4.1–5 eV region.

D. *Radiative Fluorescence Lifetimes*

Radiative or intrinsic fluorescence lifetimes are a measure of the strength of coupling between a transition and the electromagnetic field. Linear polyenes have fluorescence lifetimes in the range of 20–500 nsec. These values are much longer than expected on the basis of integration of their low-resolution absorption spectra. This is a natural consequence of the fact that the lowest energy transition between singlet states for polyenes is a forbidden transition between ^1A_g states rather than the allowed ^1A_g–^1B_u transition which dominates the absorption spectrum. The measurement of intrinsic fluorescence lifetimes is, therefore, a rather simple and convenient method for determining the excited-state ordering of polyenes. The experimental procedure consists of a determination of the fluorescence lifetime τ and the fluorescence quantum yield Q, so that the intrinsic lifetime $\tau_0(f) = \tau/Q$ can be calculated. This is then compared to the quantity $\tau_0(a)$ calculated by integration of the absorption spectra according to the procedure of Strickler and Berg (1962). If we define the quantity R by the expression

$$R = \tau_0(f)/\tau_0(a) \tag{23}$$

then a value of R, which is in excess of unity by an amount outside the range of experimental error, indicates that the low-lying excited state is the ^1A_g state rather than the ^1B_u state. Typical experimental errors and the uncertainties involved in the Strickler–Berg procedure would indicate that a value of R of 2 or greater is usually sufficient for determination of the excited-state order. When the value of R is in the region from 2 to 10, there is an indication of considerable mixing between the two excited states so that the "forbidden" transition has an oscillator strength of only 2–10-fold less than the transition to the ^1B_u state, which is, after all, a very strongly allowed transition. Values of R exceeding 100 have been observed in several cases (Table 8). These cases must correspond to forbidden transitions which

TABLE 8

FLUORESCENCE DATA FOR LINEAR CONJUGATED POLYENES

Molecule[a]	Solvent[b]	Q	τ (nsec)	$\tau_0(f)$[c] (nsec)	$\tau_0(a)$[d] (nsec)	R[e]	Reference
Diphenylpolyenes:							
DPB	CH	0.44	0.8	1.8	1.5	1.2	Birks and Dyson (1963)
DPH	BZ	0.80	6.9	8.6	1.5	5.7	Birks and Dyson (1963)
	BZ	0.68	5.5	8.1	1.5	5.4	Nikitina *et al.* (1964)
	CH	0.80	12.4	15.5	1.6	9.9	Berlman (1971)
	MCH/IH	1.0	17.5	17.5	1.9	9.2	Dalle and Rosenberg (1970)
	EPA	0.75	13.0	17.3	1.9	9.2	Dalle and Rosenberg (1970)
DPO	BZ	0.15	7.4	49	2.3	21	Birks and Dyson (1963)
	CH	0.09	6.2	69	4.1	17	Berlman (1971)
Retinyl polyenes:							
Retinol	MCH/IH	0.02	4.7	235	2.7	87	Dalle and Rosenberg (1970)
9-*cis*-retinol	MCH/IH	0.007	6.6	940	3.4	276	Dalle and Rosenberg (1970)
13-*cis*-retinol	MCH/IH	0.01	6.0	600	3.4	176	Dalle and Rosenberg (1970)
Other polyenes:							
Decatetraene	IP77K	0.2	100	500	1.8	278	Andrews and Hudson (1978a)
cPnA	CH	0.044	3.7	85	1.5	56	Sklar *et al.* (1977)
Octatetraene	H	0.02	4.4	220	1.5	147	Gavin *et al.* (1978)
	H77K	0.58	111	191	1.5	128	Gavin *et al.* (1978)

[a] All-trans isomer unless indicated: DPB, 1,4-diphenylbutadiene; DPH, 1,6-diphenylhexatriene; DPO, 1,8-diphenyloctatetraene; cPnA, *cis*-parinaric acid (*cis,trans,trans,cis*-9,11,13,15-octadecatetraenoic acid).

[b] CH, cyclohexane; BZ, benzene; MCH/IH, methylcyclohexane/isohexane 1:1; EPA, ether, *iso*-pentane, ethanol (5:5:2); IP77K, isopentane at 77 K; H, *n*-hexane at 23 C; H77K, *n*-hexane at 77 K.

[c] The radiative lifetime obtained from the ratio of τ/Q.

[d] The radiative lifetime obtained from integration of the strong absorption band.

[e] $R = \tau_0(f)/\tau_0(a)$ (see text).

are only weakly vibronically induced. The best example of behavior of this type is the case of the dimethyltetraene, decatetraene, where the intrinsic lifetime is 500 nsec or almost 300 times larger than the value which is calculated from its integrated absorption (Andrews and Hudson, 1978a). It is interesting to note that the effect of asymmetric substitution of the polyene chain, as in retinol polyenes, does not seem to result in significant admixture of the excited states. Thus, values of R of the order of 100 are still observed for these compounds (see Table 8).

The determination of an experimental radiative lifetime by dividing the observed lifetime by the quantum yield is subject to a number of kinetic assumptions. These assumptions appear to be justified, but that they are assumptions nevertheless should be kept in mind. Primarily, it is assumed that the yield of emitting states from the originally excited state(s) is unity. This means not only that there are no dark channels but also that there is no uniform suppression of all excitable channels. The first possibility leads to a fluorescence excitation spectrum different from the absorption spectrum. This also happens in the second case but can only be detected if the emitting origin line can be observed in absorption. A more general solution to this potential kinetic ambiguity has been proposed by Klochkov and Bogdanov (1978) who use light quenching of fluorescence to measure the radiative rate directly. The basis of this phenomenon is that fluorescence is decreased by stimulated emission caused by a laser pulse. There are some problems with this method due to potential excited-state absorption. Application of this technique to 1,6-diphenylhexatriene results in a value of the radiative lifetime of 7.9 nsec compared to 16.5 nsec from τ/Q and 1.6 nsec from integration of the absorption. In the absence of back transitions from metastable states, the measured lifetime is a lower bound to the radiative lifetime. It is, therefore, important to note that the measured lifetimes for polyenes with high quantum yields are greater than the value obtained from integration of the absorption.

For all but two of the linear polyene systems which have been studied, the value of R is sufficiently large that it is safe to conclude that the lowest energy excited singlet state is the ^1A_g state. The two exceptions are 1,4-diphenylbutadiene (Birks and Dyson, 1963) and cholesta-5,7,9(11)-triene-3-β-ol (Andrews and Hudson, 1979). The study of two triene steroids by Andrews and Hudson (1979) illustrates several methodological aspects of this fluorescence method and will, therefore, be discussed in somewhat more detail. The two triene steroids studied in this work have structures indicated in Fig. 30. For structure I, a steroid with an s-trans, cis, s-trans chromophore, the intrinsic fluorescence lifetime is in the range of 8–25 nsec. The lifetime calculated by integrating the solution absorption spectrum of

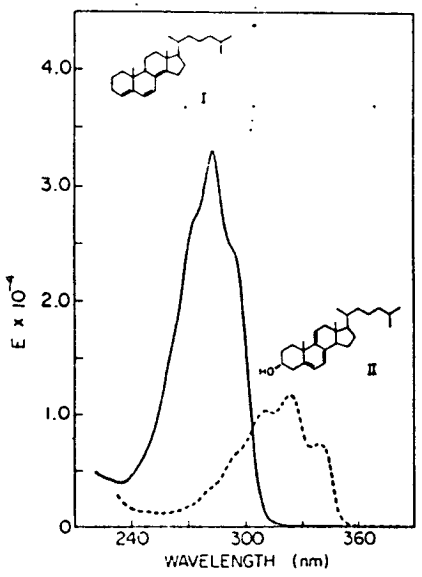

Fig. 30. The absorption spectra of the two indicated steroid trienes in cyclohexane at room temperature (Andrews and Hudson, 1979).

this species is 1.7 nsec. Thus, the value of R is in the range from 4.6 to 14.7. Structure II has an s-cis, trans, s-cis chromophore. For this species the intrinsic lifetime is 2.4–5.6 nsec, while the value calculated by integration of the absorption spectrum is 5 ± 1 nsec. Thus, in this case, the value of R is between 0.5 and 1.1 and, therefore, for this species we conclude that the absorption transition and the emission transition involve the same pair of ground and excited states.

The uncertainties in intrinsic fluorescence lifetimes and, consequently, the range of values of R cited above are due primarily to the combined uncertainty in the determination of the lifetime τ and the quantum yield. In fact, most of the uncertainty is due to the determination of the quantum yield. This becomes a particularly important factor when very low quantum yields are involved. This illustrates the primary limitation of this simple technique, namely that it requires fluorescence emission with a reasonably large quantum yield. Furthermore, if the quantum yield is only, say, 0.01, then an intrinsic lifetime of 100 nsec would result in an excited-state lifetime of only 1 nsec. Under some circumstances this is a sufficiently short lifetime that its measurement introduces additional uncertainty. However, when a species is reasonably fluorescent, or when one is prepared to make fairly exacting measurements, this simple technique has considerable utility. The primary reason for this utility is that there are no requirements concerning those structural features which appear to be required for obtaining high-resolution, vibronically resolved spectra. This makes this technique applicable to a much wider range of polyene structures than those which can be profitably studied by cryogenic mixed-crystal techniques.

Conclusions concerning the relative state ordering in polyenes based on this fluorescence comparison method have been repeatedly confirmed by other techniques. For the majority of cases where the ^1A_g excited state is below the ^1B_u state, this confirmatory evidence is discussed throughout the rest of this article. For cholestatriene-3-β-ol the value of the lifetime ratio R indicates the reverse state ordering. The comparison of the moderately resolved absorption and emission spectra of this molecule (Fig. 31) is, therefore, of interest. It is clearly seen that for this polyene there is a distinct overlap between the emission spectrum and the strongly allowed absorption (compare with Fig. 5).

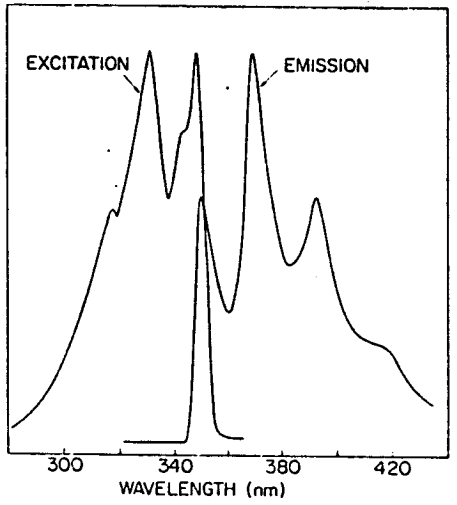

Fig. 31. The fluorescence excitation and emission spectra of cholesta-5,7,9(11)-triene-3-β-ol (II of Fig. 30) in isopentane at 77 K. (Andrews and Hudson, 1979).

This confirms the interpretation of the state ordering and strongly supports the above interpretations of both lifetime measurements and moderately resolved emission and absorption spectra comparisons. For 1,4-diphenylbutadiene, where a value of R of 1.2 was observed in cyclohexane solution, the situation is somewhat more complex. The resolved vibronic one-photon spectral studies of Hetherington (1976) noted in Section VII,A would indicate that the ^1B_u state is the lowest energy singlet state for this molecule in Shpolskii matrices, i.e., n-alkane matrices at liquid-helium temperature. However, the two-photon studies discussed in Section VII,B indicate that the excited-state order has the ^1A_g state just below the ^1B_u state. All of these

results are consistent if one postulates that the two excited states in diphenylbutadiene are quite close together and that their relative energy ordering depends on solvent interactions as discussed below. When two such excited states are quite close together, one expects the value of the fluorescence lifetime ratio R to become close to unity within experimental error because of extensive vibronic mixing of the two states.

An important aspect of this fluorescence method for the determination of state ordering in polyenes is the experimental observation that the values of the intrinsic lifetimes for linear polyenes and, therefore, the value of R, are unusually sensitive to the choice of solvent and to temperature for a particular solvent. This has led to some question as to the validity of the straightforward interpretation of intrinsic fluorescence lifetimes for polyenes. These reservations are in part based on the obvious fact that the Strickler and Berg relationship between radiative lifetimes and integrated absorption spectra is based on a theoretical development whose applicability is, in principle, limited to cases in which there are small distortions between the ground and excited states. This has led to numerous hypotheses to the effect that the excited state of linear polyenes responsible for emission is severely distorted with respect to the ground state and that this distortion is related to the long intrinsic fluorescence lifetime values. This hypothesis is discussed later, where it is shown that there is no experimental evidence to support this conclusion and that there is experimental evidence contradictory to such a large excited-state distortion. There is certainly no need to introduce such an ad hoc hypothesis since all of the available data are quantitatively explained on the basis of simple vibronic coupling between the excited ^1A_g and ^1B_u states. We illustrate this first by a discussion of the effect of solvent and temperature on the intrinsic fluorescence lifetime of polyenes.

1. *Solvent Effects on Energies and Radiative Lifetimes*

When a linear polyene is transferred from one solvent to another, the shift of the strong absorption spectrum is generally much larger than the corresponding effect on the fluorescence emission spectra. This differential effect of solvent changes on absorption and emission spectra was one of our earliest clues that two different states were involved in these processes. In this section we briefly review our understanding of this solvation effect and then apply this understanding to the phenomenon of solvent-dependent radiative lifetimes. The basic phenomenon which we need to understand is illustrated in Fig. 32. It is observed that when a polyene is dissolved in a solvent of increasing refractive index, the absorption spectrum shifts to lower energy. The transition to the excited ^1B_u state is typically 2000–3000 cm^{-1} lower in energy in solution than in the gas phase. This spectral shift does

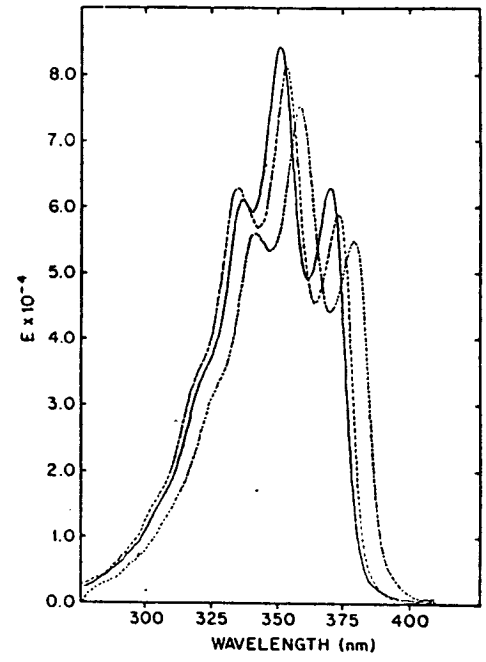

Fig. 32. Absorption spectra of diphenylhexatriene in cyclohexane, diethylether, and benzene at room temperature. (Andrews, 1978).

not appear to depend on the polarity of the solvent, but depends only on its polarizability. This suggests that the solvent effect is most easily described in terms of the mutual polarizability interaction between solute and solvent, as discussed in the works of Basu (1964), Longuet-Higgins and Pople (1957), and Ooshika (1954). According to this theory, the interaction of a nonpolar solute with a collection of nonpolar solvent molecules results in a decrease in the excitation energy of a transition by an amount given by

$$h(\nu - \nu_0) = a^{-3}[(n^2 - 1)/(n^2 + 2)][E/(E' + E)][M_{eg}^2 - E(\alpha_g - \alpha_e)] \quad (24)$$

where a is an effective solute cavity radius, n is the refractive index of the solvent, E and E' are mean excitation energies of the solvent and solute, M_{eg} is the electric dipole transition moment for the solute, and the α's are polarizabilities of the solute in the ground and excited states, respectively. This theory is based on truncation of the Coulomb interaction between solute and solvent electrons at the dipole interaction term and also on a very approximate continuum treatment of the solvent structure around the solute. For our purposes the important part of this equation is its prediction

of a linear dependence on a property of the solvent, namely the ratio $(n^2 - 1)/(n^2 + 2)$. This prediction is easily tested as shown in Fig. 33. The degree of linearity of these plots, especially their extrapolation through the gas-phase values, is a reasonable confirmation of this simple theoretical view. It should be noted that many of the solvents used in Fig. 33 are highly polar and include a great variety of structural types.

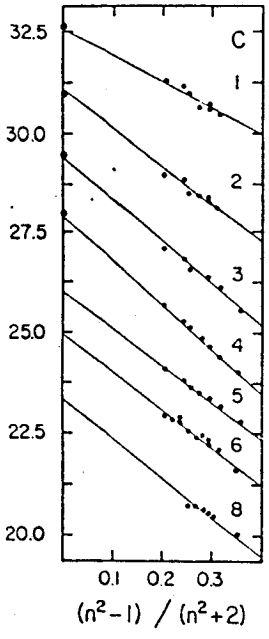

Fig. 33. Absorption spectral shifts of the diphenylpolyenes with 1–6 and 8 polyene double bonds. Reprinted with permission from Sklar *et al.* (1977). Copyright 1977 American Chemical Society.

The quantity $(n^2 - 1)/(n^2 + 2)$ is related to the solvent polarizability by the equation

$$\beta = (n^2 - 1)/(n^2 + 2) = (\rho/M)(4\pi N/3)\alpha \qquad (25)$$

Equation (24) shows that strongly allowed transitions, that is, those with large transition dipole moments M_{eg}, should have a large dependence of their excitation energy on solvent polarizability. The slopes of the lines of Fig. 33 correspond to approximately 10,000 cm^{-1} per unit change in $(n^2 - 1)/(n^2 + 2)$. The magnitude of this slope is consistent with crude estimates of quantities appearing in Eq. (24).

When the temperature of a solution is increased, expansion will occur and as a result the refractive index and, therefore, the polarizability, will decrease. The simple solvent shift theory discussed above, predicts therefore that there will be a relationship between the absorption maximum of a polyene as a

function of temperature and as a function of changes in solvent. Sklar *et al.* (1977) have in fact shown that the absorption maximum of an alkyl-substituted tetraene shifts in response to temperature in exactly the same fashion as a shift in response to solvent change. Thus, the important variable in both cases is the solvent polarizability. This is a strong confirmation of the general validity of this simple picture of the solvent shift. It also establishes a connection between the effect of temperature and solvent change on energy levels.

The comparison of solvent effects on absorption and emission spectra is of particular interest (Fig. 34). A much smaller change is observed for the emission spectra than for the absorption spectra. In fact, for the dimethyltetraene, decatetraene, the slope for the absorption data is $-10{,}150 \pm 150$ cm^{-1}, whereas that for the emission data is $+1500 \pm 3500$ cm^{-1} (Andrews, 1978). Thus, the best estimates of the slopes have opposite signs. For diphenyl-octatetraene, a small negative slope is observed for the fluorescence data.

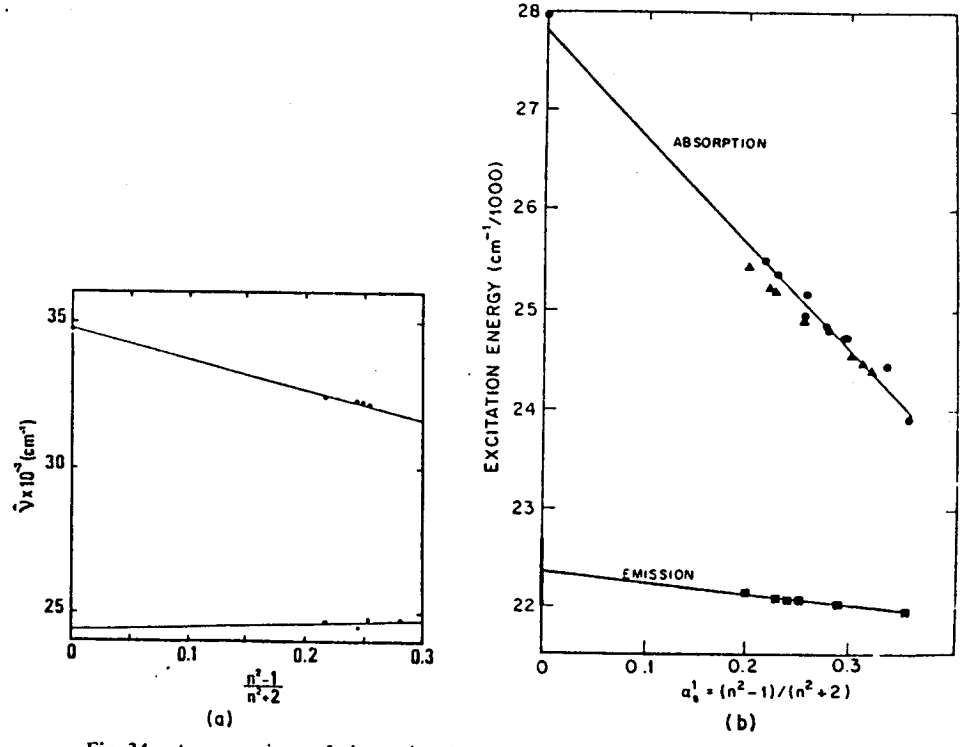

Fig. 34. A comparison of absorption (upper curve) and emission (lower curve) spectral shifts for deca-2,4,6,8-tetraene (a) and diphenyl-1,3,5,7-octatetraene (b). (Andrews, 1978; Hudson and Kohler, 1973).

Studies of absorption and emission shifts due to the polarizability increase induced by solvent compression at high pressure have been reported by Brey *et al.* (1979). Their results for diphenylhexatriene, diphenyloctatetraene, and retinylacetate demonstrate much smaller shifts for emission than for absorption. This behavior is consistent with Eq. (24) and the idea that the emission transition is associated with low oscillator strength.

The major conclusion of this analysis of solvent effects is that two different states are involved in absorption and emission. This conclusion is clearly independent of the specific formulation of the mechanism of the solvent shift itself. What is important is that the two transitions are differently affected by the solvent perturbation.

We now turn to the question of the effect of solvent changes and temperature on radiative lifetimes for linear polyenes (Andrews and Hudson, 1978b; Birks *et al.*, 1978). The basic idea behind this analysis is that the oscillator strength, and therefore the radiative rate constant, for the transition between the excited A_g state and the ground state will be related to the energy gap between the excited A_g state and the excited B_u state according to the expression

$$f = FK/(\Delta E)^2 \tag{26}$$

where f is the oscillator strength of the forbidden transition, F is the oscillator strength of the transition to the singlet B_u excited state, ΔE is the energy separation between the two excited states, and K is the matrix element connecting the excited states (Hudson and Kohler, 1973). The coupling-matrix element K is probably dominated by vibronic interactions but may also include solvent asymmetry-type interactions. The point is that the energy separation ΔE is a function of the solvent and temperature because of the differential stabilization of the excited B_u state relative to the excited A_g state in highly polarizable media. The theoretical development of this equation is given in much more detail by Andrews and Hudson (1978b). An important conclusion of that theoretical development was the demonstration that in contrast to the hypothesis of Birks and Birch (1975) and Carmichael *et al.* (1979), the excited-state coupling matrix element K is not a function of the solvent. The development of Andrews and Hudson begins with the relationship between the radiative rate constant and the matrix element between the excited A_g state and the ground state:

$$k_{ga} = (2\omega^3/hc^3)[9n^3/(n^2+2)^2]M_{ga}^2 \tag{27}$$

When this equation is combined with conventional vibronic coupling theory and the solvent-induced spectral shift discussed above, the final equation is

$$k_{ga} = \frac{1}{\tau_0} = \frac{2\omega^3}{hc^3}\frac{9n^3}{(n^2+2)^2}\frac{M_{gb}^2 h_{ab}^2}{[\Delta E_{ba}^\circ - \eta\,\Delta P_{ba}]^2} \tag{28}$$

where ΔE° is the energy difference between the excited A_g and B_u states in the gas phase and ΔP_{ba} is the difference in the slopes of the solvent-induced polarization stabilization for the excited A_g, B_u states. It is convenient to rewrite this equation in the following form:

$$K_{ga} = \left[\frac{(n^2+2)^2}{9n^2}\right]k_{ga} = \frac{\Gamma^2}{(\Delta E_{ba}^\circ - \beta\Delta P)^2} \tag{29}$$

where

$$\Gamma^2 = (2\omega^3/hc^3)|M_{gb}|^2 h_{ab}^2 \tag{30}$$

This is a relationship between the experimental quantity K_{ga} and the experimental quantity β defined by Eq. (25). The adjustable parameters are, therefore, the collection of constants Γ, the energy gap in the gas phase ΔE°, and the difference in polarization stabilization ΔP. Andrews and Hudson treat these unknowns as adjustable parameters, but there are independent experiments which provide evidence on the range of all three of these parameters. Figure 35 shows the degree of agreement of this functional form with the available experimental data for the variation of the radiative rate constant

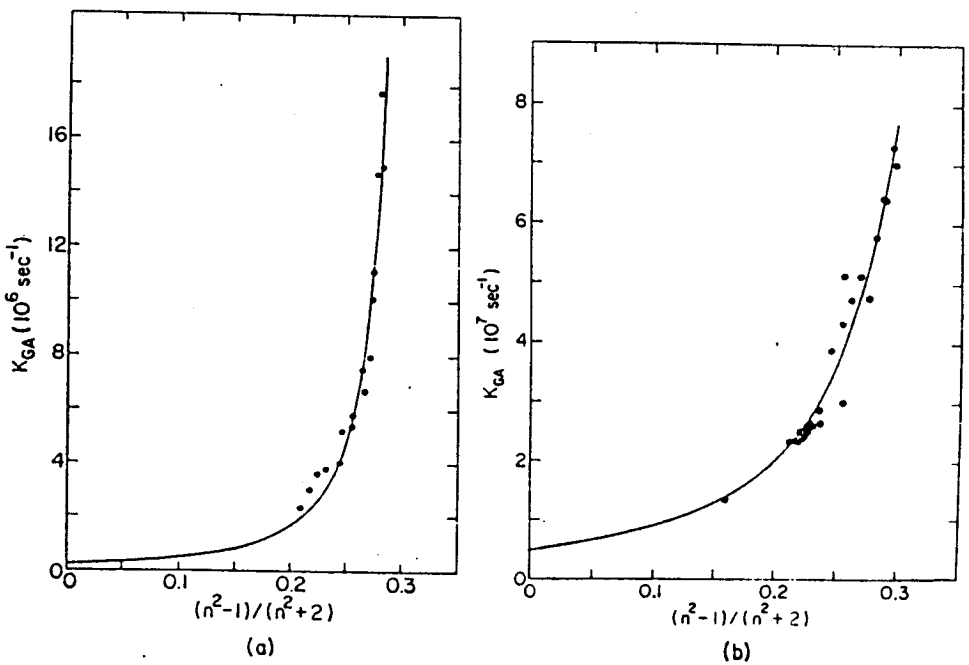

Fig. 35. The fit of Eq. (29) to radiative lifetime data for diphenylhexatriene (a) and *trans*-retinol (b) (Andrews and Hudson, 1978b).

as a function of β for diphenylhexatriene (DPH) and *trans*-retinol. The parameters obtained in the nonlinear least squares fit (Table 9) are reasonably well determined by the data and are of the proper order of magnitude based on independent estimates.

TABLE 9

PARAMETER VALUES OBTAINED FROM THE FIT OF Eq. (29) TO THE DATA OF Fig. 35

	DPH	Retinol
ΔP_{ba} (cm^{-1})	8830 ± 950	$10{,}340 \pm 2280$
ΔE_{ba} (cm^{-1})	3500 ± 66	3320 ± 48
Γ^2 ($cm^{-2}\ sec^{-1}$)	$(6.1 \pm 0.8) \times 10^{13}$	$(2.5 \pm 0.5) \times 10^{12}$
h_{ab} (cm^{-1})[a]	555	149

[a] Calculated from Γ^2 using Eq. (30). (See Andrews and Hudson, 1978b.)

The data shown in Fig. 35 include both temperature and solvent changes. The fact that all of these data fall on the same smooth curve indicates that the same basic mechanism is involved in the variation of the radiative rate constant. This conclusion has been elegantly extended by the studies of Brey *et al.* (1979). Their high-pressure studies of the relationship between the excited-state energy separation and the radiative rate constant for diphenylhexatriene and diphenyloctatetraene are quantitatively explained by Eq. (29). These high-pressure experiments are able to span a larger range of solvent polarizability and, therefore, variation in ΔE. The parameter values extracted from the fit of the above model to the diphenylhexatriene pressure data (except for the highest pressure as discussed below) are in good agreement with those obtained from the fit to solvent data. Again, this demonstrates that the important variable determining ΔE, and therefore the intrinsic lifetime, is the polarizability and not the polarity, temperature, density, or pressure.

We note here that Eq. (22) provides an explanation, in quantitative terms, of the empirical observation of Thompson (1969) and Dalle (Dalle and Rosenberg, 1970; Rosenberg, 1976) that there is a strong correlation between the "Stokes shift," a measure of ΔE, and the lifetime ratio R.

This treatment of the effect of solvent and temperature on radiative rate constants is not expected to be generally valid. In particular, if the excited states become very close together, the magnitude of the interaction and therefore the radiative rate constant will depend on the details of the vibronic-level interactions. The general trend is expected to be a decreased rate of

increase of the radiative rate constant as ΔE approaches zero. This behavior is observed in the work of Brey *et al.* (1979). However, it must also be concluded that except for this obvious case, all of the available experimental data can be nicely rationalized on the basis of this semiempirical theory using reasonable parameters. In particular, there seems to be no reason to invoke additional hypotheses concerning extreme excited-state conformational changes. This point is discussed in the next section.

2. *Conformational Distortion Hypotheses*

Several authors have repeatedly proposed that the photophysical behavior of polyenes is associated with large conformational changes upon excitation (Birks and Dyson, 1963; Thompson, 1969; Dalle and Rosenberg, 1970; Cehelnik *et al.*, 1974; Rosenberg, 1976; Birks and Birch, 1975; Cehelnik *et al.*, 1975; Birks, 1976). This hypothetical conformational change has in some cases been proposed as an explanation of the very low fluorescence quantum yield of some polyenes (e.g., Thompson, 1969) or to explain the large separation between absorption and emission spectra in terms of a Franck–Condon forbidden pattern (e.g., Mulliken, 1939; Neporent, 1973). Most workers, however, have invoked this hypothesis in order to explain the combination of the large separation between absorption and emission ("the Stokes shift") and the anomalously long lifetimes observed for polyenes, i.e., values of R greater than unity. The basic argument used by these authors is that the correlation between the separation of absorption and emission spectra with the lifetime anomaly ratio R has as its underlying cause a variation in the conformational distortion upon excitation. It must be noted that with the exception of the work by Birks and Birch (1975), this argument is applied with the assumption that the state responsible for emission is the B_u state. A large conformational distortion upon excitation will give rise to a so-called Franck–Condon forbidden transition which will have very low intensity in the origin region with a smooth increase in intensity as one approaches higher vibronic levels for either the absorption or the emission. Paralleling this argument is one which is based on an examination of the Strickler–Berg derivation of the relationship between absorption spectra and emission lifetimes. Formally, the Strickler–Berg equation is only valid for allowed transitions whose vibronic structure is described by Franck–Condon progressions. Contributions due to vibronic borrowing are not included. This, however, cannot be an important factor insofar as the transition from the ground state to the excited B_u state is concerned. Another assumption of the Strickler–Berg derivation is that the nuclear geometry of the ground and the excited states are sufficiently similar that the purely electronic transition dipole matrix element is the same for the upward and downward transitions. It has been proposed by the above authors that this assumption

is not valid for the linear polyenes. This argument has never been stated in a formal or quantitative sense. Qualitatively, however, its basis seems to be the idea that a highly twisted structure ought to have a smaller electronic transition dipole matrix element than a fully conjugated planar polyene.

A significant reason for thinking that this argument is incorrect is that it cannot account for the large magnitude of the fluorescence ratio R. It should be noted that the oscillator strength, roughly reciprocally proportional to the radiative lifetime, is only a linear function of polyene chain length. Thus, if a polyene were decomposed into its n double-bond subunits, this would have no net effect on the oscillator strength since it would now be n absorbers, each with $1/n$ of the original intensity. Factors of 100 must come from other sources. More direct experimental evidence against this large conformational change hypothesis comes from the fact that qualitatively, absorption and emission gaps, after correction for solvent contraction, are the same for polyenes in matrices at 4 K as they are in fluid solution. Radiative lifetime anomalies are also comparable at low temperatures and at room temperature. It does not seem likely that large conformational changes are possible for molecules constrained by low-temperature matrices. Similarly, the steroid triene discussed above which has a value of R of between 4.5 and 15 certainly is unable to undergo large conformational changes because of the constraints imposed by its sigma framework.

Finally, we note that the arguments presented above concerning the mechanism for the long radiative lifetime of linear polyenes, including the absolute identification of the low-lying excited state as being of singlet A_g symmetry for at least one polyene, makes it unnecessary to postulate any extreme conformational distortions associated with excitation. The study by Granville *et al.* (1979) demonstrates that octatetraene in an *n*-octane matrix maintains its center of inversion symmetry upon excitation. This precludes any large-scale conformational changes upon excitation, at least in this environment.

However, it still may be postulated that in fluid solution polyenes display twisted excited-state equilibrium geometries that are ruled out by steric interactions in low-temperature solids. Even the low-resolution absorption and fluorescence spectra are incompatible with this idea. There are no theoretical models or spectroscopic precedents for constructing anything other than a smooth vibronic profile for a Franck–Condon forbidden transition. If polyene emission is ascribed to the 1^1B_u state, a vibronic profile for the absorption or emission spectrum (or both) which has a break in intensity must be rationalized. This cannot be done. Analysis of spectra for linear polyenes with two to six double bonds in fluid solution (Granville *et al.*, 1981) shows clearly that the 1^1B_u states are only slightly distorted from the ground state geometry, mainly along the bond stretching coordinates. From the fluorescence spectra it is clear that the situation for the

2^1A_g states is similar. Though butadiene and hexatriene need further attention, as does the coupling between electronic excitation and nuclear motion in the longer polyenes, it must be accepted that those linear polyenes that emit do so from a ^1A_g state that is not substantially twisted.

E. Radiationless Decay Rates

The rates of radiationless decay of the excited singlet state of linear polyenes show several interesting trends. Butadiene and hexatriene appear to have extremely efficient radiationless decay pathways. Octatetraene, however, has a significant fluorescence yield. The longer unsubstituted polyenes are also fluorescent but with quantum yields which decrease relative to octatetraene as the chain length increases (D'Amico *et al.*, 1980). This same pattern occurs for alkyl and diphenyl polyenes. The decrease in the quantum yield with increasing chain length for longer polyenes could be due, in part, to a decreased radiative rate, even with a fixed radiationless rate. The extremely low emission yield of butadiene and hexatriene compared to that for octatetraene probably reflects a large change in C—C bond lengths on excitation for these smaller compounds and therefore very efficient internal conversion to the ground state.

Polyenes appear to have faster radiationless decays in polar sovents than when dissolved in nonpolar solvents (Dalle and Rosenberg, 1970; Birks and Birch, 1975; Thompson, 1969; Sklar *et al.*, 1977; Cehelnik *et al.*, 1975). For example, the radiationless decay rate for parinaric acid (9,11,13,15-octdecatetraenoic acid) is around 20×10^7 sec^{-1} at room temperature in nonpolar solvents and $(40–80) \times 10^7$ sec^{-1} in polar solvents (Sklar *et al.*, 1977). For diphenylhexatriene the radiationless decay rate is 1.5×10^7 sec^{-1} in perfluoro-*n*-hexane and 4.3×10^7 sec^{-1} in ethanol, both at 25°C (Cehelnik *et al.*, 1975).

The radiationless decay rates of polyenes are also quite temperature dependent. For diphenylhexatriene the radiationless decay rate of 2.5×10^7 sec^{-1} in 3-methylpentane at 22°C becomes less than 10^6 sec^{-1} at −88 C. ($Q > 0.99$). The temperature dependence is greater for polar solvents than for nonpolar solvents (Cehelnik *et al.*, 1975). Similar data are also available for retinyl polyenes (Dalle and Rosenberg, 1970) and parinaric acid (Sklar *et al.*, 1977).

Enhanced intersystem crossing and, therefore, decreased fluorescence can usually be induced by the external heavy-atom effect caused by the addition of salts such as LiBr or solvents such as iodopropane. The mechanism of this effect is increased spin–orbit coupling upon collision of the chromophore with the heavy-atom species. Song *et al.* (1976) have found that the polyenes diphenylhexatriene, diphenyloctatetraene, retinol, and retinal do not show

any fluorescence quenching upon addition of such agents. Song *et al.* (1976) actually observed an increased quantum yield for retinal when heavy-atom salts are added. Takemura *et al.* (1976) have reported that retinal is non-fluorescent in absolutely dry hydrocarbon solvents but becomes emissive when hydrogen-bonding species such as water or methanol are added. It has been claimed (Becker *et al.*, 1979) that this behavior is not observed for dodecapentaenal, a close analog of retinal, but Hudson and Loda (1981) find that this effect also occurs for this compound. This phenomenon has been interpreted by Takemura *et al.* in terms of a change in the relative ordering of $n\pi^*$ and $\pi\pi^*$ excited states. This interpretation is not unique because changes in energies of states in the triplet manifold must be considered. There do not appear to be any reports of the effect of deuterium substitution on polyene radiationless decay rates.

Overall, it must be concluded that much of the behavior of polyene radiationless decay rates is not well understood.

F. Inhomogeneous Broadening Mechanisms and Multiple Sites

Much of our new information on the low-lying excited states of linear polyenes comes from high-resolution Shpolskii matrix spectra. Because of the importance of this technique, it is of some interest to examine polyene spectra from the point of view of what they tell us about this method. The basis of the Shpolskii method or any other mixed-crystal spectroscopic technique is that an ensemble of chromophores will produce a well-resolved spectrum if the guest molecules are all in the same spectroscopic environment. The linewidth of the resulting vibronic lines is probably determined primarily by the residual multiplicity of environments, rather than by homogeneous broadening mechanisms such as lifetime broadening.

Sometimes matrix isolation in an *n*-alkane host results in several discrete environments rather than one. This is revealed as a set of absorption lines which are coincident with a set of emission lines (Fig. 20). These individual site-origin lines can be separated by as much as 300 cm^{-1}. It is, therefore, not surprising that in a random matrix, such as an organic glass, the linewidths are of this order of magnitude. The nature of the sites which give rise to these distinct origin lines is not known, but a likely possibility is that they correspond to distinct *n*-alkane crystal types (polymorphism).

The molecules in each of these environments are essentially independent species. Thus, excitation of one of the site species with narrow bandwidth radiation results in emission from only that subset of the overall ensemble. This can result in considerable spectral simplification in some cases (for example, see Hudson and Loda, 1981). In principle, a broad, continuous

spectrum generated by a set of molecules in a distribution of environments can be converted to a well-resolved emission spectrum by using narrow-band excitation and sufficiently low temperature so that interconversion between environments is slow compared to the excited-state lifetime (Kohler, 1979). This technique has not been successful with linear polyenes. Broad, continuous spectra remain amorphous with narrow bandwidth excitation at 4.2 K and below. Presumably, the reason for this is that for those polyenes such as the retinyl polyenes which produce continuous spectra, excitation at any frequency results in a population of molecules in a range of environments due to spectral congestion, the finite width of the individual environment vibronic transitions, and the fact that excitation is most likely into S_2.

Polyenes may be uniquely classified into one of two spectral types: those which produce well-resolved spectra in low-temperature matrices and those which do not. A further feature of this classification is that those polyenes which produce well-resolved spectra in one matrix, generally also have a well-resolved spectrum in one or two other matrices (although the spectrum may be different for each matrix, as discussed below). Polyenes which do not show well-resolved spectra have been examined in a great variety of matrices without success. Finally, those polyenes which produce well-resolved spectra in *n*-alkane matrices at 4.2 K have reasonably well-resolved spectra in glassy samples at 77 K (e.g., Fig. 4); polyenes with amorphous spectra at 77 K have very similar featureless spectra at 4.2 K.

The polyenes which fall into the "well-resolved" spectra class are the diphenylpolyenes, the unsubstituted polyenes with four or more double bonds, methyl-substituted polyenes with four, five, or six double bonds, and the polyene aldehyde undecapentaene. The species which have resisted spectral resolution include hexatriene and the retinyl polyenes. The reason for failure to obtain well-resolved spectra of hexatriene in matrices such as single crystals of *n*-hexane at 2 K is not clear. One possibility is that a large geometry change associated with excitation, invoked as a rationalization for the lack of fluorescence, might result in extensive phonon side-band excitation. The retinyl polyenes have a special mechanism for their generation of low-information spectra (Christensen and Kohler, 1973, 1976; Warshel and Karplus, 1972b). The ring system at the end of these compounds has an equilibrium geometry which makes the overall π-system nonplanar (Honig *et al.*, 1971). Furthermore, the potential function for the torsion of the ring relative to the main polyene chain has a rather flat minimum and it is therefore expected that a variety of conformations will be present at thermal equilibrium or trapped in a nonequilibrium state. Even the range of the zero-point motion is expected to be appreciable. The spectroscopic effect of changing this torsional angle can be viewed as a change in the effective length of the polyene chain and as a result, the distribution of electronic

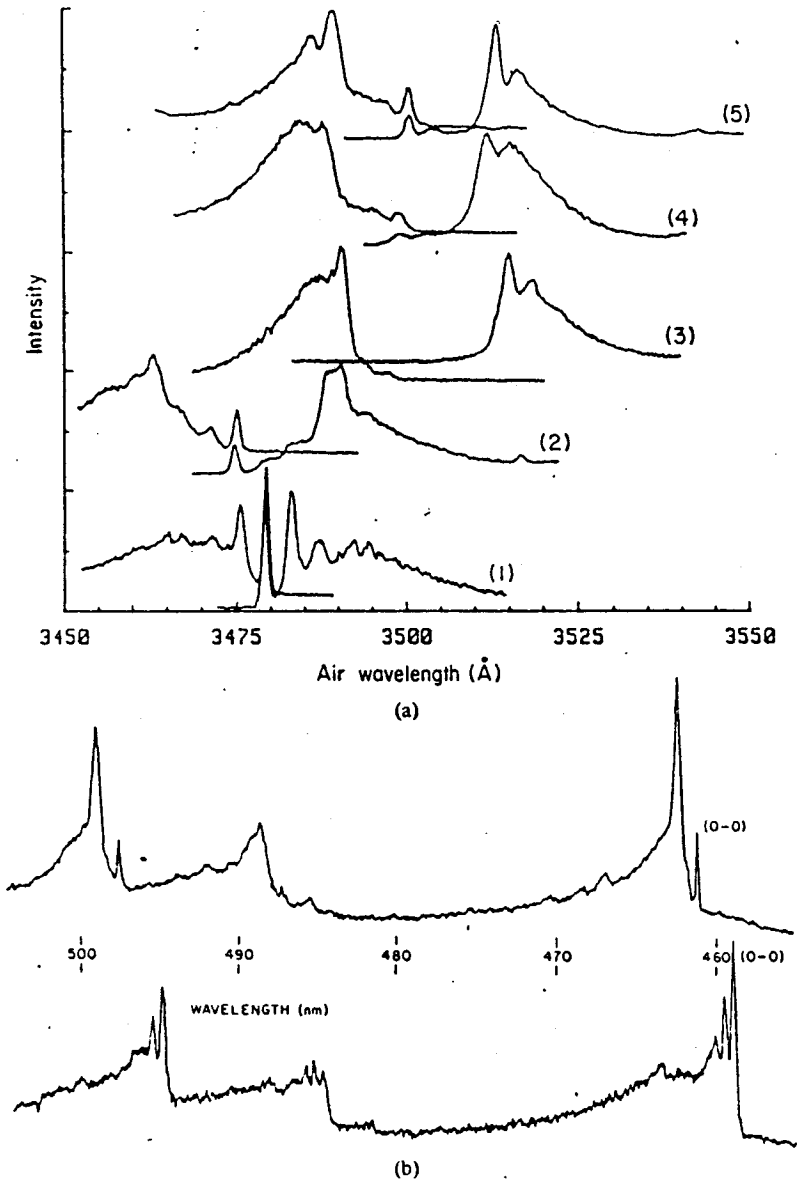

Fig. 36. Specific matrix effects on polyene spectra: (a) the excitation (left) and fluorescence (right) of octatetraene at 4.2 K in *n*-alkane matrices—(1) hexane, (2) heptane, (3) octane, (4) nonane, and (5) decane (Snow, 1980). Note that only in *n*-octane does the spectrum have a classic forbidden pattern. (b) The spectra of 2,12-dimethyltridecahexaene in slowly cooled nonane (upper) and rapidly cooled nonane (lower). Reprinted with permission from Christensen and Kohler (1976). Copyright 1976 American Chemical Society.

excitation energies. This argument has been put in more quantitative terms, and good agreement has been found between the expectations of this argument and the spectra of a set of carotenoids (Hemley and Kohler, 1977).

Finally, some interesting phenomenology related to the form of high-resolution spectra should be noted. It has been repeatedly noticed that a polyene species may produce well-resolved vibronic spectra in more than one host but that the two spectra are quite different. The most common difference is that the spectra will have a dominant allowed origin in one environment which partly or completely vanishes in another to be replaced by a false origin based on a b_u promoting mode. Some examples of this behavior are shown in Fig. 36, including a case where the only difference in the environments is generated by the rate of sample cooling.

G. *Substituent Effects*

Some data are now available that have a bearing on the effect of substituents on polyene excited-state energies. The origin of the transition to the 2^1A_g state of octatetraene in *n*-octane at 4.2 K is at 28,560 cm^{-1} (Granville *et al.*, 1979). The dimethyl tetraene 2,4,6,8-decatetraene has its origin at 28,738 cm^{-1} in *n*-undecane at 4.2 K. The origins of the transitions to the 1^1B_u states for these two tetraenes in these matrices are at roughly 32,100 and 31,280 cm^{-1}, respectively. Thus, the effect of methyl substitution is larger for the B_u state than for the A_g state, but in both cases the effects are quite small and are comparable to solvent shifts.

A similar comparison can be made for phenyl substitution. For 1,8-diphenyloctatetraene the origin of the 2^1A_g transition is at 22,570 cm^{-1}, while the ^1B_u transition is at roughly 24,300 cm^{-1} (in pentadecane at 4.2 K). Thus, relative to octatetraene, this phenyl substitution produces a red shift of 6000 and 7800 cm^{-1} for the excited A_g and B_u states. Given the uncertainties in the location of the B_u state (because of the width of the bands) and the effects of the matrix, it appears that the major effect of phenyl substitution is a uniform shift of both excited states.

Another interesting substituent effect is the replacement of a carbon atom by a carbonyl oxygen. The origin line for the A_g transition of dodecapentaenal is at 22,151 cm^{-1} (Hudson and Loda, 1981; Becker *et al.*, 1979). For comparison, the origins for a trimethylpentaene and hexaene are at 24,560 and 21,788 cm^{-1} (Christensen and Kohler, 1975; Auerbach *et al.*, 1981). The six double-bond pentaenal has almost the same 1^1A_g–2^1A_g transition energy as a hexaene. However, the allowed transition for the pentaenal is at considerably lower energy than that for this hexaene (ca. 23,500 cm^{-1} for the aldehyde, 25,800 cm^{-1} for 2,12-dimethyltridecahexaene). If we think of the

hydrocarbon as a reference molecule, the effect of aldehyde substitution is to shift the excited A_g state to lower energy by only 363 cm^{-1}, while the B_u state moves down by roughly 2300 cm^{-1}.

H. *Transition Polarizations and Intensity Borrowing*

It is believed that the polarization of the allowed transition of 1^1A_g ground state to 1^1B_u excited state is polarized along the main chain axis. The actual experimental evidence for this is fairly meager except in qualitative terms. For simple unsubstituted polyenes or any other species with C_{2h} symmetry, the transition must be in the molecular plane. Christensen (1972) has shown that the polarization of the allowed transition of all-*trans*-retinoic acid is in the plane of this polyene. A more interesting issue is the polarization of this transition in this plane, a feature which is not determined by symmetry. One reason for interest in this polarization direction is that resonance force (exciton) models (Simpson, 1951, 1956) predict a polarization direction roughly parallel to the ethylenic units, as much as 60° from the chain axis.

Semiquantitative determinations of this polarization direction have been made using stretched film (Moore and Song, 1974; Eckert and Kuhn, 1960) and oriented liquid-crystal samples (Sackmann and Rehm, 1970; Cehelnick *et al.*, 1973). The only actual quantitative determination appears to be the work of Parkhurst and Anex (1966) who used reflection spectroscopy to establish that the polarization of the allowed transition for all-*trans*-β-ionylidene crotonic acid (a retinyl-like tetraene acid) is parallel to the main chain axis.

The polarization of the fluorescence transition (2^1A_g–1^1A_g) of polyenes is in the same direction as the strong absorption (Hudson, 1972; Moore and Song, 1973b). This indicates that the intensity of the 2^1A_g–1^1A_g transition is borrowed from the nearby allowed transition. This intensity-borrowing mechanism is presupposed in the analysis of radiative fluorescence lifetimes as discussed earlier in Section VII,D. The quantitative success of this theory adds support to this intensity-borrowing mechanism. Considering the proximity and intensity of the transition to the 1^1B_u state, it is hard to imagine any other equally important intensity-borrowing routes (Hudson and Kohler, 1973). The only other potential intensity-borrowing mechanisms are coupling to higher B_u states or to out-of-plane $\sigma\pi^*$ A_u transitions. The available evidence indicates that these are not important mechanisms.

It has been proposed that the colinearity of the absorption and emission transitions of polyenes is evidence that the 1^1B_u state is in fact the lowest excited singlet state (Moore and Song, 1973b; LeClercq and LeClercq, 1980; Rosenberg, 1976; Baldry and Barltrop, 1977). However, this is not a valid argument since the forbidden transition must borrow its intensity, and this borrowing will clearly be dominated by the allowed transition (Hudson and Kohler, 1972, 1973).

I. *Excited-State Potential Surfaces and Vibronic Coupling*

We begin this section with a discussion of the b_u promoting modes identified in the spectrum of octatetraene (Granville *et al.*, 1980). The much more limited data available for 2,4,6,8-decatetraene (Andrews and Hudson, 1978a) and 2,10-dimethylundecapentaene (Christensen and Kohler, 1975) are in general agreement with the octatetraene data.

Four promoting modes were clearly identified in the octatetraene spectrum. The usual numerological analysis is strongly supported by the straightforward analysis of the two-photon spectrum which fixes the values of the totally symmetric modes. The frequencies of these four modes (in the excited state) are compared to the lowest frequency ground-state b_u modes of octatetraene in Table 10. Although this is a comparison between calculated and

TABLE 10

THE VIBRONICALLY ACTIVE PROMOTING MODES FOR THE ABSORPTION TRANSITION TO THE 2^1A_g STATE OF OCTATETRAENE COMPARED TO THE LOW-FREQUENCY MODES OF b_u SYMMETRY OF THE GROUND STATE

	Ground state	
Excited state[a] 2^1A_g (cm^{-1})	GR[b] (cm^{-1})	CFFπ[c] (cm^{-1})
93	94	106
463	401	450
538	594	600
1054	1117[d]	1187[d]

[a] From Granville *et al.* (1980).

[b] GR, Gavin and Rice (1971).

[c] The results of a CFFπ calculation as described by Warshel and Karplus (1972a) and Hudson and Andrews (1979).

[d] A mode calculated to be at 933 (or 915) cm^{-1} is omitted, as discussed in the text.

observed modes for two different states, it is believed that there are no large frequency changes for these modes upon excitation. This conclusion is based on the calculations of Lasaga *et al.* (1980) who find values of 104, 438, 594, 931, and 1188 cm^{-1} for the ground state and 103, 427, 588, 934, and 1213 cm^{-1} for the excited 2^1A_g state. It is also supported by the fact that the excitation spectrum does not appear to contain the $n = 3$ harmonic of these promoting modes which would appear if there were a large frequency change.

The lowest frequency b_u mode calculated to be at 94 or 106 cm^{-1} is known to have a ground-state value of 109 ± 5 cm^{-1} in an *n*-octane matrix based on the fluorescence and two-photon spectra (Granville *et al.*, 1979). The form of this mode, based on a CFFπ normal coordinate calculation (Hudson and Andrews, 1979), is that of an overall in-plane bend (Fig. 37).

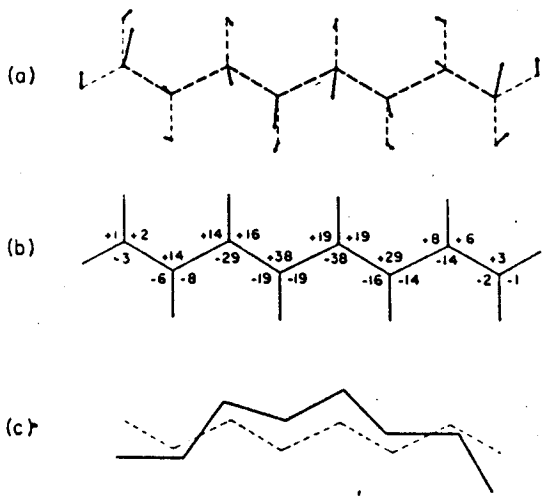

Fig. 37. Three representations of the lowest frequency b_u mode of octatetraene: (a) mass-weighted atomic displacements; (b) valence angle changes; (c) the chain without and with a displacement along the normal coordinate (Hudson and Andrews, 1979).

The other low-frequency modes of octatetraene are shown in Fig. 38, including the second b_u mode (ν_{47}) calculated to be at 450 cm^{-1}. The form of this normal mode is that of an in-plane bend with two more nodes than the 106 cm^{-1} mode. The modes calculated to be at 600 and 1187 cm^{-1} for the ground state are asymmetric accordion modes where the CCC in-plane angles are deformed such that the zigzag structure is expanded at one end and compressed at the other. The lower frequency mode at 600 cm^{-1} has its largest amplitude near the chain center, while the 1187 cm^{-1} mode has its angle deformations concentrated at the ends of the chain. The CFFπ

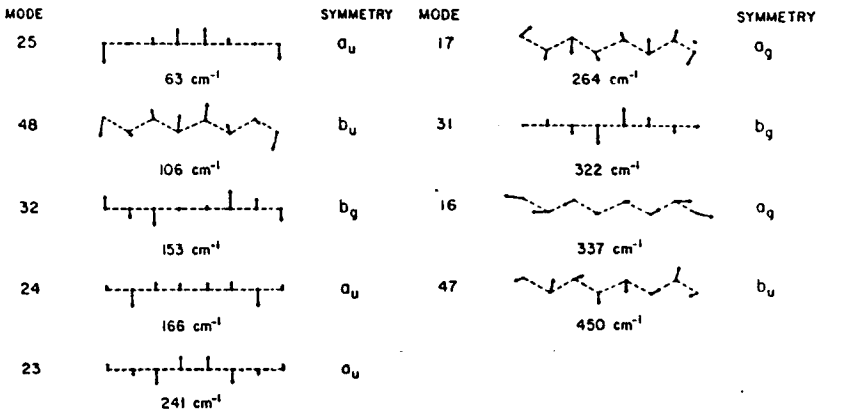

Fig. 38. Normal-mode eigenvectors for the low-frequency modes of octatetraene. The a_u and b_g modes are out-of-plane, whereas the a_g and b_u modes are in plane. (Hudson and Andrews, 1979). The indicated frequencies are from the CFFπ calculation. See Table 7 for a comparison with experiment.

mode calculated to be at 933 cm^{-1} is a purely terminal HCH angle-deformation mode and is not likely to be vibronically active for coupling $\pi\pi^*$ excited states.

One point of this discussion is that there are b_u vibrations of octatetraene with frequencies similar to those found to be promoting modes. This supports the assignment of these modes as being of b_u symmetry and, therefore, supports the excited-state 2^1A_g assignment. It is also of interest that *all* of the low-frequency b_u modes which involve the carbon skeleton are vibronically active. Further IR and far-IR studies of polyenes would be useful in the analysis of these spectra.

The totally symmetric vibrations which couple to the 1^1A_g–2^1A_g transition are also of interest. Granville *et al.* (1980) assign five modes as active a_g fundamentals in the 200–600 cm^{-1} region (220, 321, 341, 401, and 529 cm^{-1}). The vibronic peak in the two-photon spectrum for the 341 cm^{-1} mode is by far the largest in this region, with the 529 cm^{-1} mode being a factor of 5 weaker and the others weaker by another factor of 3. The 341 cm^{-1} mode is presumably the a_g mode calculated by Lasaga *et al.* (1980) to be at 336 cm^{-1} in the 2^1A_g state (see also Table 7). This is an in-plane, in-phase angle-deformation mode (Fig. 37, mode 16) in which all of the CCC angles expand or contract together. Using the conventional carbon numbering, the largest is for the 2,3,4 and 5,6,7 (penultimate) angles, the central angles 3,4,5 and 4,5,6 having a smaller change and the terminal angles 1,2,3 and 6,7,8 having the smallest change. The amplitudes are in the ratio 8:5:3. (We note that all a_g normal modes must be in-plane and not torsional as implied in Granville *et al.*, 1980.)

The vibronic mode at 529 cm^{-1} corresponds to a Raman band at 546 cm^{-1} and to a mode calculated to be at 535–593 cm^{-1}, depending on the particular calculation (see Table 7). There are no other a_g modes between the 337 cm^{-1} mode discussed above and one at 950–970 cm^{-1}. The eigenvector for the 529 cm^{-1} mode shows it to be an in-plane, out-of-phase angle-deformation mode in which the central two angles expand while the outer angles, especially the terminal angles, contract.

The very weak feature at 219 cm^{-1} probably corresponds to a Raman band at 242 cm^{-1} calculated to be at 231–264 cm^{-1}. This is an out-of-phase angular mode primarily involving expansion of the outer pair of angles (Fig. 37, mode 17).

The remaining two very weak features at 320 and 401 cm^{-1} are very difficult to assign as a_g modes since we have used all of the modes calculated to be in this region. It is very unlikely that the normal-mode calculations are in error by enough to move a_g modes into this region. A possible assignment for the 320 cm^{-1} mode, considering its intensity, is to a b_g mode calculated to be at 319–322 cm^{-1} (Table 7). This is an out-of-plane mode (see Fig. 37, mode 31) which is exclusively an out-of-phase torsion of the two interior double bonds.

The strongest vibronic bands in the two-photon and one-photon spectra of octatetraene are bond-stretching modes at 1218, 1271, and 1754 cm^{-1} with this last being the strongest by a factor of about 3. The ground-state Raman active modes with similar frequencies are at 1187, 1285, 1608, and 1612 cm^{-1} (Table 7) and the strong bands seen in fluorescence are at 1184, 1296, 1610, and 1620 cm^{-1}. The form of these normal modes was discussed above (Section VI).

The major points of interest concerning these bands are the extreme intensity of the 1754-cm^{-1} mode (1620 cm^{-1} in the ground state) and its frequency increase on excitation. The high intensity of this mode is presumably due to the parallelism between its eigenvector and the displacement on excitation as discussed in Section VI, i.e., double bonds increasing in length and single bonds decreasing in length. The best available theoretical estimate of this effect is the calculation of Lasaga *et al.* (1980). Their results for the ground and excited A_g states of octatetraene are given in Table 11. The pattern of the predicted bond-length changes parallels the normal-mode eigenvector leading to a large Franck–Condon factor (Lasaga, 1978). The intensity of this band is therefore well understood. [It is interesting to note in passing that the calculated bond-length changes for hexatriene are much larger for the double bonds (−0.077 or −0.079) than for octatetraene. This may be related to the lack of fluorescence or well-resolved spectra for this molecule, as noted above.]

TABLE 11

CALCULATED BOND LENGTHS FOR OCTATETRAENE (Å)[a]

A_g state (—)	C_1—C_2 (=)	C_2—C_3 (—)	C_3—C_4 (=)	C_4—C_5 (—)
Ground	1.347	1.461	1.361	1.457
Excited	1.398	1.409	1.432	1.408
Δ	−0.051	+0.052	−0.071	+0.049
Q^b	−0.057	+0.047	−0.071	+0.049

[a] From Lasaga *et al.* (1980).

[b] The eigenvector for the CFFπ normal mode at 1659 cm^{-1} scaled by a factor chosen to optimize comparison.

The remaining difficulty with our understanding of the potential surface of octatetraene is the observation of a frequency of 1754 cm^{-1} in the excited state compared to about 1620 cm^{-1} in the ground state. The frequencies calculated by Lasaga *et al.* (1980) are 1544 cm^{-1} for the excited ^1A_g state and 1617 cm^{-1} for the ground state. Thus, in agreement with intuition, this "double-bond" mode is calculated to have a lower frequency in the excited state. That the opposite is observed is not an isolated case peculiar to octatetraene. Other examples are 2,10-dimethyl-undecapentaene (Christensen and Kohler, 1975) and dodecapentaene (Andrews, 1978). An interesting parallel situation has been observed in the "single-bond"-stretching region for the triplet states of carotenoids (Dallinger *et al.*, 1979, 1981; Jensen *et al.*, 1980). Raman studies of several carotenoid triplets have shown an unexpected decrease in the single-bond mode near 1155 cm^{-1}. The mean decrease is about 30 cm^{-1}. The "double-bond" mode near 1520 cm^{-1} (in carotenoids) decreases, as expected from simple bonding arguments. These triplet-state effects are much smaller than the complementary singlet-state shifts.

The problem, then, is how to explain a frequency increase of 130 cm^{-1} upon excitation when a 75 cm^{-1} decrease is expected. The Duschinsky effect and changes in nearest neighbor (Dallinger *et al.*, 1981) or next-nearest-neighbor bond-interaction force constants are implicitly included in calculations such as those performed by Lasaga *et al.* (1980). Thus, the possible explanations of this unexpected frequency shift can be classified as those which are not included in this calculation or, alternatively, as defects in the calculation. An example of the former is nonadiabatic coupling between the 2^1A_g and 1^1A_g states (Auerbach *et al.*, 1981). An example of the latter is the lack of inclusion of configurations which are doubly excited with respect to the excited 2^1A_g state, since these triple and quadruple excitations may

be necessary for the next-nearest-neighbor (double bond, double bond) interaction force constants. At present, there is no clear explanation for this problem.

J. Triplet States and Higher Energy Singlet States

Most of the available data on the triplet states of linear polyenes was summarized in our earlier review. The only new information seems to be that from the electron-impact studies of Flicker *et al.* (1977) and Frueholz and Kuppermann (1978) on hexatriene. The 1^1A_g–^3B_u and 1^1A_g–^3A_g transitions have been studied in some detail (see Figs. 27–29). The lower energy transition to the ^3B_u state is found at 2.61 eV, while the upper transition to the ^3A_g state is at 4.11 eV. These are in excellent agreement with the *ab initio* calculations of Nascimento and Goddard (1979b) who calculate triplet states at 2.73 eV (^3B_u), 4.37 eV (^3A_g), and 5.28 eV (^3B_u).

The 1^1A_g–2^3A_g transition has been studied by high-resolution electron-impact spectroscopy (Frueholz and Kuppermann, 1978). The resulting vibronic pattern has been analyzed in terms of a forbidden vibronic pattern with a 1400-cm^{-1} b_u promoting mode with additional peaks 1200 and 1050 cm^{-1} higher.

The singlet-singlet transitions of butadiene higher in energy than the 4.9-eV 1^1A_g–1^1B_u transition have been extensively studied recently using a variety of techniques including optical absorption of the gas at −78°C (McDiarmid, 1975, 1976), electron-impact scattering (Mosher *et al.*, 1973b; Flicker *et al.*, 1978; Doering and McDiarmid, 1980), and multiphoton ionization (Johnson, 1976; Rothberg *et al.*, 1980). The study by Rothberg *et al.* (1980) includes both two-photon and three-photon ionization resonances. A total of 54 resonances are observed, most of which are assigned to a set of four Rydberg series all originating from the highest filled (b_g) orbital and involving s, p, d, and f atomic orbitals. Similar data are presented for three methyl-substituted dienes. No new information concerning valence excited states is obtained with this method and it is pointed out that multiphoton ionization appears to strongly favor Rydberg excited states over valence excitations so that valence excitations, although present, may be missed by this method.

The electron-impact data of McDiarmid and Doering (1980) are in good agreement with the results of Rothberg *et al.* (1980). In fact, one can read off the values of the strong peaks from the multiphoton ionization spectra and convert these to the peaks listed for the electron-impact experiments with an accuracy of ±0.01 eV. The only exceptions are the absence in the three-photon ionization spectrum of a peak at 7.61 eV, which appears to be allowed in the electron-impact spectrum, and the absence in the electron-impact spectrum of a peak at 7.78 eV, which is medium strong in the ionization

spectrum. Flicker *et al.* (1978), whose electron-impact data are generally in excellent agreement with that of Doering and McDiarmid, report peaks at 7.80 and 7.60 eV. The assignments of the Rydberg transitions adopted by Doering and McDiarmid (1980) and Rothberg *et al.* (1980) are the same (3s at 6.21 eV, $3p_1$ at 6.66 eV, $3p_2$ at 7.06 eV, and associated vibrational side bands), except for two cases. The 8-eV transition is assigned by Rothberg *et al.* as a transition to a $4p_2$ Rydberg state, while Doering and McDiarmid assign this to the 3d state. Rothberg *et al.* assign the 3d state to a band at 7.35 eV.

An underlying continuum in the 7–7.8-eV region of the electron-impact spectrum (maximum near 7.3 eV) has been assigned (Doering and McDiarmid, 1980) as the 2^1A_g excited state. The basis for this assignment is the different dependence of the continuum relative to the superimposed peaks. The continuum increases relatively at increased scattering angle. Examination of the much higher resolution data of Rothberg *et al.* shows that in the 7.0–7.8-eV region, there are 14 transitions in addition to the strong features at 7.07, 7.22, and 7.46 eV. Of these 14 transitions, 7 are unassigned, and 4 are assigned to the 3d Rydberg. This could be the one observed in the electron-impact experiments.

There have also been several recent studies of the higher singlet states of hexatriene (Flicker *et al.*, 1977; Parker *et al.*, 1976, 1978; Gavin and Rice, 1974). The results of these studies are tabulated and compared with theoretical results in Nascimento and Goddard (1979b). A transition at 6.2 eV has been firmly established as due to a ^1A_g excited state (Parker *et al.*, 1978) whose Rydberg character is indicated by a condensed-phase study using thermal lensing detection of two-photon absorption (Twarowski and Kliger, 1977). A discussion of the interpretation of the optical spectrum of hexatriene on the basis of semiempirical theory is given by Karplus *et al.* (1975). One of the difficulties in the assignment of bands in the spectra of alternate hydrocarbons is the fact that many of the transitions to excited ^1B_u states which are formally allowed have very low intensity because the upper state is a covalent ^1B_u state (see Section IV). As a result, the intensity of these "allowed" but weak transitions may be comparable to the vibronically induced intensity of symmetry-forbidden transitions. The assignment of the higher valence states of hexatriene and octatetraene (Gavin *et al.*, 1978) is still in doubt.

VIII. Infinite Polyenes: Bond Alternation and Spectral Convergence

There has been considerable recent interest in the properties of the species formed by the polymerization of acetylene. Rather than attempt to review this rapidly expanding field here, we will include a few relevant references as

part of our discussions of the structure of these materials and the extrapolations which can be made from the data available for finite chains toward the long-chain limit:

Polyacetylene, with the repeating-bond sequence double–single–double–single, should be distinguished from polydiacetylene (Wegner, 1969; Kaiser *et al.*, 1972; Baughman, 1972) with the bond sequence double–single–triple–single. Polydiacetylene is formed by a solid-state addition reaction to form crystals with highly ordered conjugated chains of essentially infinite length. Conventional polymerization of acetylene results in a material with finite conjugated chains of various lengths as components of a higher molecular weight, probably cross-linked, polymer. Polyacetylene can be formed in either cis-rich or trans-rich forms by changing the temperature of polymerization. The cis form can be converted to the trans form by heating. This interconversion is associated with the generation of unpaired electron spin believed to represent mobile boundaries between one register of the double-bond pattern and the other, i.e.,

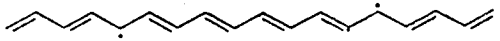

The structure drawn is a neutral "soliton" of eight methylene units. Rate constants and activation energies for soliton formation have been determined and a mechanism for soliton formation has been proposed (Chien *et al.*, 1980). Theoretical studies of soliton formation have been given by Su and Schrieffer (1980) and Su *et al.* (1980), who include references to other experimental results in this field. This phenomenon is, of course, peculiar to long polyene chains and has no direct experimental connection with results obtained with finite-length polyenes. However, it is interesting to note the similarity between the neutral soliton structure shown above and the long-bond resonance structure which dominates the excited ^1A_g state.

Several recent theoretical studies of the electronic structure of long polyenes have dealt with the origin of the ca. 2-eV band gap associated with the allowed excitation, the form of the asymptotic approach to the limiting value and the existence of spin-density waves, the infinite-chain counterpart of the 2^1A_g state (Tyutyulkov *et al.*, 1980; Duke *et al.*, 1978; Yarkony and Silbey, 1977; Szabo *et al.*, 1976; Misurkin and Ovchinnikov, 1976; Ovchinnikov *et al.*, 1973; Harris and Falicov, 1969). Recall that the Hückel treatment of the infinite polyene chain results in a band gap $\Delta E(\infty) = 2|\beta_s - \beta_l|$, i.e., twice the difference in the exchange integrals for the short and long bonds. This vanishes for equal bond lengths. It is now claimed (Tyutyulkov *et al.*, 1980) that models of the infinite polyene chain which do not include bond alternation still lead to the prediction of a finite band gap close to or larger than that observed. This conclusion, which is based on an alternative molecular orbital treatment (AMO; see Salem, 1966) within

the PPP approximation but including long-range Coulomb interactions, also results from use of the Hubbard Hamiltonian (Ovchinnikov *et al.*, 1973; Misurkin and Ovchinnikov, 1976). On the other hand, the model developed by Yarkony and Silbey (1977), a single-configuration SCF treatment, produces no band gap without bond alternation (the Hückel result). However, these authors show that within this model the major contribution to the band gap is the difference in the exchange contribution to the ground and excited state. Thus, when $|\beta_s - \beta_l|$ is only 0.12 eV so that the band gap predicted by the Hückel model is 0.24 eV, the exchange contribution is 2.29 eV. However, this exchange term vanishes when $\Delta\beta = 0$. Overall, it is not clear at present whether the existence of a finite band gap can be taken as evidence of bond alternation in long polyene chains.

The structural data presented in Section II does not really provide adequate information concerning the extent of bond alternation expected for long polyene chains. Good data for a longer chain species is clearly needed.

The vibrational data of Section VI demonstrates a decrease in the frequency of the major Raman band of polyenes as the chain length increases. The frequency of this band for polyacetylene is about 1475 cm^{-1} (Inagaki *et al.*, 1975). The decrease in this frequency is most probably due to a decreased double-bond force constant as the chain length increases. However, this normal mode has single-bond components which are 75% of the double-bond components (Table 11), so the expected increase in the single-bond force constant will eventually counteract the decrease in the double-bond strength. With equal force constants the dispersion curves of Fig. 14 will collapse into four branches for the in-plane modes, which look something like those of polyethylene but with greater dispersion. This does not necessarily result in a single Raman active band and, therefore, there is no simple relationship between the appearance of the vibrational spectrum and the absence of bond alternation.

Extrapolations of available data for the allowed electronic excitation energy of linear polyenes (e.g., Salem, 1966; Szabo *et al.*, 1976) have all been based on solution data or on a mixture of gas-phase and solution data and some have used species with different substituents. The data of Table 2 provides a set of measurements which have been consistently corrected to the gas phase using the procedure illustrated in Figs. 33 and 34. This removes the small but systematic errors introduced by the fact that the solvent correction, even for a given solvent, is not exactly the same for all polyenes. For example, a typical solvent correction for octatetraene is 3300 cm^{-1}, while for dodecahexane it is 2800 cm^{-1}. It has been claimed (Szabo *et al.*, 1976) that the allowed transition excitation energy approaches the gap limit according to the expression

$$\bar{\nu} = \bar{\nu}(\infty) + k/N \tag{31}$$

i.e., as $1/N$. The data of Table 2 do not support that conclusion but that may be due to the fact that these polyenes are too short to exhibit the general trend of the longer species.

Finally, it is interesting to note that the excitation energy for the transition to the 2^1A_g excited state appears to decrease with chain length more rapidly than the excitation energy for the allowed transition (Fig. 8; Hudson and Kohler, 1973; D'Amico *et al.*, 1980). Put another way, the gap between the excited 1^1B_u and 2^1A_g states increases with chain length. Obviously, the energy separation between these two states cannot exceed the infinite-chain band gap. However, it could approach this limit so that the 2^1A_g state (and the 1^3A_g state) would become degenerate with the ground state, as is predicted by the Hubbard Hamiltonian (Ovchinnikov *et al.*, 1973).

IX. Conclusions

Considerable progress has been made during the seven-year period since polyene spectroscopy was last reviewed. This has included a rigorous demonstration of the nature of the low-lying excited state of these species; facilitation of the comparison of theory with experiment because of the availability of data for simple methyl-substituted and unsubstituted polyenes; a systematic, quantitative understanding of the variation of polyene radiative lifetimes; the collection of data for series of homologous polyenes so that trends begin to emerge; the establishment, with reasonable certainty, that polyenes do not twist appreciably upon excitation; and the conclusion that semiempirical treatments of the low-lying excitations of long polyene chains require configuration interaction beyond the double-excitation level or possibly the use of novel methods still under development. There has also been considerable increase in our knowledge of the frequencies and forms of the promoting and symmetric modes for the lowest transition of octatetraene.

A number of observations have been made whose explanations are not fully established at the present time. One is the unexpectedly high frequency for the strongest symmetric stretch mode of polyenes in their 2^1A_g state. Another is the variation of the shape of the lowest electron-impact transition of butadiene with incident electron energy. The inability of *ab initio* calculations to describe the ionic excited states of butadiene and hexatriene remains a difficulty whose solution is not obvious.

There also remain a number of significant challenges in polyene spectroscopy in addition to the resolution of the problems posed above. One of the most important is the establishment of the excited-state order in butadiene and the two isomers of hexatriene. This could have very important photochemical implications. Another challenge is the establishment of trends in the structure and excitation energies for very long chain polyenes. Theoretical studies of this behavior should examine the extent to which conclusions can be shown to have more general validity—rather than being dependent on the model chosen.

Acknowledgments

The authors would like to acknowledge helpful conversations and the assistance of John Andrews, Robert Birge, Ron Christensen, John Doering, David Herrick, William Hetherington, Laura Hudson, Martin Karplus, David Kliger, Dylan Kohler, Aaron Kuppermann, and Guy Montelione, and the supreme patience of our editor, Ed Lim.

References

Abe, K. (1970). Thesis, University of Tokyo, as cited in Shimanouchi (1972).
Andrews, J. (1978). Thesis, Stanford University, Stanford, California.
Andrews, J., and Hudson, B. (1978a). *Chem. Phys. Lett.* 57, 600.
Andrews, J., and Hudson, B. (1978b). *J. Chem. Phys.* 68, 4587.
Andrews, J., and Hudson, B. (1979). *Chem. Phys. Lett.* 60, 380.
Aston, J. G., Szasz, G., Wooley, H. W., and Brickwedde, F. G. (1946). *J. Chem. Phys.* 14, 67.
Auerbach, R. A., Christensen, R. L., Granville, M. F., and Kohler, B. E. (1981). *J. Chem. Phys.* 74, 4.
Baldry, P. J., and Barltrop, J. A. (1977). *Chem. Phys. Lett.* 46, 430.
Bart, J. C. J., and MacGillavry, C. H. (1968). *Acta Crystallogr., Sect. B* 24, 1569.
Basu, S. (1964). *Adv. Quantum Chem.* 7, 289.
Baughman, R. H. (1972). *J. Appl. Phys.* 43, 4362.
Becker, R. S., Das, P. K., and Kogan, G. (1979). *Chem. Phys. Lett.* 67, 463.
Bennett, J. A., and Birge, R. R. (1980). *J. Chem. Phys.* 73, 4234.
Berlman, I. (1971). "Handbook of Fluorescence Spectra of Aromatic Molecules." Academic Press, New York.
Birks, J. B. (1976). *Z. Phys. Chem. (Wiesbaden)* [N.S.] 101, 91
Birks, J. B., and Birch, D. J. S. (1975). *Chem. Phys. Lett.* 31, 608.
Birks, J. B., and Dyson, D. J. (1963). *Proc. R. Soc. London, Ser. A* 275, 135.
Birks, J. B., Tripathi, G. N. R., and Lumb, M. D. (1978). *Chem. Phys.* 33, 185.
Brey, L. A., Schuster, G. B., and Drickamer, H. G. (1979). *J. Chem. Phys.* 71, 2765.
Callender, R., and Honig, B. (1977). *Annu. Rev. Biophys. Bioeng.* 6, 33.
Campion, W. J., and Karplus, M. (1973). *Mol. Phys.* 25, 30.
Carmichael, I. C., Sheng, S. J., and Hug, G. L. (1979). *J. Chem. Phys.* 70, 5339.
Carreira, L. A. (1975). *J. Chem. Phys.* 62, 3851.
Cehelnik, E. D., Cundall, R. B., Timmons, C. J., and Bowley, R. M. (1973). *Proc. R. Soc. London, Ser. A* 335, 387.
Cehelnik, E. D., Cundall, R. B., Lockwood, J. R., and Palmer, T. F. (1974). *Chem. Phys. Lett.* 27, 586.
Cehelnik, E. D., Cundall, R. B., Lockwood, J. R., and Palmer, T. F. (1975) *J. Phys. Chem.* 79, 1369.
Chien, J. C. W., Karasz, F. E., and Wnek, G. E. (1980) *Nature (London)* 285, 390.
Christensen, R. L. (1972). Ph. D. Thesis, Harvard University, Cambridge, Massachusetts.

Christensen, R. L., and Kohler, B. E. (1973). *Photochem. Photobiol.* **18**, 293.
Christensen, R. L., and Kohler, B. E. (1975). *J. Chem. Phys.* **63**, 1837.
Christensen, R. L., and Kohler, B. E. (1976). *J. Phys. Chem.* **80**, 2197.
Cole, A. R. H., Mohay, G. M., and Osborne, G. A. (1967). *Spectrochim. Acta, Part A* **23A**, 909.
Cole, A. R. H., Green, A. A., and Osborne, G. A. (1973). *J. Mol. Spectrosc.* **48**, 212.
Compton, D. A. C., George, W. O., and Maddams, W. F. (1976). *J. Chem. Soc., Perkin* Trans. 2 p. 1666.
Coulson, C. A., and Longuet-Higgins, H. C. (1948). *Proc. R. Soc. London, Ser. A* **193**, 457.
Dalle, J. P., and Rosenberg, B. (1970). *Photochem. Photobiol.* **12**, 151.
Dallinger, R. F., Guanci, J. J., Woodruff, W. H., and Rodgers, M. A. J. (1979). *J. Am Chem. Soc.* **101**, 1355.
Dallinger, R. F., Farquharson, S., Woodruff, W. H., and Rodgers, M. A. J. (1981). *J. Am. Chem. Soc.* 103, 7433.
D'Amico, K. L., Manos, C., and Christensen, R. L. (1980). *J. Am. Chem. Soc.* **102**, 1777.
Diamond, J. (1978). Ph. D. Thesis, Stanford University, Stanford, California.
Doering, J. P. (1979). *J. Chem. Phys.* **70**, 3902.
Doering, J. P., and McDiarmid, R. (1980). *J. Chem. Phys.* **73**, 3617.
Drenth, W., and Wiebenga, E. H. (1955). *Acta Crystallogr.* **8**, 755.
Duke, C. B., Paton, A., Salaneck, W. R., Thomas, H. R., Plummer, E. W., Heeger, A. J., and Macdiarmid A. G. (1978). *Chem. Phys. Lett.* **59**, 146.
Eckert, R., and Kuhn, H. (1960). *Z. Elektrochem.* **64**, 356.
Fang, H. L. B., Thrash, R. S., and Leroi, G. E. (1977). *J. Chem. Phys.* **67**, 3389.
Fang, H. L. B., Thrash, R. J., and Leroi, G. E. (1978). *Chem. Phys. Lett.* **57**, 59.
Fetter, A. L., and Walecka, J. D. (1971). "Quantum Theory of Many Particle Systems." McGraw-Hill, New York.
Flicker, W. M., Mosher, O. A., and Kuppermann, A. (1977). *Chem. Phys. Lett.* **45**, 492.
Flicker, W. M., Mosher, O. A., and Kuppermann, A. (1978). *Chem. Phys.* **30**, 307.
Frueholz, R. P., and Kuppermann, A. (1978). *J. Chem. Phys.* **69**, 3433.
Frueholz, R. P., Flicker, W. M., and Kuppermann, A. (1976). *Chem. Phys. Lett.* **38**, 57.
Gavin, R. M., Jr., and Rice, S. A. (1971). *J. Chem. Phys.* **55**, 2675.
Gavin, R. M., Jr., and Rice, S. A. (1974). *J. Chem. Phys.* **60**, 3231.
Gavin, R. M., Jr., Risemberg, S., and Rice, S. A. (1973). *J. Chem. Phys.* **58**, 3160.
Gavin, R. M., Jr., Weisman, C., McVey, J. K., and Rice, S. A. (1978). *J. Chem. Phys.* **68**, 522.
Granville, M. F., Holtom, G. R., Kohler, B. E., Christensen, R. L., and D'Amico, K. (1979). *J. Chem. Phys.* **70**, 593.
Granville, M. F., Holtom, G. R., and Kohler, B. E. (1980). *J. Chem. Phys.* **72**, 4671.
Granville, M. F., Kohler, B. E., and Snow, J. B. (1981). *J. Chem. Phys.* **75**, 3765.
Harris, R. K. (1964). *Spectrochim. Acta* **20**, 1129.
Harris, R. K., and Falicov, L. (1969). *J. Chem. Phys.* **51**, 5034.
Haugen, W., and Traetteberg, M. (1966). *Acta Chem. Scand.* **20**, 1726.
Haugen, W., and Traetteberg, M. (1967). *In* "Selected Topics in Structural Chemistry" (P. Andersen, O. Bastiansen, and S. Furberg, eds.), p. 113. Oslo Univ. Press, Oslo.
Hemley, R., and Kohler, B. E. (1977). *Biophys. J.* **20**, 377.
Herrick, D. R. (1981). *J. Chem. Phys.* **74**, 1239.
Hetherington, W. M., III (1976). Ph. D. Thesis, Stanford University, Stanford, California.
Hetherington, W. M., III, and Hudson, B. S. (1979). *Chem. Phys. Lett.* **65**, 261.
Holtom, G. R., and McClain, W. M. (1976). *Chem. Phys. Lett.* **44**, 436.
Honig, B., Hudson, B., Sykes, B. D., and Karplus, M. (1971). *Proc. Natl. Acad. Sci. U.S.A.* **68**, 1289.
Hosteny, R. P., Dunning, T. H., Jr., Gilman, R. R., Pipano, A., and Shavitt, I. (1975). *J. Chem. Phys.* **62**, 4764.

Hudson, B. (1972). Ph. D. Thesis, Harvard University, Cambridge, Massachusetts.
Hudson, B., and Andrews, J. (1979). *Chem. Phys. Lett.* **63**, 493.
Hudson, B., and Kohler, B. E. (1972). *Chem. Phys. Lett.* **14**, 299.
Hudson, B., and Kohler, B. E. (1973). *J. Chem. Phys.* **59**, 4984.
Hudson, B., and Kohler, B. E. (1974). *Annu. Rev. Phys. Chem.* **25**, 437.
Hudson, B., and Loda, R. T. (1981). *Chem. Phys. Lett.* **81**, 591.
Inagaki, F., Tasumi, M., and Miyazawa, T. (1975). *J. Raman Spectrosc.* **3**, 335.
Jensen, N.-H., Wilbrandt, R., Pagsberg, P. B., Sillesen, A. H., and Hansen, K. P. (1980). *J. Am. Chem. Soc.* **102**, 7441.
Johnson, P. M. (1976). *J. Chem. Phys.* **64**, 4638.
Jones, L. C., Jr., and Taylor, L. W. (1955). *Anal. Chem.* **27**, 228.
Kaiser, J., Wegner, G., and Fischer, E. W. (1972). *Isr. J. Chem.* **10**, 157.
Karplus, M., Gavin, R. M., Jr., and Rice, S. A. (1975). *J. Chem. Phys.* **63**, 5507.
Klochkov, V. P., and Bogdanov, V. L. (1978). *Opt. Spektrosk.* **43**, 876; *Opt. Spectrosc.* (*Engl. Transl.*) **43**, 518.
Klump, K. N., and Lassettre, E. N. (1977). *Chem. Phys. Lett.* **51**, 99.
Knoop, F. W. E., and Oosterhoff, L. J. (1973). *Chem. Phys. Lett.* **22**, 247.
Kohler, B. E. (1979). *In* "Chemical and Biochemical Applications of Lasers" (C. B. Moore, ed.), Vol. 4. Academic Press, New York.
Kuchitsu, K., Fukuyama, T., and Morino, Y. (1967). *J. Mol. Struct.* **1**, 463.
Kuppermann, A., Flicker, W. M., and Mosher, O. A. (1979). *Chem. Rev.* **79**, 77.
Lasaga, A. C. (1978). Thesis, Harvard University, Cambridge, Massachusetts.
Lasaga, A. C., Aerni, R. J., and Karplus, M. (1980). *J. Chem. Phys.* **73**, 5230.
Lassettre, E. N., and Skerbele, A. (1974). *Methods Exp. Phys.* **3**, Part B, p. 868.
LeClercq, J., and LeClercq, J. M. (1980). *Chem. Phys. Lett.* **57**, 54.
Lide, D. R., Jr. (1962). *J. Chem. Phys.* **37**, 2074.
Lipnick, R. L., and Garbisch, E. W., Jr. (1973). *J. Am. Chem. Soc.* **95**, 6370.
Lippincott, E. R., and Kenney, T. E. (1962). *J. Am. Chem. Soc.* **84**, 3641.
Lippincott, E. R., Feairheller, W. R., Jr., and White, C. E. (1959). *J. Am. Chem. Soc.* **81**, 1316.
Longuet-Higgins, H. C., and Pople, J. A. (1957). *J. Chem. Phys.* **27**, 192.
McDiarmid, R. (1975). *Chem. Phys. Lett.* **34**, 130.
McDiarmid, R. (1976). *J. Chem. Phys.* **64**, 514.
McDiarmid, R., and Doering, J. P. (1980). *J. Chem. Phys.* **73**, 4192.
Marais, D. J., Sheppard, N., and Stoicheff, B. P. (1962). *Tetrahedron* **17**, 163.
Misurkin, I. A., and Ovchinnikov, A. A. (1976). *Teor. Eksp. Khim.* **12**, 291.
Moore, T. A., and Song, P. (1973a). *Nature* (*London*), *New Biol.* **243**, 30.
Moore, T. A., and Song, P. (1973b). *Chem. Phys. Lett.* **19**, 128.
Moore, T. A., and Song, P. (1974). *J. Mol. Spectrosc.* **52**, 209.
Mosher, O. A., Flicker, W. M., and Kuppermann, A. (1973a). *Chem. Phys. Lett.* **19**, 332.
Mosher, O. A., Flicker, W. M., and Kuppermann, A. (1973b). *J. Chem. Phys.* **59**, 6502.
Mosher, O. A., Flicker, W. M., and Kuppermann, A. (1975). *J. Chem. Phys.* **62**, 2600.
Mulliken, R. S. (1939). *J. Chem. Phys.* **7**, 364.
Nascimento, M. A. C., and Goddard, W. A., III (1979a). *Chem. Phys. Lett.* **60**, 197.
Nascimento, M. A. C., and Goddard, W. A., III (1979b). *Chem. Phys.* **36**, 147.
Neporent, B. S. (1973). *Izv. Akad. Nauk SSSR, Ser. Fiz.* **37**, 236.
Nikitina, A. N., Ter-Sarkisyan, G. S., Mikhailov, B. M., and Minchenkova, L. E. (1964). *Acta Phys. Pol.* **26**, 483.
Nikitina, A. N. Ponomareva, N. A., Ter-Sarkisyan, G. S., and Yanovskaya, L. A. (1975). *Izv. Akad. Nauk SSSR, Ser. Fiz.* **39**, 1937.
Nikitina, A. N., Ponomareva, N. A., Yanovskaya, L. A., Dombrovsky, V. A., and Kucherov, V. F. (1976). *Opt. Spektrosk.* **40**, 251.

Nikitina, A. N., Ponomareva, N. A., Ter-Sarkisyan, G. S., and Yanovskaya, L. A. (1977). *Opt. Spektrosk.* 42, 889.
Novick, S., Lehn, J. M., and Klemperer, W. (1973). *J. Am. Chem. Soc.* 95, 8189.
Ohmine, I., and Schulten, K. (1982). To be published.
Ooshika, Y. (1954). *J. Phys. Soc. Jpn.* 9, 594.
Ovchinnikov, A., Ukrainiski, I., and Kventsel, G. (1973). *Sov. Phys. Usp.* (*Engl. Transl.*) **15**, 575.
Parker, D. H., Sheng, S. J., and El-Sayed, M. A. (1976). *J. Chem. Phys.* **65**, 5534.
Parker, D. H., Berg, J. O., and El-Sayed, M. A. (1978). *Chem. Phys. Lett.* **56**, 197.
Parkhurst, L. J., and Anex, B. G. (1966). *J. Chem. phys.* 45, 862.
Pitzer, K. S., and Gwinn, W. D. (1942). *J. Chem. Phys.* **10**,428.
Popov, E. M., and Kogan, G. A. (1964). *Opt. Spektrosk.* **17**, 670; *Opt. Spectrosc.* (*Engl. Transl.*) **17**, 362.
Post, D. E., Hetherington, W. M., III, and Hudson, B. (1975). *Chem. Phys. Lett.* **35**, 259.
Price, W. C., and Walsh, A. D. (1940). *Proc. R. Soc. London, Ser. A* **174**, 220.
Radom, L., and Pople, J. A. (1970). *J. Am. Chem. Soc.* **92**, 4786.
Richards, C. M., and Nielsen, J. R. (1950). *J. Opt. Soc. Am.* **40**, 438.
Rimai, L., Heyde, M. E., and Gill, D. (1973). *J. Am. Chem. Soc.* **95**, 4493.
Robin, M. D. (1975). "Higher Excited States of Polyatomic Molecules," Vol. 2. Academic Press, New York.
Rosenberg, B. (1976). *In* "Excited States of Biological Molecules" (J. B. Birks, ed.), p. 509. Wiley, London.
Rothberg, L. J., Gerrity, D. P., and Vaida, V. (1980). *J. Chem. Phys.* **73**, 5508.
Sackmann, E., and Rehm, D. (1970). *Chem. Phys. Lett.* **4**, 537.
Salem, L. (1966). "The Molecular Orbital Theory of Conjugated Systems." Benjamin, New York.
Scherer, J. R., and Overend, J. (1961). *Spectrochim. Acta* **17**, 719.
Schulten, K., and Karplus, M. (1972). *Chem. Phys. Lett.* **15**, 305.
Schulten, K., Ohmine, I., and Karplus, M. (1976). *J. Chem. Phys.* **64**, 4422.
Schulten, K., Dinur, U., and Honig, B. (1980). *J. Chem. Phys.* **73**, 3927.
Shimanouchi, T. (1949). *J. Chem. Phys.* **17**, 245, 734, 848.
Shimanouchi, T. (1972). "Tables of Molecular Vibrational Frequencies," Consolidated Vol. I. Natl. Bur. Stand., Washington, D.C.
Simonetta, M., Gianinetti, E., and Vandoni, I. (1968). *J. Chem. Phys.* **48**, 1579.
Simpson, W. T. (1951). *J. Am. Chem. Soc.* **73**, 5363.
Simpson, W. T. (1956). *J. Am. Chem. Soc.* **78**, 3585.
Sklar, L. A., Hudson, B., Petersen, M., and Diamond, J. (1977). *Biochemistry* **16**, 813.
Snow, J. (1980). Ph.D. Thesis, Wesleyan University, Middletown, Connecticut.
Song, P.-S., Chae, Q., Fujita, M., and Hiroaki, B. (1976). *J. Am. Chem. Soc.* **98**, 819.
Strickler, S. J., and Berg, R. A. (1962). *J. Chem. Phys.* **37**, 814.
Su, W. P., and Schrieffer, J. R. (1980). *Proc. Natl. Acad. Sci. U.S.A.* **77**, 5626.
Su, W. P., Schrieffer, J. R., and Heeger, A. J. (1980). *Phys. Rev. B: Condens. Matter* **22**, 2099.
Suzuki, H. (1967). "Electronic Absorption Spectra and Geometry of Organic Molecules." Academic Press, New York.
Swofford, R. L., and McClain, W. M. (1973). *J. Chem. Phys.* 59, 5740.
Szabo, A., Langlet, J., and Malrieu, J.-P. (1976). *Chem. Phys.* **13**, 173.
Takemura, T., Das, P. K., Hug, G., and Becker, R. S. (1976). *J. Am. Chem. Soc.* **98**, 7099.
Tavan, P., and Schulten, K. (1979). *J. Chem. Phys.* **70**, 5407.
Tavan, P., and Schulten, K. (1980). *J. Chem. Phys.* **72**, 3549
Thompson, A. J. (1969). *J. Chem. Phys.* **51**, 4106.

Traetteberg, M. (1968a). *Acta Chem. Scand.* **22**, 628.
Traetteberg, M. (1968b). *Acta Chem. Scand.* **22**, 2294.
Tric, C. (1969). *J. Chem. Phys.* **51**, 4778.
Twarowski, A. J., and Kliger, D. S. (1977). *Chem. Phys. Lett.* **50**, 36.
Tyutyulkov, N., Kanev, I., and Castano, O. (1980). *Theor. Chim. Acta* 55, 207.
Vaida, V., Turner, R. E., Casey, J. L., and Colson, S. D. (1978). *Chem. Phys. Lett.* **54**, 25.
Warshel, A., and Karplus, M. (1972a). *J. Am. Chem. Soc.* **94**, 5612.
Warshel, A., and Karplus, M. (1972b). *Chem. Phys. Lett.* **17**, 7.
Wegner, G. (1969). *Z. Naturforsch., B: Anorg. Chem., Org. Chem., Biochem., Biophys., Biol.* **24B**, 824.
Wilkerson, P. G., and Mulliken, R. S. (1955). *J. Chem. Phys.* **23**, 1895.
Yarkony, D. R., and Silbey, R. (1977). *Chem. Phys.* **20**, 183.
Zelikoft, M., and Watanabe, K. (1953). *J. Opt. Soc. Am.* **43**, 756.
Ziegler, L. D., and Hudson, B. S. (1982). *In* "Excited States," Vol. 5, p. 41 (E, C. Lim, ed.). Academic Press, New York.